ADECUACIÓN Y DESARROLLO DE MÉTODOS DE ANÁLISIS DE DATOS OBTENIDOS MEDIANTE ESPECTROMETRÍA GAMMA PARA LA MEDIDA DE LA RADIACTIVIDAD AMBIENTAL EN TIEMPO REAL

Elena Prieto Butillé

UNIVERSITAT ROVIRA i VIRGILI

Adecuación y desarrollo de métodos de análisis de datos obtenidos mediante espectrometría gamma para la medida de la radiactividad ambiental en tiempo real

ELENA PRIETO BUTILLÉ

TESIS DOCTORAL

2017

UNIVERSITAT ROVIRA I VIRGILI
ADECUACIÓN Y DESARROLLO DE MÉTODOS DE ANÁLISIS DE DATOS OBTENIDOS MEDIANTE ESPECTROMETRÍA GAMMA PARA LA MEDIDA DE LA RADIACTIVIDAD AMBIENTAL EN TIEMPO REAL
Elena Prieto Butillé

UNIVERSITAT ROVIRA I VIRGILI
ADECUACIÓN Y DESARROLLO DE MÉTODOS DE ANÁLISIS DE DATOS OBTENIDOS MEDIANTE ESPECTROMETRÍA GAMMA PARA LA MEDIDA DE LA RADIACTIVIDAD AMBIENTAL EN TIEMPO REAL
Elena Prieto Butillé

UNIVERSITAT ROVIRA I VIRGILI
ADECUACIÓN Y DESARROLLO DE MÉTODOS DE ANÁLISIS DE DATOS OBTENIDOS MEDIANTE ESPECTROMETRÍA GAMMA PARA LA MEDIDA DE LA RADIACTIVIDAD AMBIENTAL EN TIEMPO REAL
Elena Prieto Butillé

Adecuación y desarrollo de métodos de análisis de datos obtenidos mediante espectrometría gamma para la medida de la radiactividad ambiental en tiempo real

Tesis Doctoral

Elena Prieto Butillé

Dirigida por: Dr. Marçal Salvadó Artells y Dr. Ramon Casanovas Alegre

Unitat de Física Mèdica, Departament de Ciències Mèdiques Bàsiques

UNIVERSITAT
ROVIRA i VIRGILI

Reus

Junio de 2017

UNIVERSITAT ROVIRA I VIRGILI
ADECUACIÓN Y DESARROLLO DE MÉTODOS DE ANÁLISIS DE DATOS OBTENIDOS MEDIANTE ESPECTROMETRÍA GAMMA PARA LA MEDIDA DE LA RADIACTIVIDAD AMBIENTAL EN TIEMPO REAL
Elena Prieto Butillé

UNIVERSITAT
ROVIRA i VIRGILI

HAGO CONSTAR que el presente trabajo, titulado "**Adecuación y desarrollo de métodos de análisis de datos obtenidos mediante espectrometría gamma para la medida de la radiactividad ambiental en tiempo real**", que presenta Elena Prieto Butillé para la obtención del título de Doctor, ha sido realizado bajo mi dirección en el Departamento Ciencias Médicas Básicas de esta universidad.

Reus, 1 de Junio de 2017

Los directores de la Tesis Doctoral

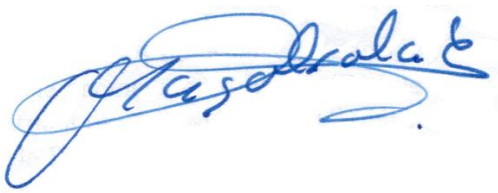

Dr. Marçal Salvadó Artells

Dr. Ramon Casanovas Alegre

UNIVERSITAT ROVIRA I VIRGILI
ADECUACIÓN Y DESARROLLO DE MÉTODOS DE ANÁLISIS DE DATOS OBTENIDOS MEDIANTE ESPECTROMETRÍA GAMMA PARA LA MEDIDA DE LA RADIACTIVIDAD AMBIENTAL EN TIEMPO REAL
Elena Prieto Butillé

Als meus pares

UNIVERSITAT ROVIRA I VIRGILI
ADECUACIÓN Y DESARROLLO DE MÉTODOS DE ANÁLISIS DE DATOS OBTENIDOS MEDIANTE ESPECTROMETRÍA GAMMA PARA LA MEDIDA DE LA RADIACTIVIDAD AMBIENTAL EN TIEMPO REAL
Elena Prieto Butillé

Agradecimientos / Agraïments

En la realització d'aquesta tesi hi han intervingut vàries persones directa o indirectament a les quals m'agradaria agrair la seva aportació.

En primer lloc, vull donar les gràcies al director de la tesi i cap de la Unitat de Física Mèdica, el Dr. Marçal Salvadó. Moltes gràcies per haver-me donat la oportunitat d'incorporar-me al projecte de les Xarxes de Vigilància Radiològica Ambiental de la Generalitat de Catalunya. Gràcies per estar al capdavant del projecte i abastar totes les vessants que se'n deriven, des de la gestió, la part tecnològica, la informàtica i, sobretot, l'anàlisi de dades. Per tenir i aportar sempre noves idees per poder fer proves i estudis en aquest camp. I, sobretot, m'agradaria destacar tota l'ajuda i la dedicació que m'ha proporcionat en els últims mesos per tal que jo pogués finalitzar els articles i la tesi. Gràcies també per haver-me fet professora associada de la URV. En la vessant més personal, m'agradaria agrair la flexibilitat i el suport que m'ha donat per compaginar la tesi amb el naixement de la meva filla i el meu actual segon embaràs.

Voldria agrair molt especialment al Dr. Ramon Casanovas, co-director de la tesi, la seva gran aportació al projecte de les Xarxes i sobretot gràcies per haver-me acompanyat i guiat des del principi, sempre amb entusiasme i paciència. Va ser un molt bon exemple a seguir i espero que pugui continuar vinculat al projecte de cara al futur. Encara que sabem que podem comptar amb tu, se't troba a faltar!

Gràcies al Diego Molina per ser capaç d'implementar tots els requisits i càlculs interminables als seus programes, fins i tot millorant les nostres demandes. Moltes gràcies per estar sempre disponible i obert a ajudar-me immediatament amb qualsevol problema que sorgís.

Al Sr. Enric Batalla, cap del Servei de Coordinació d'Activitats Radioactives de la Generalitat de Catalunya: moltes gràcies per comptar amb la Unitat de Física Mèdica de la URV per l'anàlisi de dades i també per apostar fort per la investigació en vigilància ambiental en temps real basada en l'espectrometria gamma i la seva implementació a Catalunya.

Al Sr. Miguel López, antic cap de la Unitat de Física Mèdica. Encara que no vam coincidir treballant a la facultat, m'agradaria agrair-li tota la feina feta per tal que la Unitat pogués optar al projecte de les Xarxes.

A la Maria Cros, companya de feina i amiga. Gràcies per tot, perquè parlar amb tu és molt fàcil i els dies de feina són molt millors quan hi som les dues. Ah, i sobretot gràcies perquè aquestes últimes setmanes m'has aguantat i ajudat molt amb tots els tràmits de la tesi.

A la Irene Hernández. Irene, sense tu estar dos (o tres?) anys a la cova hagués sigut insuportable! M'alegro que hagis pogut trobar una feina que t'ompli, llàstima que hagis hagut de marxar tant lluny. Gràcies per haver-me ajudat sempre que ho necessitava.

Molt especialment m'agradaria agrair als meus pares, a qui dedico aquesta tesi, tot l'esforç, el suport i l'ajuda que m'han donat per a poder arribar fins aquí. Per totes les fronteres que han creuat per acompanyar-me i per haver-me animat sempre a seguir el meu propi camí. Gràcies per tot, per estimar-me sempre. Sóc molt afortunada perquè sé que sempre puc comptar amb vosaltres i que sempre esteu pendents de mi. Mai us podré agrair suficientment tot el que heu fet per mi.

A les meves germanes, Rosa i Cutxi, gràcies per animar-me, ajudar-me i aconsellar-me. Gràcies per ser les meves amigues i tenir la vostra confiança i suport. A tu també Marco, per ser el "sorello" des de que et vaig conèixer en aquell viatge de final de curs a Itàlia. A les nebodes: Livia, Chiara i Bianca. L'alegria que aporteu a la família és incomparable! la Plànan us estima molt.

A tota la família política: gràcies a la meva sogra Maria Rosa per rebre'm a casa seva i a la seva família, escoltar-me i sempre animar-me. Als meus cunyats i nebots, gràcies per ser tan generosos amb nosaltres.

Al Lorenzo, company, amic i marit. Gràcies per creure més en mi que jo mateixa, animar-me a treure el millor de mi i estar sempre disposat a ajudar-me. Gràcies per fer-me costat en les meves decisions i fer que també siguin teves.

Finalment, m'agradaria donar unes gràcies molt especials. Gràcies Giulia, per ser el millor que m'ha passat a la vida. Per fer que, per tu, vulgui ser millor persona. Per omplir de felicitat cada dia i donar sentit a aquest món. Per la teva alegria, simpatia, espontaneïtat, curiositat. Per ser trapella i divertida i deixar-me reviure moments que tenia oblidats. Perquè gràcies a tu m'he adonat de tot el què és una mare. "La mami t'estima infinit".

Listado de contribuciones

Artículos de la tesis

Esta tesis se basa en los artículos científicos siguientes, a los que se hará referencia en números romanos en el cuerpo central del texto.

[I] E. Prieto, R. Casanovas y M. Salvadó, "Calibration and performance of a real-time gamma-ray spectrometry water monitor using a $LaBr_3$(Ce) detector," Enviado a una revista indexada en Mayo de 2017.

[II] R. Casanovas, E. Prieto y M. Salvadó, "Calculation of the ambient dose equivalent H*(10) from gamma-ray spectra obtained with scintillation detectors," *Appl. Radiat. Isot.*, 2016. vol. 118, pp. 154–159, 2016.

[III] E. Prieto, R. Casanovas y M. Salvadó, "Spectral windows analysis method for monitoring anthropogenic radionuclides in real-time environmental gamma-ray scintillation spectrometry," Enviado a una revista indexada en Junio de 2017.

Presentaciones y comunicaciones a congresos

Investigaciones previas y relacionadas con esta tesis se han presentado en distintos congresos:

- E. Prieto, R. Casanovas y M. Salvadó, "Estudio comparativo del equivalente de dosis ambiental H*(10) obtenido mediante diferentes tipos de detectores de radiación," en

IX Jornadas sobre el control de la radiactividad ambiental. Sitges, 2016. Disponible en http://www.ub.edu/IXjcradiactividadbcn2016/wp-content/uploads/2016/07/1-6-Elena_Prieto_Calibraci%C3%B3n_H10.pdf

- E. Prieto, R. Casanovas y M. Salvadó, "Estudio de los datos obtenidos mediante espectrometría gamma en tiempo real por un monitor de agua con detectores de centelleo de NaI(Tl) y $LaBr_3$(Ce)," en *VIII Jornadas sobre el control de la radiactividad ambiental*. Huelva, 2014. Disponible en https://www.csn.es/documents/10182/914809/COE-04-07+VIII+Jornadas+sobre+calidad+en+el+control+de+la+radiactividad+ambiental+-+Huelva%2C+11%2C+12+y+13+de+junio+de+2014

- E. Prieto, R. Casanovas y M. Salvadó, "Estudio comparativo entre medidas radiológicas adquiridas mediante espectrometría gamma con cristales de NaI(Tl) y $LaBr_3$(Ce) y aquéllas obtenidas con detectores Geiger," en *39 Reunión Anual de la Sociedad Nuclear Española*. Reus, 2013.

- R. Casanovas, E. Prieto y M. Salvadó, "Calibración y estudio de las capacidades de medida de los equipos de espectrometría gamma en tiempo real desarrollados para la renovación de la red de estaciones automáticas de vigilancia radiológica ambiental de la Generalitat de Catalunya," en *39 Reunión Anual de la Sociedad Nuclear Española*. Reus, 2013.

- E. Prieto, R. Casanovas y M. Salvadó, "Método para anailzar espectros y establecer alertas tempranas en medidas de espectrometría gamma ambiental en tiempo real," en *III Congreso Conjunto de las Sociedades Españolas de Física Médica y Protección Radiológica*. Cáceres, 2013.

Resumen ejecutivo

Introducción

La Red de Vigilancia Radiológica Ambiental de la Generalitat de Catalunya está constituida por varios tipos de detectores para la medida automática en continuo y en tiempo real de la radiación ambiental. Dicha Red está formada por varias subredes según los tipos de monitores de radiación: La Red de Vigilancia General, la Red de Vigilancia alrededor de las centrales nucleares, la Red de Espectrometría y la Red de equivalente de dosis ambiental H*(10). Desde 2006, la *Unitat de Física Mèdica* de la *Universitat Rovira i Virgili* (URV) se encarga de la evaluación del significado radiológico de los datos adquiridos y de tareas de investigación dentro del proyecto de la Red de Vigilancia Radiológica Ambiental de la Generalitat de Catalunya.

La Red de Espectrometría, situada en distintos puntos de Catalunya y dentro del recinto de las centrales nucleares, consta de veintiséis equipos: monitores de medida de radiación gamma sobre filtro de papel con detectores de NaI(Tl) y $LaBr_3$(Ce), monitores de medida directa de radiación con detectores de NaI(Tl) y $LaBr_3$(Ce), monitores de medida directa sin apantallamiento de NaI(Tl) y $LaBr_3$(Ce) y dos monitores de agua de río con detector de NaI(Tl). Dada la condición experimental de la Red, para poder llevar a cabo estudios de investigación, las medidas de los dos tipos de detectores de centelleo utilizados son diferentes en algunos monitores. Así, la Red dispone de equipos con detectores de NaI(Tl) de 2”×2” y 3”×3” y detectores de $LaBr_3$(Ce) de 1”×1” y 2”×2”.

Objetivos

El objetivo principal perseguido en esta tesis es el desarrollo y la realización de distintas tareas de I+D para mejorar los procesos de análisis de datos que realiza la *Unitat de Física Mèdica* en el marco del proyecto de la Red de Espectrometría de Catalunya.

En particular, los objetivos específicos son:

1. Adecuar los espectros obtenidos por un monitor de agua de río de espectrometría gamma en tiempo real con detector de $LaBr_3(Ce)$ para el análisis espectrométrico: estabilizar espectros, calibrar el equipo en energía, resolución y eficiencia y sustraer el fondo intrínseco.

2. Analizar los datos obtenidos por el monitor de agua de río con un detector de $LaBr_3(Ce)$ durante un incremento natural y compararlos con los del monitor de agua de río con un detector de NaI(Tl) para evaluar la elección más adecuada del equipamiento en distintas situaciones.

3. Desarrollar e implementar una metodología para el cálculo del equivalente de dosis ambiental H*(10) a partir de los datos obtenidos con los monitores de la Red de Espectrometría.

4. Comparar los valores obtenidos de H*(10) a partir de datos espectrométricos con los proporcionados por la Red de equivalente de dosis ambiental H*(10), formada por contadores GM.

5. Desarrollar un método de análisis de espectros gamma mediante regiones espectrales útil para solventar el solapamiento de picos y eliminar la contribución adicional aportada por la presencia de isótopos naturales en medidas ambientales en tiempo real.

6. Aplicar el método de análisis por regiones espectrales a medidas de laboratorio para cuantificar la concentración de actividad de isótopos de interés, tanto naturales (^{214}Bi y ^{214}Pb) como artificiales (^{131}I y ^{137}Cs).

7. Comprobar que el método es adecuado para el establecimiento de alarmas automáticas asociadas a incrementos de concentración de actividad de isótopos artificiales.

Material y métodos y Resultados

Esta tesis está formada por tres artículos científicos, uno de ellos publicado y otros dos en proceso de revisión en revistas indexadas.

En la primera publicación (**[I]**), se caracteriza un monitor de agua de espectrometría gamma de centelleo con un detector de 2"×2" de $LaBr_3$(Ce) que registra espectros gamma de agua del río Ebro. Los espectros registrados carecen de significado radiológico si no se aplican métodos para la estabilización de espectros y para la calibración del monitor. Así, se realiza una calibración completa del equipo: la calibración en energía y en resolución se ha llevado a cabo experimentalmente, mientras que la eficiencia se ha determinado mediante simulaciones de Montecarlo con el código EGS5. También se proporcionan valores de la concentración de actividad mínima detectable para los isótopos ^{131}I y ^{137}Cs en distintos tiempos de integración. Finalmente, para comprobar el funcionamiento del monitor calibrado, se estudia un incremento radiológico registrado durante un episodio de lluvia y se comparan los resultados con los obtenidos por otro monitor de agua con detector de NaI(Tl).

En el artículo **[II]**, se describe la metodología del cálculo del equivalente de dosis ambiental H*(10) a partir de simulaciones de Montecarlo y su aplicación a medidas reales de espectrometría gamma tomadas con detectores de centelleo con cristales de $LaBr_3$(Ce). La medida del equivalente de dosis ambiental H*(10) con monitores automáticos de espectrometría gamma en tiempo real aporta información valiosa en tiempos de integración cortos y se presenta como una alternativa al análisis convencional por ajuste de Gaussianas. La metodología presentada comprende el cálculo de los factores de conversión de fluencia a H*(10) y un método para obtener la fluencia a partir de espectros gamma. Los resultados obtenidos en este estudio se comparan con los de un detector Geiger-Muller (GM) calibrado en H*(10). Finalmente, se calcula la concentración de actividad necesaria para producir cierto aumento de H*(10) para distintos isótopos. De este modo se pueden comparar las capacidades de detección de los detectores de espectrometría frente a los detectores GM.

El último artículo (**[III]**) propone una metodología de análisis basada en la técnica de las regiones espectrales dirigida a espectros gamma ambientales tomados en tiempo real por detectores de centelleo. El método permite la monitorización de concentraciones de actividad de isótopos naturales y artificiales, como el ^{137}Cs y ^{131}I, ya que elimina la dispersión Compton (y otras contribuciones) y solventa el solapamiento de picos dentro de las regiones espectrales. Se presentan concentraciones de actividad de ^{137}Cs, ^{131}I, ^{214}Bi y ^{214}Pb obtenidas aplicando el método particularizado para un monitor de medida directa con detector de $LaBr_3$(Ce).

Conclusiones

Los estudios presentados en el cuerpo central de esta tesis hacen referencia a distintas aportaciones que la *Unitat de Física Mèdica* de la URV ha realizado para la evaluación del significado radiológico de los datos adquiridos y en tareas de investigación en el marco del proyecto de la Red de Vigilancia Radiológica Ambiental de la Generalitat de Catalunya.

Las principales conclusiones alcanzadas en la realización de los diferentes estudios que ha abordado este trabajo son:

- Se han adecuado los espectros registrados por un monitor de agua de río con detector de $LaBr_3$(Ce) para el análisis espectrométrico, aplicando metodologías para la estabilización de espectros y la calibración del equipo en energía, resolución y eficiencia.

- Se ha comparado su funcionamiento con otro monitor de agua de río con detector de NaI(Tl) durante un episodio de lluvia. La concentración de actividad calculada para el ^{214}Bi ha dado un resultado equiparable con ambos monitores.

- Debido a la gran dispersión de las medidas de fondo, aportada por el valor elevado del fondo intrínseco, el monitor de agua de río con detector de $LaBr_3$(Ce) requiere un incremento de cps mucho mayor que el monitor de NaI(Tl) para superar el criterio de discriminación de análisis de espectros establecido en la Red.

- Se ha desarrollado una metodología para el cálculo del equivalente de dosis ambiental H*(10) en monitores de espectrometría gamma en tiempo real con

detectores de centelleo que puede ser aplicada a todos los tipos de detectores de espectrometría, a distintas geometrías, materiales y rango de energías gamma.

- Se ha aplicado la metodología a un monitor con detector de $LaBr_3(Ce)$ y se han comparado los valores obtenidos de H*(10) con los proporcionados por un contador GM calibrado. Además, se han calculado las concentraciones de actividad necesarias para producir cierto incremento del equivalente de dosis ambiental H*(10).

- Se ha desarrollado un método de análisis por regiones espectrales para la monitorización de la concentración de actividad de isótopos artificiales en medidas ambientales de espectrometría gamma en tiempo real tomadas con detectores de centelleo.

- En cada región espectral, el método sustrae las contribuciones externas que sobreestiman la concentración de actividad de un cierto isótopo, como la dispersión Compton de la radiación natural o las cuentas provenientes de otras emisiones gamma cercanas.

- Se ha ajustado el método a un monitor de medida directa con detector de $LaBr_3(Ce)$, para evitar los falsos positivos de ^{137}Cs y ^{131}I en espectros de fondo y espectros con una notable presencia de descendientes del ^{222}Rn. En espectros registrados con fuentes de ^{137}Cs y ^{131}I, la metodología obtiene un valor de concentración de actividad equiparable con el obtenido por un programa comercial de ajuste de Gaussianas.

ÍNDICE

1. Introducción

1.1 Justificación

El Artículo 36 del Tratado Euratom (Comunidad Europea de la Energía Atómica) [1] insta a los Estados Miembros de la Unión a informar a la Comisión Europea, de manera periódica y constante, sobre los niveles de radioactividad al que está expuesta la población. Los Estándares Básicos de Seguridad de la Comisión requieren una monitorización de dichos niveles en aire, agua y suelo, así como en muestras biológicas (productos alimenticios) [2]. También requieren una monitorización de la tasa de dosis ambiental para poder cuantificar la exposición externa de la población.

En España, el Consejo de Seguridad Nuclear (CSN) es el organismo competente en materia de seguridad nuclear y protección radiológica. Su misión es la protección de los trabajadores, el público y el ambiente de los efectos dañinos de las radiaciones ionizantes. Para cumplir con el Tratado Euratom, el CSN gestiona una red de ámbito nacional formada por estaciones automáticas y de muestreo, llamada Red de Vigilancia Radiológica Ambiental (REVIRA). Las estaciones automáticas (Red de Estaciones Automáticas – REA) miden en continuo variables radiológicas (tasa de dosis gamma, concentración de radón, radioyodos, emisores alfa y beta en aire) y variables meteorológicas (temperatura, humedad relativa, dirección y velocidad del viento, precipitación y presión atmosférica) mientras que la vigilancia de muestreo (Red de Estaciones de Muestreo - REM) consiste en realizar medidas de la radiactividad en suelos, aire, agua potable, leche y dieta tipo, agua de río y de mar en distintos puntos del territorio.

La gestión de la red REVIRA de Cataluña está encomendada al *Servei de Coordinació d'Activitats Radioactives* (SCAR) de la Generalitat de Catalunya. En el caso de la REA, la Generalitat dispone de redes automáticas propias para la detección de la radiactividad

ambiental en tiempo real. Desde 2006, la *Unitat de Física Mèdica* de la *Universitat Rovira i Virgili* (URV) se encarga de la evaluación del significado radiológico de los datos adquiridos y de tareas de investigación en la Red de Vigilancia Radiológica Ambiental de la Generalitat de Catalunya. Así, la Red de Vigilancia Radiológica Ambiental instalada en Catalunya está constituida por varios tipos de detectores para la medida automática en continuo y en tiempo real de la radiación ambiental. Dicha Red está formada por varias subredes según los tipos de monitores de radiación: La Red de Vigilancia General, la Red de Vigilancia alrededor de las centrales nucleares, la Red de Espectrometría y la Red de equivalente de dosis ambiental H*(10).

Inicialmente, se implantaron la Red de Vigilancia General y la Red de Vigilancia alrededor de las centrales nucleares. La Red de Vigilancia General consta de nueve equipos automáticos (Berthold BAI-9850) para la monitorización de la concentración de actividad en aire (emisores alfa y beta, tasa de dosis gamma y concentración de radón) situados alrededor del perímetro de Catalunya y en puntos estratégicos del interior, cerca de las centrales nucleares de Vandellòs y Ascó. La Red de Vigilancia alrededor de las centrales nucleares está formada por ocho monitores Geiger (Berthold LB-6500) calibrados en tasa de dosis equivalente ambiental, situados dentro y fuera del recinto de las centrales nucleares, y por dos monitores de agua de río (BertholdLB/BAI 9110) que miden la concentración total de actividad gamma en agua, colocados antes y después del paso del río Ebro por la central nuclear de Ascó.

Posteriormente, a raíz del análisis de los datos registrados durante el incidente de diciembre de 2007 catalogado como nivel 2 de la Escala Internacional de Eventos Nucleares (*INES* en sus siglas en inglés) [3], se identificó la necesidad de obtener más información radiológica [4] y se inició un trabajo de desarrollo de equipos de espectrometría con detectores de NaI(Tl) y $LaBr_3$(Ce), juntamente con la *Universitat Politècnica de Catalunya* y *Raditel Serveis i Subministraments Tecnològics S.L.* Los equipos desarrollados fueron patentados[1]

[1] Patente Nacional ES201230408 ES2425801 por "ESTACIÓN DE IDENTIFICACIÓN Y MEDIDA EN TIEMPO REAL DE LA RADIACTIVIDAD AMBIENTAL GAMMA MEDIANTE ESPECTROMETRÍA SOBRE FILTRO DE PAPEL", a nombre de UNIVERSITAT ROVIRA I VIRGILI y UNIVERSITAT POLITECNICA DE CATALUNYA

Patente Nacional ES201230236 ES2423236 por "ESTACIÓN DE IDENTIFICACIÓN Y MEDIDA EN TIEMPO REAL DE LA RADIACTIVIDAD AMBIENTAL GAMMA, MEDIANTE ESPECTROMETRÍA CON DOS CRISTALES DE CENTELLEO", a nombre de UNIVERSITAT ROVIRA I VIRGILI

y dieron lugar al nacimiento de la Red de Espectrometría. Así, la Red de Espectrometría, situada en distintos puntos de Catalunya y dentro del recinto de las centrales nucleares, consta de veintiséis equipos: monitores de medida de radiación gamma sobre filtro de papel con detectores de NaI(Tl) y $LaBr_3$(Ce) [5], monitores de medida directa de radiación con detectores de NaI(Tl) y $LaBr_3$(Ce) [6], monitores de medida directa sin apantallamiento de NaI(Tl) y $LaBr_3$(Ce) y dos monitores de agua de río con detector de NaI(Tl) [7], que sustituyeron a los monitores de agua de la Red de Vigilancia General (ver Figura 1). Dada la condición experimental de la Red, para poder llevar a cabo estudios de investigación, las medidas de los dos tipos de detectores de centelleo utilizados son diferentes en algunos monitores. Así, la Red dispone de equipos con detectores de NaI(Tl) de 2”×2” y 3”×3” y detectores de $LaBr_3$(Ce) de 1”×1” y 2”×2”.

a)

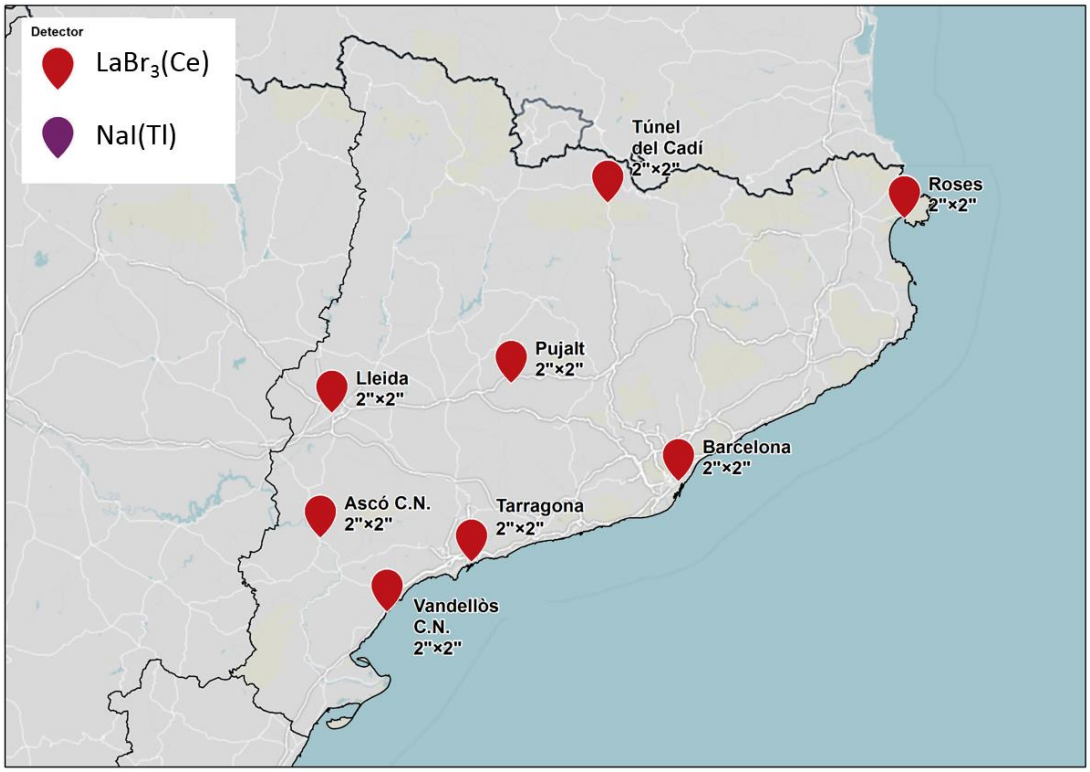

b)

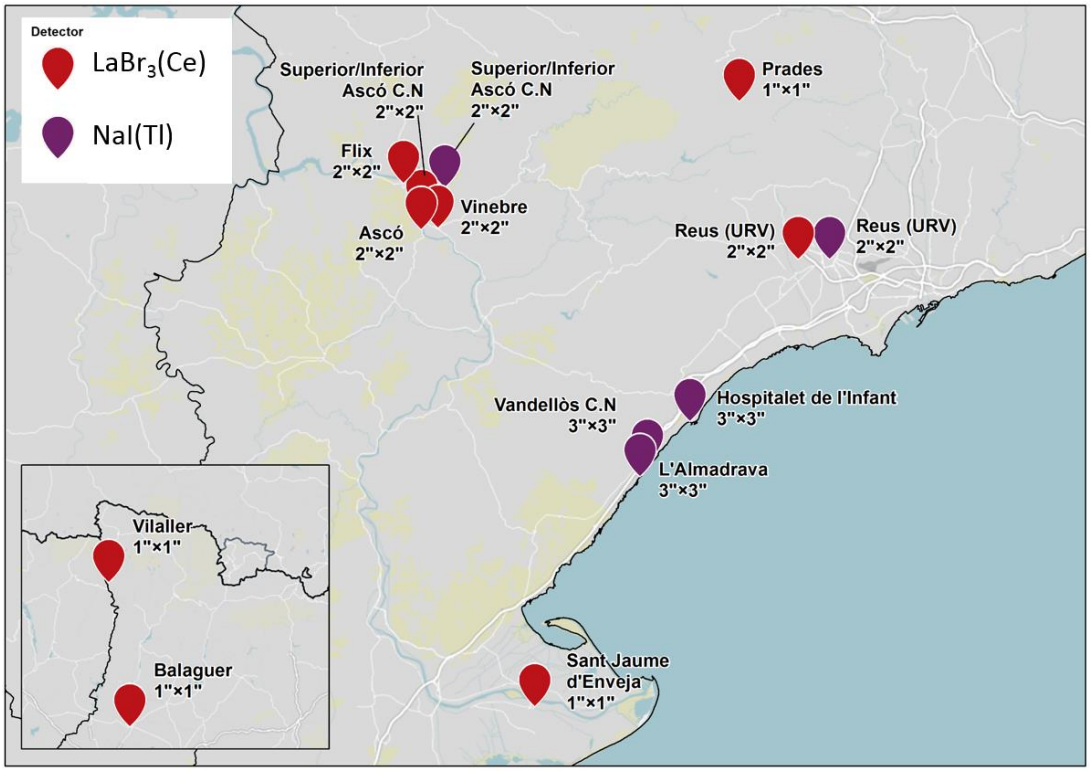

c)

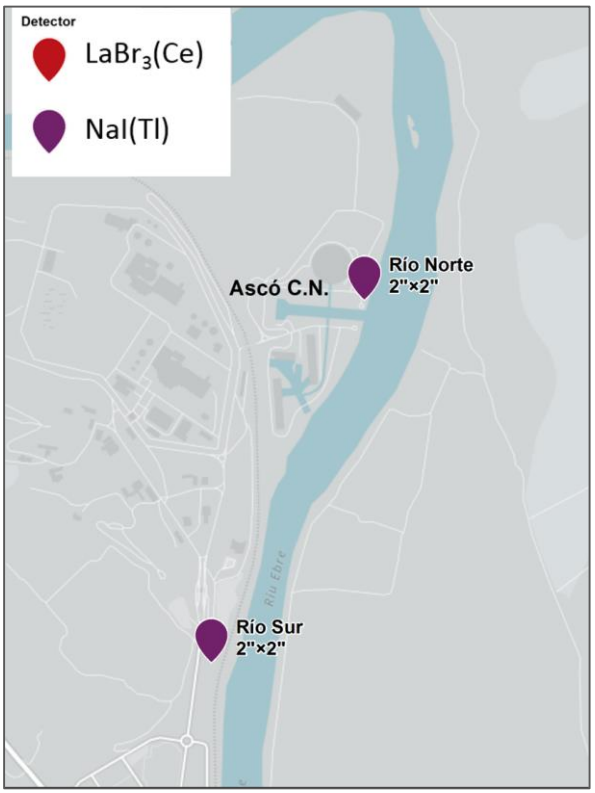

Figura 1. Localización de los monitores de medida de radiación gamma sobre filtro de papel (a), monitores de medida directa con y sin apantallamiento (b) y monitores de agua de río (c).

Finalmente, se instaló la Red de dosis equivalente ambiental H*(10) compuesta por seis estaciones con sondas Geiger Intelligent Gamma Probe IGS421-H de la compañía alemana Envinet GmbH (Technidata) calibradas en H*(10) y situadas en distintos lugares de la geografía catalana, uno de ellos dentro del recinto de la central nuclear de Ascó.

Todas las estaciones de la Red se acompañan de una estación meteorológica que registra diversas variables meteorológicas: lluvia, tasa de lluvia, presión atmosférica, temperatura exterior, temperatura exterior máxima, temperatura mínima exterior, temperatura interior, humedad relativa exterior, humedad relativa interior, velocidad del viento, velocidad del viento máxima, dirección del viento, dirección predominante del viento, distancia recorrida por el viento, irradiación solar, irradiación solar máxima, energía solar, punto de rocío y temperatura de bochorno.

Además de los monitores de radiación mencionados, la *Unitat de Física Mèdica* dispone de equipamiento de laboratorio para hacer estudios y pruebas que después pueden implantarse en los equipos de la Red situados en campo. Los detectores de espectrometría gamma de centelleo utilizados en el laboratorio son un detector de NaI(Tl) de 2”×2” y otro de $LaBr_3$(Ce) de 2”×2”. El detector de NaI(Tl) es el Modelo 905-3 de ORTEC®, y el detector de $LaBr_3$(Ce) un BrilLanCe™380 de Saint-Gobain Crystals. El analizador multicanal al que se conectan los detectores de centelleo es un analizador multicanal digital (ORTEC® digiBASE™) de 2000 canales que se conecta directamente a un puerto USB o por Ethernet. También se dispone de una sonda Geiger Intelligent Gamma Probe IGS421-H de Envinet GmbH (Technidata) y un contador proporcional RS04L de BITT Technology (modelo NPGD 02), ambos calibrados en equivalente de dosis ambiental H*(10).

Los datos registrados por los distintos tipos de monitores de radiación y las sondas meteorológicas de la Red tienen un tiempo de integración de 10 min para obtener información en tiempo real, aunque los equipos de laboratorio se han utilizado para realizar pruebas con tiempos de integración mucho más cortos, de hasta 30 s. Los detectores de espectrometría del laboratorio han sido adaptados para la medida portátil que ha demostrado ser útil para la adecuación de parámetros de adquisición y la comparación con los equipos en campo.

1.2 Adecuación de datos espectrométricos

1.2.1 Intervención en equipos

Una parte fundamental del análisis de datos obtenidos en espectrometría gamma de centelleo recae en la manipulación de los equipos para variar y ajustar los espectros gamma obtenidos a las necesidades que se deseen satisfacer en cada situación. Así, a parte de la elección del tipo de cristal de centelleo, se modifican parámetros de adquisición relacionados con la forma del pulso a través de las opciones del analizador multicanal digital, que en los monitores de la Red de Espectrometría es un ORTEC® digiBASE de 1000 canales. Los parámetros que afectan a la forma final del espectro obtenido son el alto voltaje, la ganancia, el tiempo de subida (*risetime*), la puerta (*gate*), el *flattop* y el modo apilado (*pile-up mode)*.

Aun así, los espectros obtenidos no aportan información radiológicamente significativa hasta que se someten a varios procesos de adecuación: la estabilización de espectros y la calibración en energía, en resolución y en eficiencia.

1.2.2 Estabilización de espectros

El proceso de estabilización corrige la deriva de picos y la distorsión de espectros causada por cambios en la ganancia provocados por variaciones en las condiciones de medida en la electrónica del equipo, causados principalmente por cambios de temperatura. En los equipos situados en campo, los cambios de temperatura diarios y estacionales originan grandes diferencias entre espectros registrados por un mismo monitor. El método utilizado en este estudio consiste en identificar un pico de referencia y asignarle una posición en el espectro. El resto del espectro se ubica de manera proporcional a la posición del pico de referencia [8]. Así, una vez han sido estabilizados, todos los espectros presentan los distintos fotopicos en los mismos canales. Este método ha demostrado ser adecuado para los distintos tipos de monitores en campo.

1.2.3 Calibración en energía, resolución y eficiencia

El uso adecuado de detectores de radiación conlleva la calibración de los mismos. En el caso de los detectores de centello para espectrometría gamma, el proceso de calibración se lleva a cabo en tres partes: calibración en energía, calibración en resolución y calibración en eficiencia. Así, la calibración en energía asigna valores de energía al rango de canales del

analizador multicanal; la calibración en resolución contempla las diversas anchuras de picos debidas a la respuesta no proporcional de los distintos cristales centelladores; y, por último, la calibración en eficiencia relaciona el número de cuentas debajo de un pico de un isótopo determinado con su concentración de actividad. En este estudio, las calibraciones en energía y resolución utilizadas han sido determinadas experimentalmente con fuentes radiactivas de test. Ambas calibraciones se han ajustado a polinomios de 2º grado. La calibración en eficiencia ha sido determinada por métodos de Montecarlo con un programa de simulación validado basado en el código EGS5 [9].

1.2.4 Sustracción del fondo

Opcionalmente, existe la posibilidad de mejorar el análisis de datos para la detección de isótopos sustrayendo las cuentas del espectro correspondientes al propio detector (fondo intrínseco) o al valor mínimo constante de la localización del detector (fondo natural). En el caso de los monitores de $LaBr_3(Ce)$, la sustracción del fondo intrínseco puede ser beneficiosa debido a la propia contaminación interna del cristal centellador por la presencia de ^{138}La y ^{227}Ac. En los espectros obtenidos con este tipo de detectores se observa típicamente un pico a 1468 keV que corresponde con la emisión gamma de 1436 keV del ^{138}La en coincidencia con una emisión de rayos-X, la emisión gamma de 789 keV en coincidencia con una partícula beta y los picos asociados a los decaimientos alfa del ^{227}Ac en la región de 1850-3000 keV [10]. En la Figura 2 se observan los picos típicos mencionados en dos fondos intrínsecos de $LaBr_3(Ce)$: uno corresponde a un cristal de 1"×1" y el otro de 2"×2" [11].

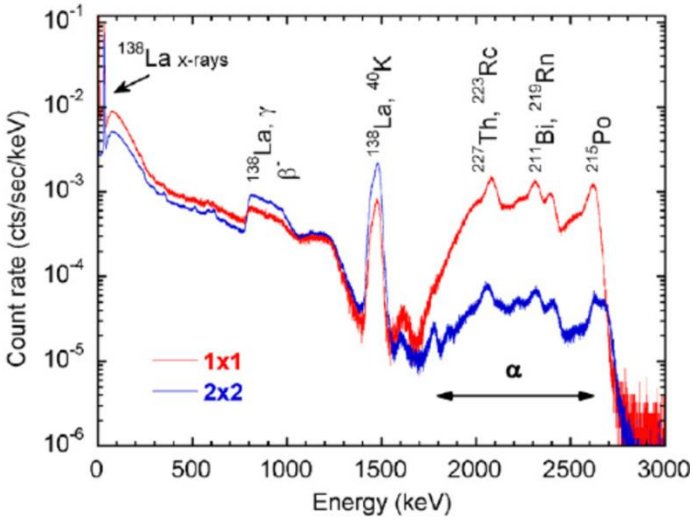

Figura 2. Espectro intrínseco de dos cristales de $LaBr_3(Ce)$. En rojo, un cristal de 1"×1" y, en azul, otro cristal de 2"×2". En el estudio de Quarati et al. [11] se observa que, al aumentar el tamaño del

cristal, la marca comercial Saint Gobain Crystals® mejoró el proceso de fabricación y disminuyó la contaminación interna de ^{227}Ac en la región de altas energías.

En este estudio, los procesos para la adecuación de espectros gamma se aplican a un monitor de agua de río de espectrometría gamma con cristal de $LaBr_3(Ce)$. Teniendo en cuenta que los monitores de agua de la Red funcionan con detectores de NaI(Tl), se llevó a cabo una investigación para analizar el funcionamiento de uno de los monitores de agua con un detector de $LaBr_3(Ce)$. Después de aplicar los procesos de adecuación, las medidas registradas durante un incremento radiológico se compararon con las obtenidas por el monitor con detector de NaI(Tl).

1.3 Análisis de datos espectrométricos

1.3.1 Análisis de espectros

La técnica más extendida para el análisis de espectros gamma tomados con detectores de centelleo es el ajuste de Gaussianas, que consiste en determinar el área debajo de un pico para poder obtener un valor de la concentración de actividad asociada al isótopo estudiado. Sin embargo, existen otros métodos para evaluar la presencia de isótopos, naturales o artificiales, en espectros registrados en tiempo real que permiten obtener una estimación global de la radiación total detectada o bien un valor de concentración de actividad de los isótopos que se quieren analizar. Estos métodos, que se presentan en este estudio para ser aplicados de manera automática, son el cálculo de la dosis equivalente ambiental H*(10) y el análisis de espectros mediante regiones espectrales o Regiones De Interés (*Region of Interest*, ROI en sus siglas en inglés).

1.3.2 Cálculo del equivalente de dosis ambiental H*(10)

Según la *International Commission on Radiological Protection* (ICRP) equivalente de dosis ambiental H*(10) se define como la energía por unidad de masa (J/kg) depositada por un campo alineado y expandido de radiación en un punto a 10 mm de profundidad de la esfera ICRU [12]. La esfera ICRU es una esfera de 30 cm de diámetro y densidad 1 g/cm^3 que está compuesta por O (76,2%), C (11,1%), H (10,1%) y N (2,6%) [13].

El equivalente de dosis ambiental H*(10) obtenido a partir de espectros gamma puede compararse con las medidas registradas por una sonda Geiger calibrada, como las instaladas en las estaciones de la Red de equivalente de dosis ambiental H*(10) de Catalunya. Para

poder estimar la tasa del equivalente de dosis ambiental H*(10) son necesarios dos elementos: los factores de conversión de fluencia de rayos gamma a H*(10) y el cálculo de la fluencia de rayos gamma a partir de los espectros. La metodología para su obtención se presenta en este estudio.

1.3.3 Análisis de espectros mediante ROIs

La vigilancia ambiental en tiempo real realizada con espectrometría gamma de centelleo comporta ciertas dificultades. La mayoría de las medidas ambientales registradas en tiempos de integración cortos (10 min) aportan bajas tasas de dosis y valores altos de ruido. En este sentido, un método útil para analizar espectros con dichas características es el método de las regiones espectrales o regiones de interés (ROIs).

El método consiste en definir varias ventanas o ROIs alrededor de las energías de las emisiones gamma de los isótopos estudiados y, considerando las contribuciones externas en dicha ROI, obtener una evolución temporal de la concentración de actividad del isótopo. Los isótopos de interés para este estudio son los isótopos artificiales más representativos de un posible vertido gaseoso procedente de una central nuclear: el ^{131}I y el ^{137}Cs. Éstos son responsables de la mayor parte de la exposición radiológica recibida por la población en caso de vertido [14]. Sin embargo, a la hora de determinar su actividad, el cálculo mediante ROIs debe tener en cuenta y sustraer las contribuciones externas a cada ROI. Dichas contribuciones son debidas al fondo intrínseco, al solapamiento de picos causado por emisiones gamma cercanas y a la contribución de fenómenos de interacción, como la dispersión Compton, proveniente de emisiones de isótopos naturales.

2. Motivación, hipótesis y objetivos

La *Unitat de Física Mèdica* de la *Universitat Rovira i Virgili* se encarga de la evaluación del significado radiológico de los datos adquiridos y de tareas de investigación dentro del proyecto de la Red de Vigilancia Radiológica Ambiental de la Generalitat de Catalunya. Estas tareas abarcan distintos aspectos. Por una parte, la *Unitat* interviene en los equipos implementando distintos parámetros, investiga con distintos detectores y realiza la puesta a punto de equipos mediante la aplicación de calibraciones. Por otra, se desarrollan métodos para el análisis de datos espectrométricos para ser implantados en la Red de Espectrometría de Catalunya y poder realizar una vigilancia automática preliminar de los valores de radiactividad del ambiente. Así, el presente estudio es un compendio de distintos procesos de investigación, desarrollo y transferencia tecnológica que la *Unitat de Física Mèdica* ha llevado a cabo para la Generalitat en el marco de la Red de Espectrometría.

Por este motivo, este trabajo se basa en la hipótesis que la espectrometría gamma puede ser aplicada en vigilancia radiológica ambiental en tiempo real para el establecimiento de alertas tempranas. Dichas alertas serían establecidas al superar ciertos niveles de concentración de actividad de los isótopos artificiales más probables de ser emitidos por una central nuclear en caso de vertido gaseoso.

Por todo lo expuesto, el objetivo principal perseguido en esta tesis es el desarrollo y la realización de distintas tareas de I+D para mejorar los procesos de análisis de datos que realiza la *Unitat de Física Mèdica* en el marco del proyecto de la Red de Espectrometría de Catalunya.

En particular, los objetivos específicos son:

1. Adecuar los espectros obtenidos por un monitor de agua de río de espectrometría gamma en tiempo real con detector de $LaBr_3(Ce)$ para el análisis espectrométrico:

estabilizar espectros, calibrar el equipo en energía, resolución y eficiencia y sustraer el fondo intrínseco.

2. Analizar los datos obtenidos por el monitor de agua de río con un detector de $LaBr_3$(Ce) durante un incremento natural y compararlos con los del monitor de agua de río con un detector de NaI(Tl) para evaluar la elección más adecuada del equipamiento en distintas situaciones.

3. Desarrollar e implementar una metodología para el cálculo del equivalente de dosis ambiental H*(10) a partir de los datos obtenidos con los monitores de la Red de Espectrometría.

4. Comparar los valores obtenidos de H*(10) a partir de datos espectrométricos con los proporcionados por la Red de equivalente de dosis ambiental H*(10), formada por contadores GM.

5. Desarrollar un método de análisis de espectros gamma mediante regiones espectrales útil para solventar el solapamiento de picos y eliminar la contribución adicional aportada por la presencia de isótopos naturales en medidas ambientales en tiempo real.

6. Aplicar el método de análisis por regiones espectrales a medidas de laboratorio para cuantificar la concentración de actividad de isótopos de interés, tanto naturales (^{214}Bi y ^{214}Pb) como artificiales (^{131}I y ^{137}Cs).

7. Comprobar que el método es adecuado para el establecimiento de alarmas automáticas asociadas a incrementos de concentración de actividad de isótopos artificiales.

3. Material y métodos y Resultados

Esta sección está formada por tres artículos científicos, uno de ellos publicado y otros dos en proceso de revisión en revistas indexadas. Los artículos se ordenan según su contenido para seguir los objetivos especificados en la Sección 2. Cada artículo será referenciado con números romanos en el texto.

[I] E. Prieto, R. Casanovas y M. Salvadó, "Calibration and performance of a real-time gamma-ray spectrometry water monitor using a $LaBr_3$(Ce) detector," Enviado para su publicación.

[II] R. Casanovas, E. Prieto y M. Salvadó, "Calculation of the ambient dose equivalent H*(10) from gamma-ray spectra obtained with scintillation detectors," Applied Radiation and Isotopes, vol. 118, pp. 154–159, 2016.

[III] E. Prieto, R. Casanovas y M. Salvadó, "Spectral windows analysis method for monitoring anthropogenic radionuclides in real-time environmental gamma-ray scintillation spectrometry," Enviado para su publicación.

3.1 Calibración y puesta a punto de un monitor de agua de espectrometría gamma en tiempo real con detector de $LaBr_3$(Ce)

[I] E. Prieto, R. Casanovas and M. Salvadó.

Calibration and performance of a real-time gamma-ray spectrometry water monitor using a $LaBr_3$(Ce) detector.

(Enviado para su publicación)

Resumen

En este estudio se caracteriza un monitor de agua de espectrometría gamma de centelleo con un detector de 2"×2" de $LaBr_3$(Ce). Este monitor registra espectros gamma de agua de río. La calibración en energía y en resolución se ha llevado a cabo experimentalmente, mientras que la eficiencia se ha determinado mediante simulaciones de Montecarlo con el código EGS5. Se han calculado valores de concentración de actividad mínima detectable para los isótopos ^{131}I y ^{137}Cs en distintos tiempos de integración. Para comprobar el funcionamiento del monitor calibrado, se estudia un incremento radiológico registrado durante un episodio de lluvia.

Abstract

A scintillation gamma-ray spectrometry water monitor with a 2"×2" $LaBr_3$(Ce) detector was characterized in this study. This monitor measures gamma-ray spectra of river water. Energy and resolution calibrations were performed experimentally, whereas the detector efficiency was determined using Monte Carlo simulations with EGS5 code system. Values of the minimum detectable activity concentrations for ^{131}I and ^{137}Cs were calculated for different integration times. As an example of the monitor performance after calibration, a radiological increment during a rainfall episode was studied.

Calibration and performance of a real-time gamma-ray spectrometry water monitor using a $LaBr_3$(Ce) detector

E. Prieto[1], R. Casanovas[1] and M. Salvadó[1].

[1] Unitat de Física Mèdica, Facultat de Medicina i Ciències de la Salut, Universitat Rovira i Virgili, ES-43201 Reus (Tarragona), Spain

Abstract

A scintillation gamma-ray spectrometry water monitor with a 2"×2" $LaBr_3$(Ce) detector was characterized in this study. This monitor measures gamma-ray spectra of river water. Energy and resolution calibrations were performed experimentally, whereas the detector efficiency was determined using Monte Carlo simulations with EGS5 code system. Values of the minimum detectable activity concentrations for ^{131}I and ^{137}Cs were calculated for different integration times. As an example of the monitor performance after calibration, a radiological increment during a rainfall episode was studied.

Key words: **scintillation gamma-ray spectrometry, $LaBr_3$(Ce), Monte Carlo simulation, efficiency calculation, MDAC**

1 Introduction

Ascó nuclear power plant is located in the village of Ascó, Catalonia (ES-E, Spain-East), beside the Ebre river. The water of the river is used for cooling the two pressurised water reactors of the plant. However, this water is also used for human consumption and irrigation of agricultural crops. Therefore, a continuous radiological surveillance of the water of the Ebre river is required.

For this purpose, two real-time water gamma-ray spectrometry monitors with NaI(Tl) detectors, located before and after the river flows through Ascó nuclear power plant were improved, calibrated and tested in a previous study of our research group (Casanovas et al., 2013).

This improvement was part of a more ambitious project where the measurement capabilities of the automatic real-time surveillance network in Catalonia (ES-E, Spain-East) were enhanced using real-time gamma-ray spectrometry. For this, two other type of monitors using either NaI(Tl) or $LaBr_3$(Ce) scintillation detectors were also developed, calibrated and implemented: an aerosol monitor using a particulate filter (RARM-F) (Casanovas et al., 2014a) and a monitor using two shielded detectors measuring directly to the environment (RARM-D2) (Casanovas et al., 2014b).

The better performance of $LaBr_3$(Ce) detectors in comparison with NaI(Tl) ones has been clearly observed in both RAMR-F and RARM-D2 monitors. The advantages of $LaBr_3$(Ce) detectors for environmental monitoring have been widely studied (Toivonen et al., 2008), (Mattila et al., 2010). The better resolution of $LaBr_3$(Ce) detectors from 100 keV permits the identification of artificial photopeaks of importance for environmental monitoring that are close to natural emissions (Casanovas et al., 2014a). For example, the ^{131}I emission of 364 keV is resolved from the 352 keV peak of ^{214}Pb when spectra are obtained with $LaBr_3$(Ce) (Toivonen et al., 2008). Moreover, these

detectors present a linear energy response, good stopping power and higher light yield than NaI(Tl) detectors (Quarati et al., 2007), (Menge et al., 2007).

Hence, an improvement in the performance of the river water monitors is also expected if a $LaBr_3$(Ce) detector is used instead of a NaI(Tl) one. In fact, $LaBr_3$(Ce) detectors showed good properties when used for marine water monitoring in other studies (Su et al., 2011), (Zeng et al., 2017). In this paper, the measurement capabilities of the river water monitors when using $LaBr_3$(Ce) detectors were evaluated. The new system, where the $LaBr_3$(Ce) detector was implemented, was calibrated in energy, resolution and efficiency. Minimum detectable activity concentrations (MDAC) were calculated for ^{131}I and ^{137}Cs for different integration times.

2 Materials

2.1 Water Monitor System

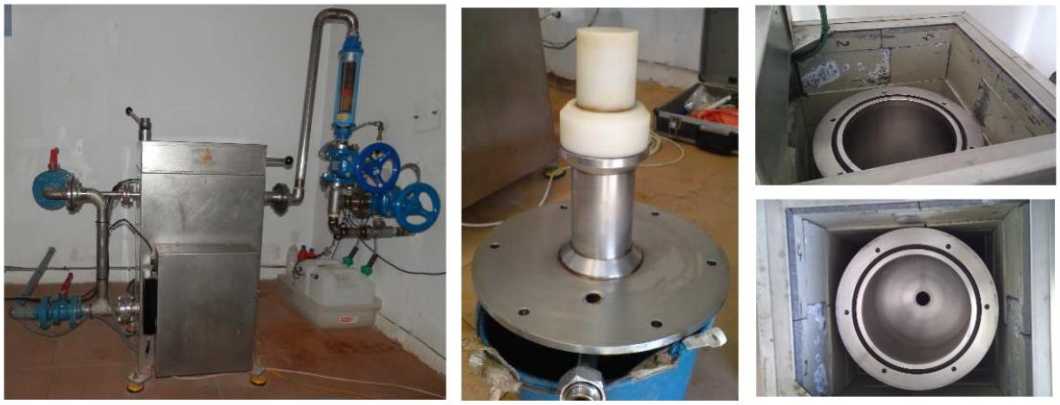

Figure 1. Water monitor (left), vessel cover with detector enclosure (middle), vessel with Pb shielding (right)

The river monitor, whose measurement capabilities using a $LaBr_3$(Ce) were tested, was the one located upstream of the nuclear power plant, known as North Ebre River Monitor. Due to regulatory issues related to the availability of the river monitors, the time dedicated to study the monitor with a $LaBr_3$(Ce) detector was limited. During the trial period, the river monitor located after the nuclear power plant (South Ebre River Monitor) continued functioning with a NaI(Tl) detector.

The monitor used in this study (see Figure 1) was a Berthold LB/BAI 9110 (Berthold Technologies GmbH & Co. KG, Germany) that was enhanced with different features in a previous study (Casanovas et al., 2013). The original NaI(Tl) detector was replaced by a 2"×2" $LaBr_3$(Ce) from Saint Gobain Crystals®. The detector was connected to a digital multichannel analyser (ORTEC® Digibase) of 1000 channels which was in turn connected to a computer. All collected data are transferred to an external server and stored in a SQL database using an ADSL connection. The system is prepared for remote control of the monitor and interaction with the server through an external computer.

The measurement process begins when the water is collected from the river by a pump. The water flows continuously through a 25 L vessel inside of which the scintillator detector is placed. The vessel and the detector are surrounded by a lead shielding to minimize the external radiation contribution. In addition, the system is connected to two 15 L water sampling recipients aimed

for posterior analysis that can be filled manually and automatically up to a selected level in case of exceeding established radiological criteria. Figure 2 shows a scheme of this process.

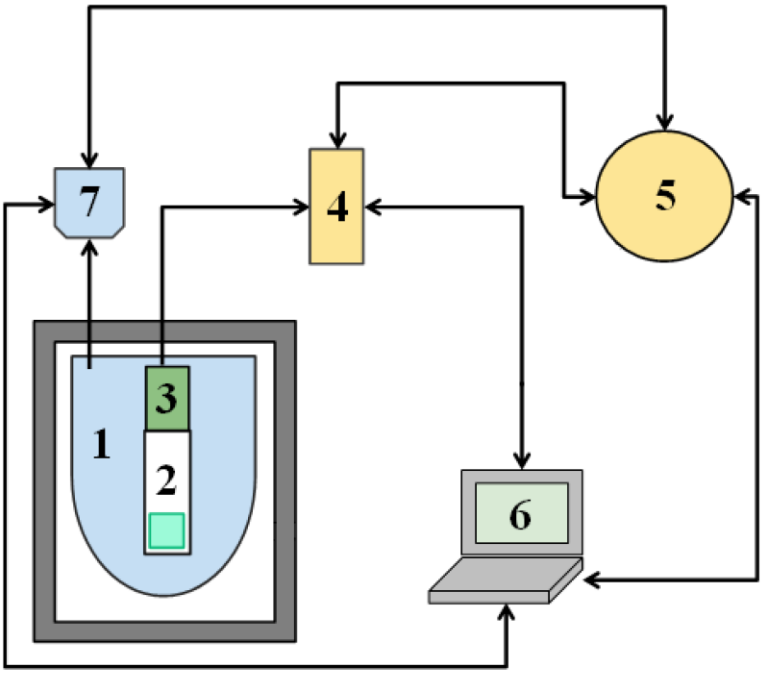

Figure 2. Scheme of the Water Monitor System. (1) vessel; (2) $LaBr_3(Ce)$ detector; (3) digital MCA, (4) local computer; (5) SQL server; (6) external computer; (7) sampling recipients.

The remote control of the system is done via TCP/IP protocol. The system is also equipped with sensors for electronic checking such as a flow meter, a detector temperature probe or a meteorological station measuring wind speed and direction, air temperature, humidity, barometric pressure, rainfall and solar radiation.

2.2 Calibration sources

For calibration purposes, different radioactive sources were used in this study. They encompassed point-sources of ^{152}Eu, ^{137}Cs and ^{60}Co, a hermetically sealed natural source of ^{226}Ra (with its corresponding ^{214}Pb and ^{214}Bi daughters) and ^{138}La emissions from the self-contamination of the detector $LaBr_3(Ce)$ crystal.

3 Methods

3.1 $LaBr_3(Ce)$ self-activity determination

The typical shape of spectra obtained with $LaBr_3(Ce)$ detectors in low count rate scenarios is due to the presence of radioactive ^{138}La and ^{227}Ac in the detector crystal (Quarati et al., 2012). For analysis purposes, it was convenient to quantify the intrinsic activity arising from the $LaBr_3(Ce)$ detector crystal in a low background environment. For that, the detector was placed inside the water monitor, which is shielded with lead, when the vessel was empty. The absence of any photopeak from natural origin was checked after an integration time of several hours.

3.2 Calibration

3.2.1 Spectra stabilisation

Prior to calibration, the spectra need to be stabilised to correct the peak positions that can be affected by water temperature variations. The stabilisation is performed by fitting two Gaussian curves to the ^{138}La double peak at 1440 keV and 1470 keV to find their position and correct the entire spectrum using the second method described in a previous study (Casanovas et al., 2012a). This process is performed automatically and stabilized spectra are stored into the database.

3.2.2 Energy and resolution calibrations

The applied calibration methodology (Casanovas et al., 2012b) was adapted to the particular characteristics of the water monitor with a $LaBr_3$(Ce) detector.

The calculation of the energy and resolution calibrations was performed using the radioactive sources described in Section 2.2. A second-degree polynomial was adjusted to obtain the energy calibration:

$$E = a_0 + a_1 \cdot C + a_2 \cdot C^2 \quad (1)$$

where C is the channel number, E is the energy and a_k are the fitting coefficients.

In order to properly analyse the obtained spectra, it is necessary to perform the resolution calibration. The resolution calibration was determined adjusting the experimental values of the Full Width at Half Maximum (FWHM) to a second-degree polynomial:

$$FWHM(E) = b_0 + b_1 \cdot E + b_2 \cdot E^2 \quad (2)$$

where $FWHM(E)$ is the Full Width at Half Maximum, E is the energy and b_k are the fitting coefficients.

However, the calculation of the FWHM in energy units cannot be simply determined applying equation (1) straightforward. The FWHM was obtained subtracting the energy value of the lower channel to the higher channel determined by Equation (1).

3.2.3 Monte Carlo simulated efficiencies

The efficiency calibration was determined using Monte Carlo (MC) simulations with the EGS5 user code that was previously validated (Casanovas et al. 2012). The information regarding the diluted radiation source, the geometry (shape and dimensions) and materials of the system (e.g. vessel, shielding, detector, detector water around the detector, etc.) was implemented into the code. Thus, a model of the monitor based on the real characteristics was simulated. The density and composition of the monitor materials were taken from Berger et al. (2005). The modelled monitor is shown in Figure 3. The simulated radiation was set at a cut-off energy of 10 keV for photons and electrons.

Each point of the efficiency curve was calculated considering a monoenergetic source in the range of 20 to 2000 keV distributed homogeneously in the water volume. The obtained spectra for the simulated monoenergetic sources were convoluted with the resolution function obtained with

Equation (2) by using the method described in a previous study (Casanovas et al. 2012). After that, the broadened spectra were used to calculate the efficiencies using the spectra analysis software ScintiVision™ from ORTEC®.

The efficiency was calculated as:

$$\varepsilon_{MC} = \frac{N_{counts}}{N_{hist}} \tag{3}$$

where N_{counts} is the number of net counts under the full energy peak and N_{hist} is the number of simulated histories (i.e. the number of primary source-particles simulated and all of the secondary particles produced by it), which was set at 10^7.

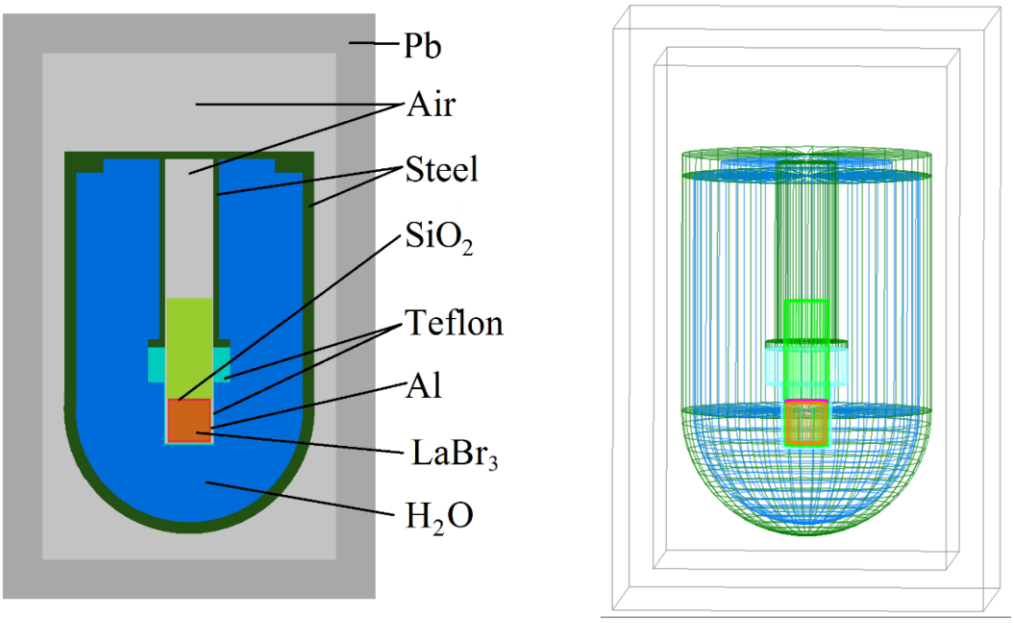

Figure 3. Implemented geometry model and materials for the MC efficiency simulation.

The efficiency calculations were fitted to the following function:

$$\log \varepsilon_V = \sum_{n=0}^{6} a_n (\log E)^n \tag{4}$$

where ε_V is the volumetric efficiency at the gamma-ray energy E and a_n represents the fitting coefficients.

3.3 Activity Concentration and Minimum Detectable Activity Concentration (MDAC)

The activity concentration (e.g. Bq L^{-1}) related to each peak can be written as:

$$a = \frac{N}{\varepsilon_V \cdot t \cdot p_\gamma} \tag{5}$$

where N is the number of counts under the peak, t the counting time, p_γ is the emission probability of the gamma-ray and $\varepsilon_V \equiv \varepsilon \cdot V$ is the volumetric efficiency, where ε is the peak-efficiency and V is the volume of the vessel, which was 25 L in this study.

The Minimum Detectable Activity Concentration corresponds to the activity measured from the detection limit, L_D. The detection limit is the minimum number of counts under a peak that one can be confident of detecting with a certain probability.

From Equation (5) the MDAC can be determined as:

$$MDAC = \frac{L_D}{\varepsilon_V \cdot t \cdot p_\gamma} \tag{6}$$

where the detection limit L_D (with a 95% confidence limit) for a certain Region of Interest (ROI) is calculated using the Currie expression for the standard deviation of the background (Currie, 1968):

$$L_D = 2.71 + 3.29\sigma_B \tag{7}$$

where σ_B is the standard deviation of the background (natural plus intrinsic) measured in counts in the considered ROI. The background and σ_B were obtained with the filled vessel during a period of low count rates from natural origin (e.g. no precipitation present).

The width of the ROI is determined by the width of the expected peak, which is proportional to the *FWHM(E)* function:

$$n = n(E) = \alpha \cdot FWHM(E) \tag{8}$$

where α is the proportionality constant to set the desired peak coverage and *FWHM(E)* is obtained using Equation (2). In this study, $\alpha = 2.548$ for a 99.73% peak area coverage.

3.4 Data analysis discrimination criterion

The spectrometry monitors of the automatic real-time surveillance network of Catalonia provide new data every 10 min. In order to simplify the analysis task, a discrimination criterion was implemented to identify suspicious spectra. The total counts per second (cps) of each registered spectrum are counted, x_i, and the value is checked to be in the following interval:

$$\mu - k\sigma \le x_i \le \mu + k\sigma \tag{9}$$

where μ is the mean value of the total cps of spectra in a long period, σ the standard deviation and k a confidence factor.

If the value fails the established criterion, especially above the interval, the spectrum is analysed in detail. This criterion is used in all types of monitors of the Catalan radiological surveillance network with the confidence factor k set at 2 (Casanovas et al., 2011).

4 Results and Discussion

4.1 Energy and resolution calibrations

During the period analysed in this study, the water temperature variations were very low. However, the applied stabilisation method corrected the relative drift of the peaks that could be affected by temperature changes.

The energy calibration was carried out using an internally developed software for fitting Gaussian peaks using the Levemberg-Marquardt algorithm. The software provides the exact centre of the Gaussian and the corresponding FWHM in channels among many other parameters.

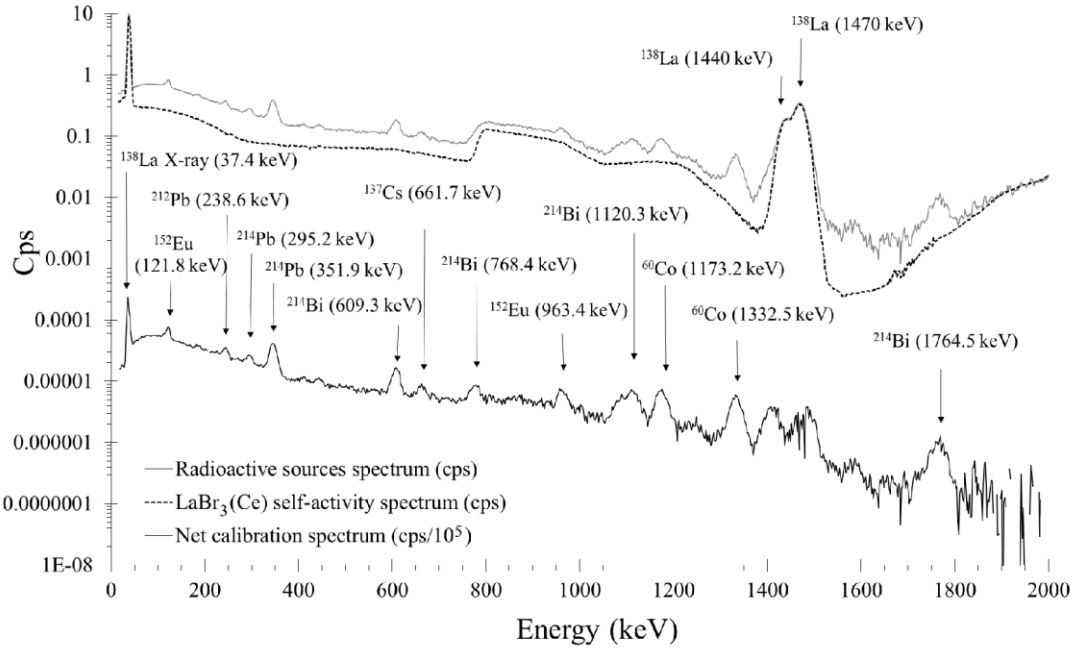

Figure 4. Spectra used for the energy calibration (black line). The Radioactive sources spectrum (grey line) and the $LaBr_3(Ce)$ self-activity spectrum (dotted line) are shown in cps, whereas the Net calibration spectrum (black line) is shown in cps/10^5 for illustrative purposes. The main peaks of the used radioactive sources are labelled.

Figure 4 shows the spectra used for the energy calibration with the main peaks used. The grey line and the dotted line correspond to the radioactive sources spectrum and to the self-activity of the detector, respectively. Both spectra are shown in cps. Below them, the net calibration spectra (black) shows the radioactive source spectrum resulting from subtracting the intrinsic activity. It is presented in cps/10^5 for illustrative purposes. It is remarkable that the two peaks from the $LaBr_3(Ce)$ self-activity at 1440 keV and 1470 keV are not well defined in the resulting net calibration spectrum. Thus, the information of the peaks position was taken from the radioactive sources spectrum and incorporated to the energy calibration. The subtraction of the detector self-activity is advantageous to distinguish hidden contributions, such as the 768.4 keV emission of ^{214}Bi, which is completely hidden by the gamma emission at 789 keV of ^{138}La and its associated beta continuum (Nicolini et al., 2007). However, this process incorporates some difficulties. For example, the temperature peak shift stabilisation and the energy calibration must be continuously checked for the acquired spectra in order to properly subtract the recorded self-activity spectra, as little variations between them could result in a misleading spectral analysis.

The energy calibration of the system is shown in Figure 5. Data used for the calibration were fitted to Equation (1) and gave a coefficient of determination of $R^2 = 0.99999$.

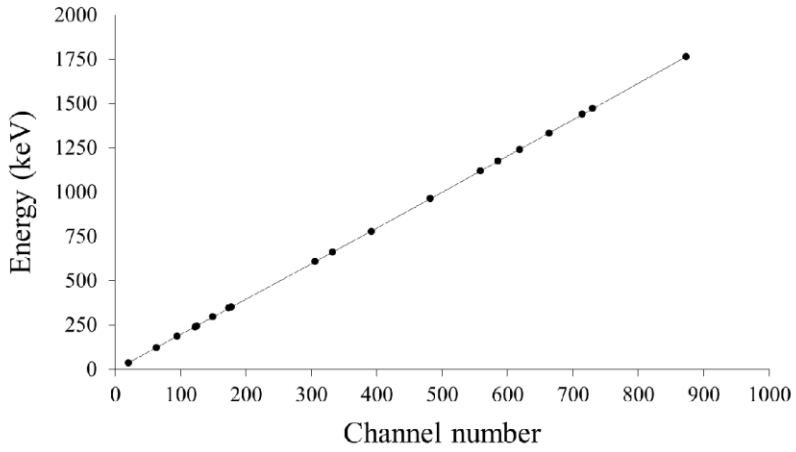

Figure 5. Energy calibration of the $LaBr_3(Ce)$ detector. The solid line corresponds to the 2nd degree polynomial fit.

By way of example, the energy value obtained for the 661.7 keV photopeak of ^{137}Cs was 660.7 keV, which represents a relative difference of 0.15%. The maximum relative difference obtained in the energy calibration was 0.9% for the 238.6 keV photopeak of ^{212}Pb giving an energy of 240.8 keV, which corresponds to a 2.2 keV deviation.

The energy resolution of the system was determined using Equation (2), which resulted in a coefficient of determination $R^2 = 0.995$. The data used for the resolution calibration are drawn in Figure 6.

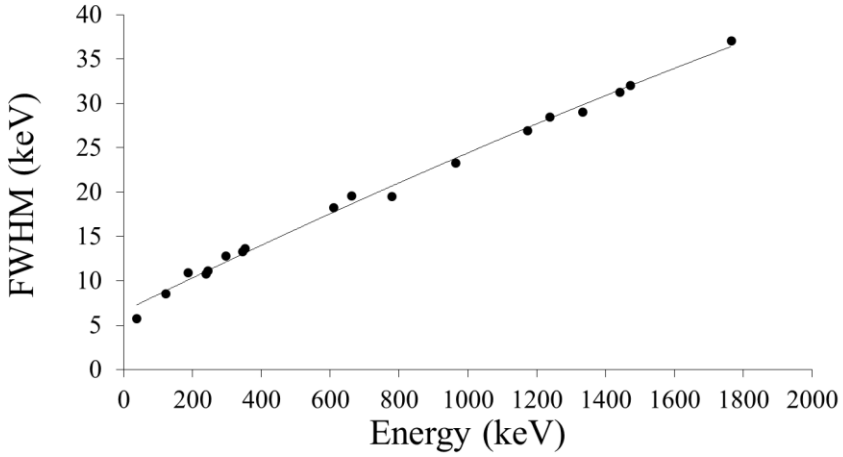

Figure 6. FWHM calibration of the $LaBr_3(Ce)$ detector. The solid line corresponds to the 2nd degree polynomial fit.

The obtained FWHM curve is adequate for its purposes and the determination of the values was precise due to the resolution of the $LaBr_3(Ce)$ detector crystal. At 661.7 keV, the FWHM obtained for ^{137}Cs is 19.6 keV, giving a resolution of 2.9%, which is similar to the value of 3% obtained for a 2"×2" $LaBr_3(Ce)$ detector (Quarati et al., 2007). In other studies, the resolution obtained for

different $LaBr_3(Ce)$ crystal sizes is also < 3%: 2.9% for a 3"×3" crystal size (Saint-Gobain Crystals, n.d.) and 2.8% for a 1.5"× 1.5" crystal size (Iltis et al., 2006).

4.2 Efficiency calculation

The efficiency curve for the $LaBr_3(Ce)$ water monitor obtained with MC simulations is drawn in Figure 7. In addition, the efficiency curve obtained for the water monitor with a NaI(Tl) detector in Casanovas et al. (2013) is shown for comparison purposes.

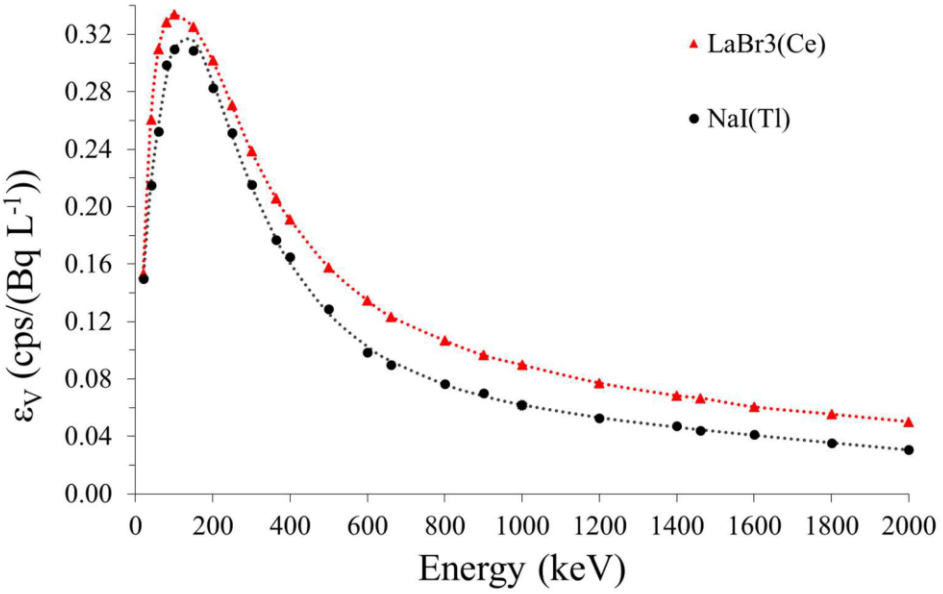

Figure 7. Efficiency curves obtained for the $LaBr_3(Ce)$ water monitor (triangles) and for the NaI(Tl) water monitor dots) calculated using MC simulations (Casanovas et al., 2013). The dotted lines correspond to the fitted curve given by equation (4).

Given that the water monitor is implemented for continuous surveillance, the water flows permanently through the shielded vessel. Therefore, it was not possible to fill the vessel with certified radioactive liquid sources and compare the simulated values with experimental results. However, the efficiency curve was obtained using an EGS5 MC user code previously validated for efficiency calculations (Casanovas et al. 2012).

The obtained values for the efficiency of $LaBr_3(Ce)$ water monitor are higher than those obtained for the NaI(Tl) water monitor in all the energetic range (Figure 7). The quotient between efficiency values, $\varepsilon_{V_{LaBr}} / \varepsilon_{V_{NaI}}$, is close to 1 for low energies (below 250 keV) and near 1.4 for medium energies (from 600 keV to 1400 keV), which is in agreement to the value of the detector densities quotient, ρ_{LaBr} / ρ_{NaI} , where ρ_{LaBr} = 5.3 g/cm^3 and ρ_{NaI} = 3.7 g/cm^3. Thus, this was used as an acceptance criteria for the calculated values, as the NaI(Tl) ones were validated experimentally.

The efficiency values given by the simulation could not be strictly compared to those obtained in other studies with $LaBr_3(Ce)$ detectors, due to the unique characteristics of the river water monitor vessel. Another study determined the efficiency for a 2"×2" sea water monitor using $LaBr_3(Ce)$ detectors (Zeng et al., 2017) where the detector was placed in the middle of a sea water cylindrical tank of Ø2.0 m × 2.3 m. The simulated results for a 2"×2" $LaBr_3(Ce)$ detector gave a volumetric

efficiency value of 0.0867 cps/(Bq L^{-1}) for ^{137}Cs (Zeng et al., 2017), which is lower that the efficiency computed in this work of 0.125 cps/(Bq L^{-1}).

4.3 MDAC

The minimum detectable activity concentrations were calculated for ^{131}I and ^{137}Cs, as these are typical isotopes that are susceptible of being released by the nuclear power plant in case of accident (Nuclear Energy Agency, 2002). MDAC values were calculated using equation (6) and are shown in Table 1. The widths of the ROI of the expected peaks were set with $\alpha = 2.548$ to obtain a 99.73% peak area coverage.

	MDAC (Bq L^{-1})	
Time	^{131}I	^{137}Cs
10 min	1.07	1.76
1 h	0.45	0.69
4 h	0.24	0.34
12 h	0.14	0.15
24 h	0.10	0.08

Table 1. MDAC values for ^{131}I and ^{137}Cs obtained for different integration times.

The self-activity of the $LaBr_3(Ce)$ detector rises the values of the MDAC compared to the ones obtained with NaI(Tl) detectors (Su et al., 2011). Note that the MDAC results are independent from the intrinsic background and are only related to the dispersion of the background values, σ_B. Given that σ_B is higher in the monitor with a $LaBr_3(Ce)$ detector, so are the calculated MDAC. By means of example, for ^{137}Cs, the MDAC calculated in the river monitor using a NaI(Tl) detector for 10 min was 0.6 Bq L^{-1}, whereas for $LaBr_3(Ce)$ is 1.76 Bq L^{-1}.

4.4 Rainfall episode spectrum analysis

An episode of rainfall occurred during the period that the $LaBr_3(Ce)$ detector was installed in the water monitor. Spectra were collected and analysed to check the calibration and the proper functioning of the monitor. Figure 8 shows the total (summed) number of counts per second (cps) of each acquired 10 min spectrum without the detector self-activity from 60 to 1980 keV (red dots) with the rain measures (blue line). The temporal coincidence of the rain with the increase of cps is clearly shown. The grey areas mark the periods that were analysed by spectrum analysis.

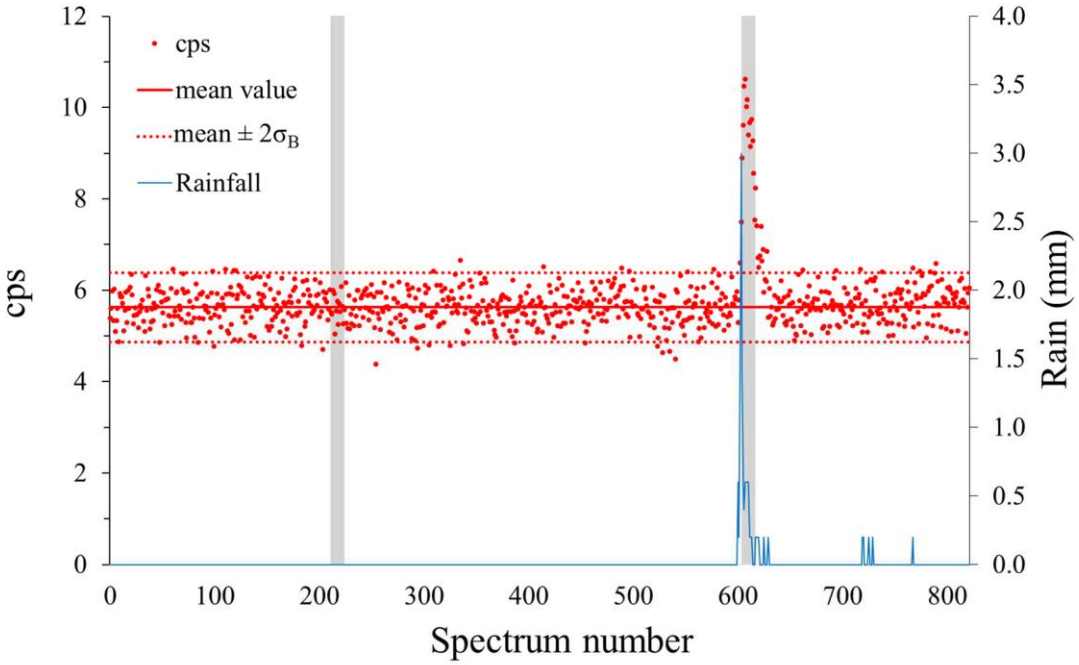

Figure 8. Radiological increments measured in cps (red dots), correlated with rainfall (blue line). The cps mean value (red line) with the statistical discrimination criterion (red dotted line) are added. The grey areas indicate the total spectra considered for the analysis, corresponding to the spectra shown in Figure 9. (For interpretation of the references to colour in this figure legend, the reader is referred to the web version of this article.)

Figure 9 shows two spectra, one obtained during rainfall (red) and another registered in a period without precipitation (black), which correspond to the areas marked in grey in Figure 8. Both spectra were obtained by summing all the 10 min spectra marked by the grey regions in Figure 8, which was equivalent to an integration time of 2 h and 10 min. The intrinsic self-activity of the detector crystal was removed in both spectra. It is worth mentioning that the shielded vessel of the water monitor attenuates a great amount of background radiation. And thus, the augments of the registered spectra with the $LaBr_3(Ce)$ detector were very close to its self-activity spectrum during all the trial period, excluding the rain episode.

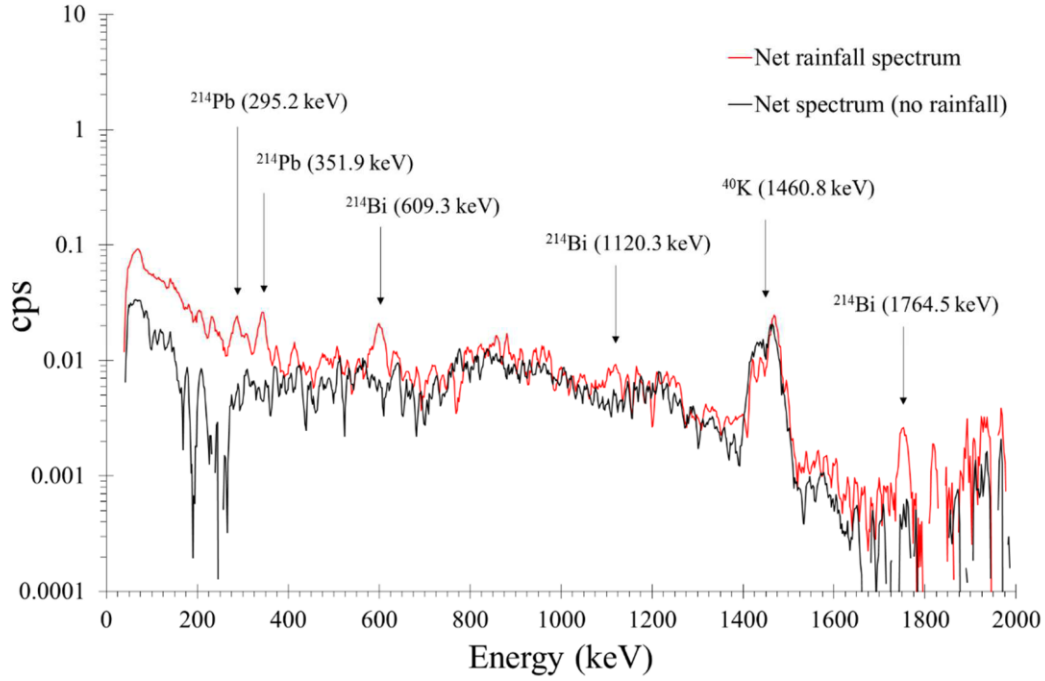

Figure 9. Rainfall spectrum without the detector self-activity (red) and background spectrum without the detector self-activity (black). Peaks of the identified isotopes are labelled. (For interpretation of the references to colour in this figure legend, the reader is referred to the web version of this article.)

In Figure 9, the peak located between 1400 and 1500 keV corresponds to the contribution from the emission of ^{40}K at 1460.8 keV, which is dissolved in the river water, plus the remains of the subtraction of the self-emission peaks of ^{138}La at 1440 keV and 1470 keV. Below 700 keV, some peaks corresponding to natural emissions can be identified, such as those from ^{214}Bi (609.3 keV, 1120.3 keV and 1764.5 keV) and ^{214}Pb (295.2 keV and 351.9 keV). The Compton contribution is remarkable below 400 keV.

The activity of ^{214}Bi was calculated using the 609.3 keV emission during the rain episode giving a value of 3.7 Bq L^{-1}. The counts under the 609.3 keV peak were determined subtracting the net spectrum from the net rain spectrum. The same activity calculation was performed for the South Ebre River Monitor with a NaI(Tl) detector for the same rain episode. The value obtained for ^{214}Bi was 3.4 Bq L^{-1}. In view of the results and attending that the efficiency calibration of the NaI(Tl) detector was validated experimentally, the efficiency calibration that was performed in this study for the $LaBr_3$(Ce) was considered to be acceptable.

4.5 Data analysis discrimination criterion

The maximum increase in cps (see Figure 8) during the rain episode for the $LaBr_3$(Ce) monitor was 10.6 cps, which corresponds with 5.0 cps over a 5.63 cps background mean value with a standard deviation σ_{LaBr} = 0.38 cps. For the NaI(Tl) monitor, the increase was of 3.5 cps over a 3.2 cps background with a standard deviation σ_{NaI} = 0.08 cps.

As the river water monitors are part of the radiological surveillance network of Catalonia, the spectra that surpass in total cps a statistical threshold are studied in detail (see Section 3.4). The spectra that are analysed in detail are those that surpass the threshold $\frac{\Delta Ncps}{2\sigma_B} > 1$, which can be fulfilled either with high cps increases or low values of σ. Considering the values presented for the two water monitors, the increase registered with both detectors exceeded the threshold, giving

$\frac{\Delta Ncps_{LaBr}}{2\sigma_{LaBr_B}} = 6.6$ and $\frac{\Delta Ncps_{NaI}}{2\sigma_{NaI_B}} = 21.9$ It should be noted that the cps variation was greater in the monitor with a $LaBr_3(Ce)$ detector than with the NaI(Tl) one, but the increment was less notable due to the major dispersion of the background values compared to the monitor with NaI(Tl). For that reason, the river water monitor with the $LaBr_3(Ce)$ detector requires of higher variations to surpass the statistical threshold established by the value of σ. Precisely, a measurement that barely passes the threshold in the NaI(Tl) monitor should be 4.7 times greater to be statistically noticed with the $LaBr_3(Ce)$ one. The higher dispersion in the background values of the monitor with the $LaBr_3(Ce)$ detector could be due to its intrinsic activity.

A similar behaviour of the two monitors is found when studying a ROI centred at the 609.3 keV emission of ^{214}Bi. In both monitors, the widths of the ROIs were determined using Equation (8) with $\alpha = 2.548$ that gives a 99.73% peak area coverage. Figure 10 shows the evolution of the ^{214}Bi ROIs of $LaBr_3(Ce)$ and NaI(Tl) before and during the rain episode.

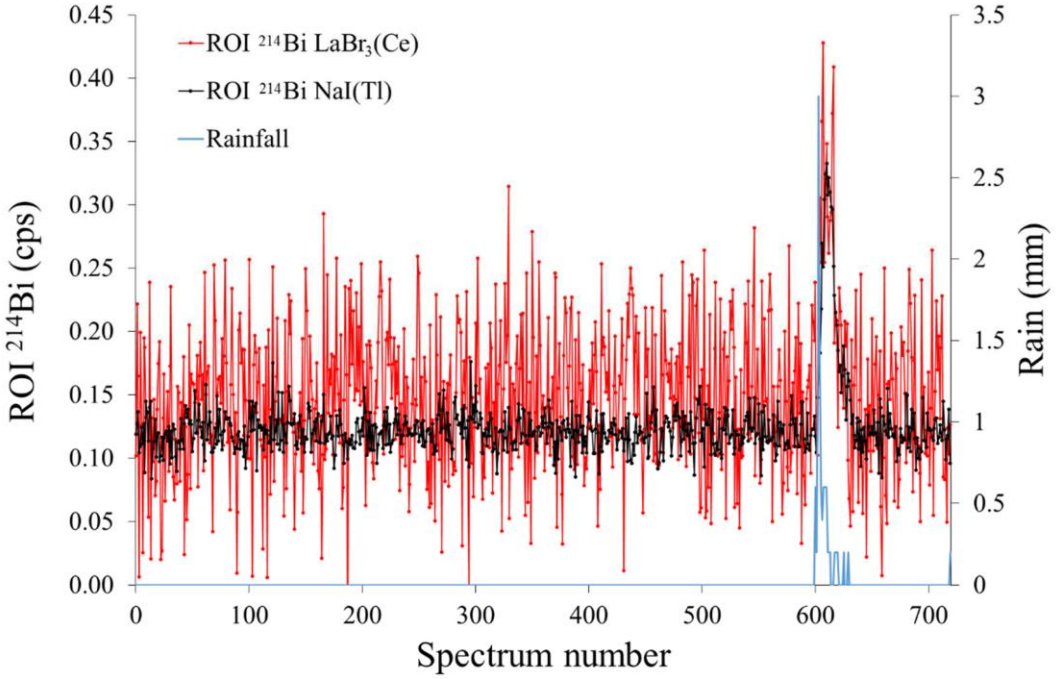

Figure 10. Cps registered in the ^{214}Bi ROI of the $LaBr_3(Ce)$ monitor (red) without its intrinsic background and NaI(Tl) ^{214}Bi ROI (black), correlated with rainfall (blue line). (For interpretation of the references to colour in this figure legend, the reader is referred to the web version of this article.)

Table 2 shows the registered values of the ROIs drawn in Figure 10 during the rain episode along with the associated increment and threshold criterion for a 10 min integration time. Additionally, values for the monitor with a NaI(Tl) detector are given in the same energetic range as the $LaBr_3(Ce)$ monitor ROI. This narrower NaI(Tl) ROI would avoid possible counts from ^{137}Cs that could be included in the wider NaI(Tl) ROI due the lower resolution of the NaI(Tl) crystal.

	ROI range		Background (no rain)		Maximum value (rain episode)	Increment	
	E_{min} (keV)	E_{max} (keV)	μ_B	σ_B	N_{cps}	ΔN_{cps}	$\Delta N_{cps}/2\sigma_B$
$LaBr_3(Ce)$	587	632 [a]	1.96	0.057	2.25	0.29	2.5
NaI(Tl)	556	663 [b]	0.12	0.014	0.33	0.21	7.6
NaI(Tl)	587	632 [a]	0.05	0.009	0.20	0.15	8.2

[a] Energy range corresponds to interval ($E_{609.3} \pm 2.548 \cdot FWHM_{LaBr}(609.3)$)

[b] Energy range corresponds to interval ($E_{609.3} \pm 2.548 \cdot FWHM_{NaI}(609.3)$)

Table 2. Values of ^{214}Bi ROI cps registered during the rain episode compared to background. Increments and threshold criterion are given for both types of detectors.

As can be observed in Table 2, the total increment in counts of the ^{214}Bi ROI is still greater in the $LaBr_3(Ce)$ monitor than in the NaI(Tl) one and the dispersion of the background is more than 4 times greater in the $LaBr_3(Ce)$ monitor. Moreover, the ratio of the total cps increment to the background dispersion is still more than 3 times higher in the NaI(Tl) monitor. It is worth noting that the intrinsic background value of the ^{214}Bi ROI in the $LaBr_3(Ce)$ monitor from the self-activity spectrum is 1.83 cps, which is close to the value obtained before the rain episode (1.96 cps).

Even if the better resolution of $LaBr_3(Ce)$ allows us to determine a narrower ROI, there is little difference between the two ROIs of ^{214}Bi implemented for the NaI(Tl) monitor, as both of them behave similarly when compared to the $LaBr_3(Ce)$ monitor, giving higher values of $\frac{\Delta Ncps}{2\sigma_B}$ than $LaBr_3(Ce)$ in both cases.

5 Conclusions

A real-time gamma-ray spectrometry river water monitor was fully calibrated for operating with a 2”×2” $LaBr_3(Ce)$ detector. After the experimental energy and FWHM calibrations together with the MC simulated efficiency computations, the monitor was ready to provide spectra suitable for carrying out isotopic analysis of the river water. Therefore, the water monitor with a $LaBr_3(Ce)$ detector is adequate to quantify and identify radionuclides due to the good characteristics of its crystal (resolution, efficiency, density, linearity, etc.). However, the higher dispersion of the background values compared to the monitor with NaI(Tl) implies that a signal should be much greater to surpass the statistical criterion used in the Catalan network, which is related to the standard deviation of the background measurements. Thus, despite the greater dispersion, the water monitor with a $LaBr_3(Ce)$ detector would be a better choice when spectra are registered in high count rate scenarios, where the counts of the measured spectra are remarkably superior to the intrinsic background of the detector. In the other hand, the use of a NaI(Tl) detector in the water monitor could be convenient to assure radiological quality in low count rate situations.

References

Berger, M.., Coursey, J.., Zucker, M.., Chang, J., 2005. ESTAR, PSTAR, and ASTAR: Computer Programs for Calculating Stopping-Power and Range Tables for Electrons, Protons, and Helium Ions (version 1.2.3) [WWW Document]. URL https://www.nist.gov/pml/stopping-power-range-tables-electrons-protons-and-helium-ions

Casanovas, R., Morant, J.J., López, M., Hernández-Girón, I., Batalla, E., Salvadó, M., 2011. Performance of data acceptance criteria over 50 months from an automatic real-time environmental radiation surveillance network. J. Environ. Radioact. 102, 742–748. doi:10.1016/j.jenvrad.2011.04.001

Casanovas, R., Morant, J.J., Salvado, M., 2014a. Development and calibration of a real-time airborne radioactivity monitor using gamma-ray spectrometry on a particulate filter. IEEE Trans. Nucl. Sci. 61, 727–731. doi:10.1109/TNS.2014.2299715

Casanovas, R., Morant, J.J., Salvado, M., 2014b. Development and calibration of a real-time airborne radioactivity monitor using direct gamma-ray spectrometry with two scintillation detectors. Appl. Radiat. Isot. doi:10.1016/j.apradiso.2014.01.026

Casanovas, R., Morant, J.J., Salvadó, M., 2013. Implementation of gamma-ray spectrometry in two real-time water monitors using NaI(Tl) scintillation detectors. Appl. Radiat. Isot. 80, 49–55. doi:10.1016/j.apradiso.2013.06.003

Casanovas, R., Morant, J.J., Salvadó, M., 2012a. Temperature peak-shift correction methods for NaI(Tl) and LaBr3(Ce) gamma-ray spectrum stabilisation. Radiat. Meas. 47, 588–595. doi:10.1016/j.radmeas.2012.06.001

Casanovas, R., Morant, J.J., Salvadó, M., 2012b. Energy and resolution calibration of NaI(Tl) and LaBr 3(Ce) scintillators and validation of an EGS5 Monte Carlo user code for efficiency calculations. Nucl. Instruments Methods Phys. Res. Sect. A Accel. Spectrometers, Detect. Assoc. Equip. 675, 78–83. doi:10.1016/j.nima.2012.02.006

Currie, L. a., 1968. Limits for qualitative detection and quantitative determination. Application to radiochemistry. Anal. Chem. 40, 586–593. doi:10.1021/ac60259a007

Iltis, A., Mayhugh, M.R., Menge, P., Rozsa, C.M., Selles, O., Solovyev, V., 2006. Lanthanum halide scintillators: Properties and applications. Nucl. Instruments Methods Phys. Res. Sect. A Accel. Spectrometers, Detect. Assoc. Equip. 563, 359–363. doi:10.1016/j.nima.2006.02.192

Mattila, A., Toivonen, H., Vesterbacka, K., Leppänen, M., Salmelin, S., Pelikan, A., 2010. Radiation monitoring network with spectrometric capabilities: implementation of LaBr3 spectrometers to the Finnish network, in: Proceedings of the Third European IRPA Congress. Helsinki, pp. 1958–1966.

Menge, P.R., Gautier, G., Iltis, A., Rozsa, C., Solovyev, V., 2007. Performance of large lanthanum bromide scintillators. Nucl. Instruments Methods Phys. Res. Sect. A Accel. Spectrometers, Detect. Assoc. Equip. 579, 6–10. doi:10.1016/j.nima.2007.04.002

Nicolini, R., Camera, F., Blasi, N., Brambilla, S., Bassini, R., Boiano, C., Bracco, A., Crespi, F.C.L., Wieland, O., Benzoni, G., Leoni, S., Million, B., Montanari, D., Zalite, A., 2007. Investigation of the properties of a 1“x1” LaBr3:Ce scintillator. Nucl. Instruments Methods Phys. Res. Sect. A Accel. Spectrometers, Detect. Assoc. Equip. 582, 554–561. doi:10.1016/j.nima.2007.08.221

Nuclear Energy Agency, 2002. Assessment of Radiological and Health Impacts 2002 Update of

Chernobyl : Ten Years On. Chernobyl, Assess. Radiol. Heal. Impacts.

Quarati, F., Bos, A.J.J., Brandenburg, S., Dathy, C., Dorenbos, P., Kraft, S., Ostendorf, R.W., Ouspenski, V., Owens, A., 2007. X-ray and gamma-ray response of a 2“x2” LaBr3:Ce scintillation detector. Nucl. Instruments Methods Phys. Res. Sect. A Accel. Spectrometers, Detect. Assoc. Equip. 574, 115–120. doi:10.1016/j.nima.2007.01.161

Quarati, F.G.A., Khodyuk, I. V., Van Eijk, C.W.E., Quarati, P., Dorenbos, P., 2012. Study of 138La radioactive decays using LaBr 3 scintillators. Nucl. Instruments Methods Phys. Res. Sect. A Accel. Spectrometers, Detect. Assoc. Equip. 683, 46–52. doi:10.1016/j.nima.2012.04.066

Saint-Gobain Crystals, n.d. BrilLanCeTM Scintillators Performance Summary (Revision: January, 2009).

Su, G., Zeng, Z., Cheng, J., 2011. Monte carlo simulation of in situ LaBr gamma-ray spectrometer for marine environmental monitoring. Radiat. Prot. Dosimetry 146, 103–106. doi:10.1093/rpd/ncr122

Toivonen, H., Vesterbacka, K., Pelikan, A., Mattila, A., Karhunen, T., 2008. LaBr3 Spectrometry for Environmental Monitoring, in: Proceedings of the 12th International Congress of the International Radiation Protection Association. Buenos Aires.

Zeng, Z., Pan, X., Ma, H., He, J., Cang, J., Zeng, M., Mi, Y., Cheng, J., 2017. Optimization of an underwater in-situ LaBr3:Ce spectrometer with energy self-calibration and efficiency calibration. Appl. Radiat. Isot. 121, 101–108. doi:10.1016/j.apradiso.2016.12.016

3.2 Cálculo del equivalente de dosis ambiental H*(10) a partir de espectros gamma obtenidos con detectores de centelleo.

[II] R. Casanovas, E. Prieto, and M. Salvadó.

Calculation of the ambient dose equivalent H*(10) from gamma-ray spectra obtained with scintillation detectors.

Applied Radiation and Isotopes, vol. 118, pp. 154–159, 2016.

Resumen

La medida del equivalente de dosis ambiental H*(10) con monitores automáticos de espectrometría gamma en tiempo real aporta información valiosa en tiempos de integración cortos. Además, se presenta como una alternativa al análisis convencional por ajuste de Gaussianas. Este artículo describe la metodología de cálculo de dicha magnitud a partir de simulaciones de Montecarlo y su aplicación a medidas reales de espectrometría gamma tomadas con detectores de centelleo con cristales de $LaBr_3$(Ce). La metodología comprende el cálculo de los factores de conversión de fluencia a H*(10) y un método para obtener la fluencia a partir de espectros gamma. Los resultados obtenidos se comparan con los de un detector Geiger-Muller (GM) calibrado en H*(10). Finalmente, se calcula la concentración de actividad necesaria para producir cierto aumento de H*(10) para distintos isótopos. De este modo se pueden comparar las capacidades de detección de los detectores de espectrometría frente a los detectores GM.

Abstract

The measurement of the ambient dose equivalent H*(10) with automatic real-time radioactivity monitors using gamma-ray spectrometry provides valuable information at short integration times and serves as an alternative to conventional peak analysis of spectra. In this paper, a full methodology for the calculation of this quantity using Monte Carlo (MC) simulations is described and applied to real spectrometric measurements with $LaBr_3$(Ce) scintillation detectors. The methodology involves the calculation of the fluence-to-H*(10) conversion factors and a method for obtaining the fluence from gamma-ray spectra. The combination of this two elements makes it possible to calculate the H*(10). The obtained

results are compared with the H*(10) measurements of a Geiger-Müller (GM) detector. Finally, the necessary activity concentration to produce a certain increment on the H*(10) is discussed for some isotopes. This is used to discuss the analysis capabilities of the spectrometric detectors when compared to GM ones.

Applied Radiation and Isotopes 118 (2016) 154–159

Contents lists available at ScienceDirect

Applied Radiation and Isotopes

journal homepage: www.elsevier.com/locate/apradiso

Calculation of the ambient dose equivalent H*(10) from gamma-ray spectra obtained with scintillation detectors

Ramon Casanovas*, Elena Prieto, Marçal Salvadó

Unitat de Física Mèdica, Facultat de Medicina i Ciències de la Salut, Universitat Rovira i Virgili, Reus, Tarragona, ES-43201 Spain

ARTICLE INFO

Keywords:
H*(10)
Scintillation gamma-ray spectrometry
$LaBr_3$(Ce)
Monte Carlo simulation

ABSTRACT

The measurement of the ambient dose equivalent H*(10) with automatic real-time radioactivity monitors using gamma-ray spectrometry provides valuable information at short integration times and serves as an alternative to conventional peak analysis of spectra. In this paper, a full methodology for the calculation of this quantity using Monte Carlo (MC) simulations is described and applied to real spectrometric measurements with $LaBr_3$(Ce) scintillation detectors. The methodology involves the calculation of the fluence-to-H*(10) conversion factors and a method for obtaining the fluence from gamma-ray spectra. The combination of these two elements makes it possible to calculate the H*(10). The obtained results are compared with the H*(10) measurements of a Geiger-Müller (GM) detector. Finally, the necessary activity concentration to produce a certain increment on the H*(10) is discussed for some isotopes. This is used to discuss the analysis capabilities of the spectrometric detectors when compared to GM ones.

1. Introduction

Article 35 of the Euratom Treaty (2000/473/Euratom, 2000) requires each Member State to establish the necessary facilities to carry out real-time monitoring of the level of radioactivity in air, water, and soil and to ensure compliance with the basic standards. Following these requirements, there is an automatic real-time surveillance network in Catalonia (ES-E, Spain-East).

Recently, a project for the implementation of environmental radioactivity monitors using real-time gamma-ray spectrometry in this network has started. The project began after the findings of a previous study (Casanovas et al., 2011), which recommended this implementation for obtaining new and better radiological information.

Therefore, three different types of radiation monitors using either NaI(Tl) or $LaBr_3$(Ce) scintillation detectors have been recently developed, calibrated, and implemented into the Catalan real-time surveillance network: a water monitor (Casanovas et al., 2013), an aerosol monitor using a particulate filter (RARM-F) (Casanovas et al., 2014a), and a monitor using two shielded detectors measuring directly to the environment (RARM-D2) (Casanovas et al., 2014b).

However, to obtain real-time information from gamma-ray spectrometry (i.e. to obtain information in short integration times, e.g. 10 min), conventional peak analysis of gamma-ray spectra may not be useful as a consequence of having poor statistics. For this, other analysis methods are being developed to maximize the information extracted from the spectra. In particular, one of them is obtaining the ambient dose equivalent H*(10) from gamma-ray spectra.

The ambient dose equivalent H*(10) is recommended by the ICRP as the operational quantity for assessing effective dose in area monitoring (ICRP 103, 2007). In most practical situations of external radiation exposure, the ambient dose equivalent fulfils the aim of providing a conservative estimate or upper limit for the value of the limiting quantities.

The calculation of dosimetric quantities from gamma-ray or neutron spectra has been addressed in other studies by using different methodologies applied to several types of detectors (Camp and Vargas, 2014; Kim et al., 2002; Sato et al., 2005; Terada et al., 1980).

In this work, a full methodology for the calculation of the ambient dose equivalent H*(10) using Monte Carlo (MC) simulations is described and applied to real spectrometric measurements with $LaBr_3$(Ce) scintillation detectors.

2. Materials

2.1. Detectors

The gamma-ray spectrometry detectors that were used in this study were two 2″x2″ $LaBr_3$(Ce) scintillation detectors, which are part of the RARM-D2 monitor (Casanovas et al., 2014b). RARM-D2 monitor consists of two scintillation detectors (see Fig. 1), one pointing up (1) and the other pointing down (2), which are shielded with Pb (3) to permit the separate measurement of the airborne isotopes with respect

* Corresponding author.
E-mail address: ramon.casanovas@urv.cat (R. Casanovas).

http://dx.doi.org/10.1016/j.apradiso.2016.09.001
Received 28 June 2016; Received in revised form 27 August 2016; Accepted 3 September 2016
Available online 09 September 2016

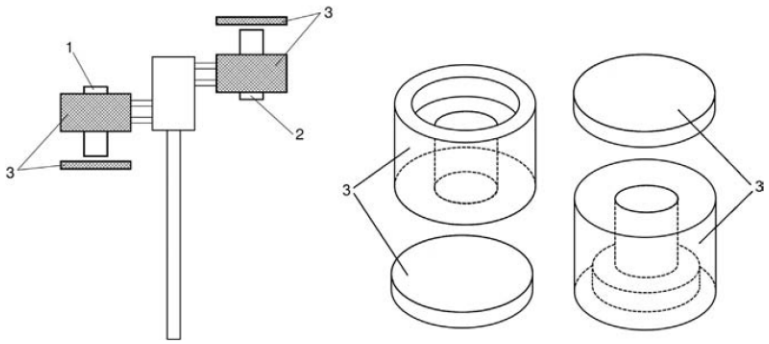

Fig. 1. General scheme of the RARM-D2 (left) and detailed scheme of the Pb shielding (right). The main elements are: detector pointing up (1), detector pointing down (2) and Pb shielding (3).

to the deposited isotopes. Both $LaBr_3(Ce)$ detectors were BrilLanCe™380 from Saint-Gobain Crystals. Each of the detectors was connected to a multichannel pulse-height analyzer of 2000 channels.

For comparison purposes, a Geiger-Müller (GM) Intelligent Gamma Probe IGS421 from Envinet was also used (Envinet, 2011). This GM monitor is composed of three detectors (two for low dose rates and one for higher ones) that are calibrated to measure the ambient dose equivalent rate in the range from 10 nSv/h to 10 Sv/h.

Both monitors, the RARM-D2 and the GM, were installed in the owner controlled area of the Ascó Nuclear Power Plant, in an open environment far from buildings or vegetation to avoid interferences with measurements. To ensure that detectors were exposed to the same radiation field, the monitors were positioned so that their active parts were at the same height (at about 2 m).

2.2. Radioactive sources

The certified radioactive sources that were used in this study for calibration purposes were five point sources of ^{241}Am, ^{133}Ba, ^{137}Cs, ^{60}Co, and ^{152}Eu. Besides, an ^{238}U ore was used to calibrate through some of the gamma lines of its progeny (^{226}Ra, ^{214}Bi, ^{214}Pb, etc.).

3. H*(10) calculation method

For the measurement of the ambient dose equivalent H*(10) with scintillation detectors using gamma-ray spectrometry, two elements are necessary: the conversion factors from gamma-ray fluence to H*(10) and the calculation of gamma-ray fluence from spectra. Combining these two elements, it is possible to obtain the H*(10) from spectra.

3.1. Calculation of the fluence-to-H*(10) conversion factors

3.1.1. H*(10) and ICRU sphere definition

The definition provided by the International Commission on Radiation Protection (ICRP 103, 2007) for the H*(10) is: "The ambient dose equivalent, H*(10), at a point in a radiation field, is the dose equivalent that would be produced by the corresponding expanded and aligned field in the ICRU sphere at a depth of 10 mm on the radius vector opposing the direction of the aligned field". The ICRU sphere (ICRU 39, 1985) is a 30 cm diameter sphere of unit density (1 g/cm^3) tissue-equivalent material (mass composition: 76.2% O, 11.1% C, 10.1% H and 2.6% N).

3.1.2. Monte Carlo simulations

The conversion factors F from gamma-ray fluence Φ to ambient dose equivalent H*(10) were calculated using Monte Carlo simulations with the EGS5 code system (Hirayama et al., 2005), which is a general-purpose package that enables the simulation of the coupled transport of electrons and photons in an arbitrary geometry. For this, an EGS5 user code was specifically programmed, which controls the EGS5 subroutines and contains all of the information about the radiation source (type of particles, energy of the particles and geometrical distribution) and the details of the ICRU sphere (geometry, density and composition).

Thus, several beams of 10^7 monoenergetic gamma rays covering the range from 0 to 2000 keV were simulated. The gamma rays were distributed in a 30 cm diameter circle and emitted towards the ICRU sphere following parallel trajectories and propagated through the vacuum. For each of the gamma-ray energies, the absorbed dose in a 1 mm-side cube was recorded. The cube was located at a depth of 10 mm in the sphere, according to the H*(10) definition. Then, at those energies, the conversion factors F were calculated by dividing the simulated fluence with the absorbed dose in the cube at a depth of 10 mm.

To improve statistics without the need of increasing the number of simulated gamma rays, a variance reduction technique was used. This technique consists in increasing the number of gamma rays that deposit energy in the small cube where the dose is computed. As the cube is located around the axis, this can be achieved using a distribution of gamma rays that is more peaked on the axis. Thus, the distribution given by Eq. (1) was used (Ferrari and Pelliccioni, 1994):

$$r = R \cdot \xi^{\frac{1}{1-\alpha}} \tag{1}$$

where r is the radial coordinate, R the radius of the gamma rays beam, $\xi \in U(0,1)$ a random number, and $\alpha = 1/2$ a constant parameter.

To obtain an unbiased result, the scored quantities need to be weighted with the statistical weight w given in Eq. (2):

$$w = \frac{2}{1-\alpha}\frac{r^{1+\alpha}}{R^{1+\alpha}} \tag{2}$$

Statistical uncertainties were estimated by performing all calculations in several batches and computing the standard deviation of the average (Casanovas et al., 2012a).

3.2. Calculation of the gamma-ray fluence from spectra

When a gamma ray interacts with a scintillation detector, it can either depose all of its energy or suffer a partial absorption (e.g. a Compton interaction after which the resulting electron deposits its energy in the detector and the gamma ray leaves the detector). Thus, the response of a scintillation detector does not only include full energy peaks corresponding to the energies of the gamma-rays emitted by the source, but also the effect of several partial absorptions.

The relation between the measured spectrum $\vec{M}$ and the fluence of incident gamma-ray spectrum $\vec{\phi}$ can be written as a matrix equation:

$$M = R\cdot\phi \begin{pmatrix} M_1 \\ M_2 \\ \vdots \\ M_n \end{pmatrix} = \begin{pmatrix} R_{11} & R_{12} & \cdots & R_{1n} \\ R_{21} & \ddots & & R_{2n} \\ \vdots & & \ddots & \vdots \\ R_{n1} & R_{n2} & \cdots & R_{nn} \end{pmatrix} \begin{pmatrix} \phi_1 \\ \phi_2 \\ \vdots \\ \phi_n \end{pmatrix} \tag{3}$$

where $\vec{M}$ and $\vec{\phi}$ are $n\times1$ vectors representing the measured spectrum and the incident gamma-ray fluence spectrum, respectively, and R an $n\times n$ matrix containing the information of the detector response (including the effect of the partial absorptions). A square response matrix was specifically chosen to ease solving the system of linear equations.

The response matrix R was calculated by means of Monte Carlo simulations using EGS5. For this, a user code was programmed to include all the information about the source term and the detector geometry, and to record the necessary quantities. For the calculations, the dimension of vectors and matrices was set to $n=40$, which was identified as appropriate in another study (Camp and Vargas, 2014). The R matrix was built by recording the response of the detector to different gamma ray energies, ranging from 0 to 2000 keV in steps of 50 keV (40×40 matrix). The gamma rays were distributed in a circle of 15 cm radius, similarly to the ICRU sphere calculations.

3.3. Calculation of H*(10)

After having the fluence-to-H*(10) conversion factors and the response matrix, the calculation of the H*(10) from gamma-ray spectra is straightforward. If $\vec{F}$ is a $n\times1$ vector containing the conversion factors from fluence to H*(10) at the same energies than the components of $\vec{M}$ and $\vec{\phi}$, then the H*(10) can be written as the following scalar product:

$$H^*(10) = F\cdot\phi$$

$$H^*(10) = \begin{pmatrix} F_1 & F_2 & \cdots & F_n \end{pmatrix}\cdot\begin{pmatrix} \phi_1 \\ \phi_2 \\ \vdots \\ \phi_n \end{pmatrix} \tag{4}$$

From Eq. (3), the fluence vector can be written as:

$$\vec{\phi}=R^{-1}\cdot\vec{M} \tag{5}$$

And combining Eq. (4) and Eq. (5):

$$H^*(10) = F\cdot\phi = F\cdot R^{-1}\cdot M = \chi\cdot M$$

$$H^*(10) = \begin{pmatrix} \chi_1 & \chi_2 & \cdots & \chi_n \end{pmatrix}\cdot\begin{pmatrix} M_1 \\ M_2 \\ \vdots \\ M_n \end{pmatrix} = \chi_1 M_1 + \chi_2 M_2 + \cdots + \chi_n M_n \tag{6}$$

where the vector $\vec{\chi}$ is defined as:

$$\chi \equiv F\cdot R^{-1}\begin{pmatrix} \chi_1 & \chi_2 & \cdots & \chi_n \end{pmatrix} \equiv \begin{pmatrix} F_1 & F_2 & \cdots & F_n \end{pmatrix}\cdot\begin{pmatrix} R_{11} & R_{12} & \cdots & R_{1n} \\ R_{21} & \ddots & & R_{2n} \\ \vdots & & \ddots & \vdots \\ R_{n1} & R_{n2} & \cdots & R_{nn} \end{pmatrix}^{-1} \tag{7}$$

From Eq. (6), the ambient dose equivalent H*(10) can be calculated by dividing the measured spectra in n Regions of Interest (ROIs), adding the counts in each of the ROIs (M_i), and summing them weighted by the calculated χ_i factors.

However, as a consequence of the smooth variation of the χ_i factors, it is possible to expand the calculations to all channels in the spectrum, avoiding the need of adding the counts in each of the ROIs and obtaining more precision in the calculations. Thus, the χ_i factors are fitted to a sixth order polynomial to get the $\bar{\chi}_j$ factors for each of the channels. Then, the calculation of H*(10) is performed using:

$$H^*(10) = \sum_{j=1}^{N_{channels}} \bar{\chi}_j\cdot C_j \tag{8}$$

where C_j are the counts in the channel j.

3.4. Experimental spectra preparation

Before using Eq. (8) for H*(10) calculation, some steps need to be performed to prepare the acquired spectra. These steps encompass spectra stabilization, energy calibration, and background subtraction.

3.4.1. Spectra stabilization

When detectors are operated under unstable temperature conditions in the environment, a peak shift in spectra and a consequent spectral distortion is observed. Thus, it is necessary to stabilize the acquired spectra.

For this purpose, software was specifically designed and used to perform the stabilization of spectra. This software automatically searches the position of reference peaks and uses them to stabilize the spectrum by applying a method that was previously developed in another study (Casanovas et al., 2012b).

3.4.2. Energy calibration

After spectrum stabilization, the energy calibration was applied using a 2nd grade polynomial. In a previous study (Casanovas et al., 2012a), this function was identified as appropriate for describing the relation between energy and channel number. This relation was established experimentally using the radioactive sources described in Section 2.2.

3.4.3. Background subtraction

Finally, before using Eq. (8), the self-contamination background of the $LaBr_3$(Ce) detector spectra (Quarati et al., 2012) needed to be removed. For doing so, a reference spectrum was recorded in a low background environment and was subtracted to all the spectra before the calculation of the H*(10).

3.5. H*(10) vs concentration of activity

After having a method for the calculation of H*(10) from spectra, it is possible to determine the activity concentration (Bq/m^3) of a certain isotope that is necessary to produce a certain H*(10) increment.

For doing so, it is necessary to recall to the detector efficiency curve, which provides the relation between the counts per second (cps) in the detector and the activity concentration (Bq/m^3) at different gamma-ray energies. This curve was calculated in a previous study using Monte Carlo simulations (Casanovas et al., 2014b).

Having the relation between the cps and Bq/m^3 and the methodology for calculating the H*(10) from the spectra (cps for different gamma-ray energies), it is possible to establish a relationship between the activity concentration and the H*(10).

In this study, the interest was focused on calculating the activity concentration of some isotopes that produce an H*(10) increment equivalent to the Investigation Level that was defined in a previous study for GM monitors (Casanovas et al., 2011), which corresponds to an increment of 0.008 μSv/h. The calculations were performed for the following isotopes: ^{241}Am, ^{131}I, ^{137}Cs and ^{60}Co. These isotopes are of interest in environmental gamma-ray spectrometry and cover a broad range of gamma-ray energies.

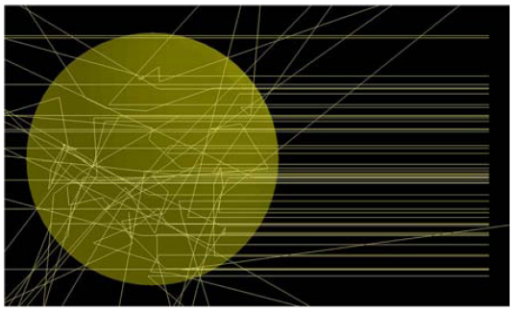

Fig. 2. MC simulation of a parallel beam of gamma-rays distributed in a circle of 15 cm radius and incident to the ICRU sphere where several interactions take place.

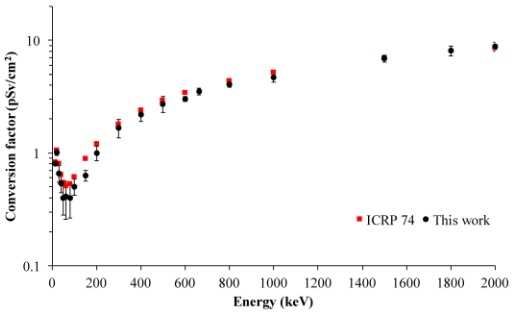

Fig. 3. Fluence-to-H*(10) conversion factors calculated in this study (circles) and compared with those in ICRP 74 publication (squares).

4. Results and discussion

4.1. Fluence-to-H*(10) conversion factors

The geometrical arrangement for the MC simulations is shown in Fig. 2, which includes a parallel beam of gamma rays distributed in a circle of 15 cm radius and incident to the ICRU sphere where several interactions take place.

The calculated fluence-to-H*(10) conversion factors are shown in Fig. 3. The obtained values were compared with those from ICRP 74 publication (ICRP 74, 1996) and found to be in good agreement with them.

4.2. Calculation of the gamma-ray fluence from spectra

For the calculation of the response matrix R, the arrangement shown in Fig. 4 was used, which included the detector (geometry and materials composition) and the parallel beam of gamma rays.

The obtained results for the response matrix R were combined with the fluence-to-H*(10) conversion factors to calculate the χ_i factors using Eq. (7). The calculated χ_i factors from cps to nSv/h are shown in Fig. 5.

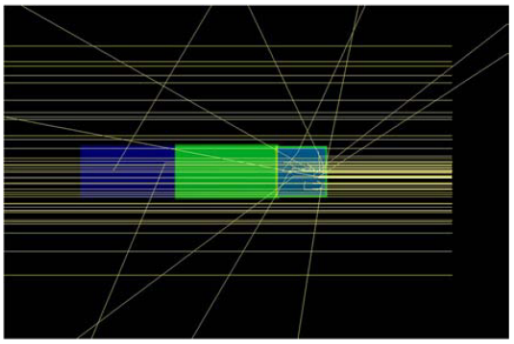

Fig. 4. MC simulation of a parallel gamma rays beam distributed in a 15 cm radius circle and incident to a scintillation detector.

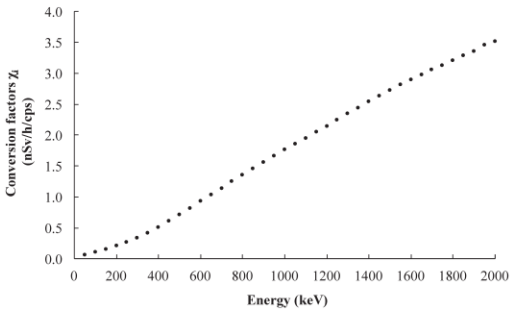

Fig. 5. Conversion factors χ_i (from cps to nSv/h) for H*(10) calculation.

4.3. Calculation of H*(10)

The calculation of H*(10) was performed separately at each of the two detectors of the RARM-D2 monitor by using Eq. (8) with the interpolated coefficients from Fig. 5. Then, both values were added to obtain the total H*(10). This enabled the comparison with the GM monitor, which is sensible to both gamma radiation coming from the airborne isotopes and from the soil isotopes.

4.3.1. H*(10) comparison

By way of example, a comparison between the ambient dose equivalent rate H*(10) obtained during one month from the $LaBr_3$(Ce) spectrometric detectors and the measurements from the GM monitor is provided in Fig. 6.

The results in Fig. 6 show that both monitors provide similar relative measurements. The observed H*(10) fluctuations are consequence of daily variations of ^{222}Rn and ^{220}Rn concentrations in air, which strongly depend on different meteorological variables (insolation, atmospheric pressure, humidity, rain, etc.). Radon isotopes emanate from the subsoil to the atmosphere and decay to different daughters that are gamma emitters (such as ^{214}Bi, ^{214}Pb or ^{208}Tl). As it can be observed between day 21 and day 25, this effect becomes relevant during rain episodes.

Regarding absolute values, the results in Fig. 6 show that the GM monitor provides higher values than that calculated for the $LaBr_3$(Ce) detector. On average, the absolute differences between them were about 0.02 μSv/h. However, the radiological increments above the average value were of similar magnitude.

Based on the information that is given in the technical data sheet of the GM monitor (Envinet, 2011), an overestimation of the dose rate in the GM monitor was expected since it provides a higher response for gamma rays with energies above that of ^{137}Cs (as some from ^{226}Ra progeny that are always present in the environment). An overestimation of +67% is expected for 2.5 MeV gamma rays.

Similar results on H*(10) overestimation with GM monitors were also observed in another study (Sáez-Vergara et al., 2002), where different GM monitors were compared with the readings of an ion chamber and some TLDs. The same study concluded that the GM detectors have an inherent background that needs to be compensated and that they usually provide a higher response to gamma rays with energies above 662 keV as a consequence of being only calibrated with ^{137}Cs.

Another justification of the GM providing greater values is that the cosmic radiation component is difficult to be measured separately from

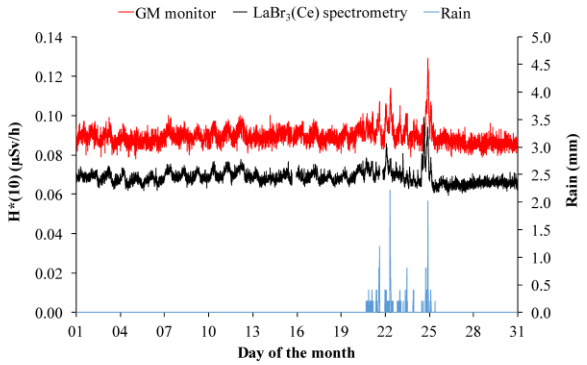

Fig. 6. Comparison of the ambient dose equivalent rate H*(10) obtained with a $LaBr_3$(Ce) spectrometry detector (black) and obtained with a GM monitor (red). The rainfall during the period is also provided (blue).(For interpretation of the references to color in this figure legend, the reader is referred to the web version of this article.)

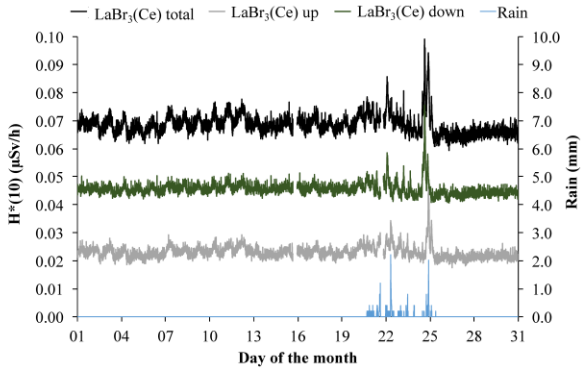

Fig. 7. Contribution to the total H*(10) (black) of the up detector (gray) and down detector (green) of RARM-D2. The rainfall during the period is also provided (blue).(For interpretation of the references to color in this figure legend, the reader is referred to the web version of this article.)

Table 1
Activity concentration increments for different isotopes to produce an H*(10) increment of 0.008 μSv/h in a 2″x2″ $LaBr_3$(Ce) detector.

Isotope	Activity concentration (Bq/m^3)
^{241}Am	48.6
^{131}I	19.1
^{137}Cs	51.1
^{60}Co	141.4

the internal background of the $LaBr_3$(Ce) detectors, and thus, it is lost when subtracting this internal background. Consequently, this component must be obtained by other means and added to the measurements. A value of 0.033 μSv/h for the cosmic dose rate in Barcelona is given in (Camp and Vargas, 2014), which could be assumed as similar to that in the location where the experimental measurements of this study were carried out.

Finally, it is important to remark that if the internal background of the $LaBr_3$(Ce) had not been subtracted, and so the counts had been interpreted as external dose rate, it would have added a surplus to the ambient dose equivalent rate H*(10) of 0.115 μSv/h (more than 1 mSv/y). The background subtraction process could also be a source of uncertainty that justifies the differences with the GM.

In view of the discrepancies on the obtained results, a more complete study of inter-comparison needs to be performed. The inter-comparison should be done by using other type of detectors (e. g. TDLs or proportional counters) that could provide other estimates of the H*(10).

4.3.2. H(10) contributions*

The contribution to the H*(10) of the upwards- and downwards-pointing detectors of the RARM-D2 is not the same (see Fig. 7). In average, the contribution of the up detector is about 1/3 and the one for the down detector is about 2/3. This is a consequence of the vertical distribution of the radon concentration, which is higher close to the ground and becomes lower with height as a consequence of its atmospheric dispersion.

4.4. H(10) vs concentration of activity*

The results for the activity concentration of some isotopes that produce an H*(10) increment of 0.008 μSv/h in a $LaBr_3$(Ce) detector are provided in Table 1. The calculated activity concentrations provide an idea of the contribution to the H*(10) of each of the isotopes, considering that they emit gamma rays at different energies and with different probabilities.

The same methodology could be applied in the other way to obtain the H*(10) increment that is produced after a given concentration of activity. This could be valuable in assessing doses and establishing radiation protection measures.

Results in Table 1 can be also interpreted as the necessary activity concentration to produce the H*(10) increment in the GM monitor, and so they can be also used to compare the sensitivity of both types of detectors to gamma rays.

By way of example, the necessary activity concentration of ^{137}Cs for triggering the investigation level in the GM monitors, which is set at 0.008 μSv/h, is 51.1 Bq/m^3. However, the Minimum Detectable Activity Concentration (MDAC) in a 10 min spectrum for ^{137}Cs is 5.3 Bq/m^3 (Casanovas et al., 2014b). Hence, it can be concluded that the spectrometric capabilities would provide better sensitivity, since the presence of ^{137}Cs would be detected before using conventional spectrometric analysis rather than realizing an abnormal increment of the ambient dose equivalent H*(10).

5. Conclusions

A full methodology for the calculation of the ambient dose equivalent H*(10) in automatic real-time radioactivity monitors using gamma-ray spectrometry was provided. This methodology encompasses the calculation of the fluence-to-H*(10) conversion factors and a method for obtaining the fluence from gamma-ray spectra. Both calculations were performed using Monte Carlo simulations with the EGS5 code system.

The methodology was applied in a $LaBr_3$(Ce) detector and the obtained results for the H*(10) were compared with the measurements of a GM detector. In view of the results, a more complete study of inter-comparison needs to be performed.

The method was also used for calculating the necessary activity concentrations of some isotopes to produce a determined increment on the H*(10). This was used to compare the capabilities of gamma-ray spectrometry with that of the GM detector.

Finally, the developed methodology can be adapted for obtaining the H*(10) in other types of spectrometric detectors, either detectors with different materials or from different sizes, and the calculations can be also performed for other gamma-ray energy ranges.

Acknowledgments

The work was partially financed by the *Consejo de Seguridad Nuclear* (CSN, Nuclear Safety Council) of Spain [funding for R & D projects related to radiation protection, BOE No. 178 of 26th July 2012]

and the *Servei de Coordinació d'Activitats Radioactives* (SCAR, Radioactive Activities Coordination Service) of the Generalitat de Catalunya [administrative contract for research and data analysis associated with the monitors of the environmental radioactivity surveillance network of the Generalitat de Catalunya, EMO 2013 613, Lot 2]. The Monte Carlo simulations were performed in the supercomputers of the *Consorci de Serveis Universitaris de Catalunya* (CSUC).

References

2000/473/Euratom, 27 July 2000. Commission Recommendation of 8 June 2000, Official Journal of the European Commission, No. 191. (Available from: ⟨http://ec.europa.eu/energy/nuclear/radioprotection/doc/legislation/00473_en.pdf⟩)

Camp, A., Vargas, A., 2014. Ambient dose estimation H*(10) from $LaBr_3$(Ce) Spectra. Radiat. Prot. Dosim. 160, 264–268.

Casanovas, R., Morant, J.J., Lopez, M., Hernandez-Giron, I., Batalla, E., Salvadó, M., 2011. Performance of data acceptance criteria over 50 months from an automatic real-time environmental radiation surveillance network. J. Environ. Radioact. 102, 742–748.

Casanovas, R., Morant, J.J., Salvadó, M., 2012a. Energy and resolution calibration of NaI (Tl) and $LaBr_3$(Ce) scintillators and validation of an EGS5 Monte Carlo user code for efficiency calculations. *Nucl. Intrum. Methods Phys. Res. A* 675, 78–83.

Casanovas, R., Morant, J.J., Salvadó, M., 2012b. Temperature peak-shift correction methods for NaI(Tl) and $LaBr_3$(Ce) gamma-ray spectrum stabilisation. Radiat. Meas. 47, 588–595.

Casanovas, R., Morant, J.J., Salvadó, M., 2013. Implementation of gamma-ray spectrometry in two real-time water monitors using NaI(Tl) scintillation detectors. Appl. Radiat. Isot. 80, 49–55.

Casanovas, R., Morant, J.J., Salvadó, M., 2014a. Development and calibration of a real-time airborne radioactivity monitor using gamma-ray spectrometry on a particulate filter. IEEE Trans. Nucl. Sci. 61, 727–731.

Casanovas, R., Morant, J.J., Salvadó, M., 2014b. Development and calibration of a real-time airborne radioactivity monitor using direct gamma-ray spectrometry with two scintillation detectors. Appl. Radiat. Isot. 89, 103–108.

Envinet. Intelligent Gamma Probe IGS421A/B-H. Technical Data Sheet IGS421A/B-H/00EN/09/2011. (Available at): ⟨http://www.envinet.com⟩

Ferrari, A., Pelliccioni, M., 1994. On the conversion coefficients from fluence to ambient dose equivalent. Radiat. Prot. Dosim. 51, 251–255.

Hirayama, H., Namito, Y., Bielajew, A.F., Wilderman, S.J., Nelson, W.R., 2005. The EGS5 Code System. SLAC-R-730 and KEK Report 2005–8.

International Commission on Radiation Units and Measurements, 1985. Determination of Dose Equivalents Resulting from External Radiation Sources. ICRU Report 39.

International Commission on Radiological Protection, 1996. Conversion Coefficients for Use in Radiological Protection against External Radiation. ICRP Publication 74.

International Commission on Radiological Protection, 2007. The 2007 Recommendations of the International Commission on Radiological Protection. ICRP Publication 103.

Kim, E., Endo, A., Yamaguchi, Y., Nakamura, T., Shiomi, T., 2002. Measurement of neutron dose with an organic liquid scintillator coupled with a spectrum weight function. Radiat. Prot. Dosim. 102, 31–40.

Quarati, F.G.A., Khodyuk, I.V., van Eijk, C.W.E., Quarati, P., Dorenbos, P., 2012. Study of ^{138}La radioactive decays using $LaBr_3$ scintillators. Nucl. Instrum. Methods Phys. Res. A 683, 46–52.

Sáez-Vergara, J.C., Romero, A.M., Vila Peña, M., Rodriguez, R., Muñiz, J.L., 2002. The use of passive environmental TLDs in the operation of the Spanish early warning network "REVIRA". Radiat. Prot. Dosim. 101, 249–252.

Sato, T., Satoh, D., Endo, A., Yamaguchi, Y., 2005. Development of dose monitoring system applicable to various radiations with wide energy ranges. J. Nucl. Sci. Technol. 42, 768–778.

Terada, H., Sakai, E., Katagiri, M., 1980. Environmental gamma-ray exposure rates measured by in-situ Ge(Li) spectrometer. J. Nucl. Sci. Technol. 17, 281–290.

3.3 Método de análisis por regiones espectrales para la monitorización de isótopos artificiales en espectrometría gamma de centelleo en tiempo real

[III] E. Prieto, R. Casanovas and M. Salvadó.

Spectral windows analysis method for monitoring anthropogenic radionuclides in real-time environmental gamma-ray scintillation spectrometry.

(Enviado para su publicación)

Resumen

Este artículo propone una metodología de análisis basada en la técnica de las regiones espectrales dirigida a espectros gamma ambientales registrados en tiempo real por detectores de centelleo. El método permite la monitorización de concentraciones de actividad de isótopos artificiales, como el ^{137}Cs y ^{131}I, ya que elimina la dispersión Compton (y otras contribuciones externas) y solventa el solapamiento de picos dentro de las regiones espectrales. Se presentan concentraciones de actividad de ^{137}Cs, ^{131}I, ^{214}Bi y ^{214}Pb, obtenidas aplicando el método particularizado para un monitor de medida directa con detector de $LaBr_3$(Ce).

Abstract

This paper proposes an analysis methodology based on the spectral windows technique aimed for environmental real-time gamma-ray spectra obtained with scintillation detectors. The method permits to monitor activity concentrations of selected isotopes, such as anthropogenic radionuclides like ^{137}Cs and ^{131}I, by removing the Compton scattering plus other external contributions and resolving peak overlapping within any window. Activity concentrations are presented for ^{137}Cs, ^{131}I, ^{214}Bi and ^{214}Pb obtained applying the method particularised for a monitor using a $LaBr_3$(Ce) detector.

Spectral windows analysis method for monitoring anthropogenic radionuclides in real-time environmental gamma-ray scintillation spectrometry

E. Prieto[1], R. Casanovas[1] and M. Salvadó[1].

[1] Unitat de Física Mèdica, Facultat de Medicina i Ciències de la Salut, Universitat Rovira i Virgili, ES-43201 Reus (Tarragona), Spain

Abstract

This paper proposes an analysis methodology based on the spectral windows technique aimed for environmental real-time gamma-ray spectra obtained with scintillation detectors. The method permits to monitor activity concentrations of selected isotopes, such as anthropogenic radionuclides like ^{137}Cs and ^{131}I, by removing the Compton scattering plus other external contributions and resolving peak overlapping within any window. Activity concentrations are presented for ^{137}Cs, ^{131}I, ^{214}Bi and ^{214}Pb when applying the method to a monitor using a $LaBr_3$(Ce) detector.

Key words: **scintillation gamma-ray spectrometry, real-time, $LaBr_3$(Ce), ^{137}Cs, ^{131}I, windows technique, activity concentration**

1 Introduction

Over the past few years, the Medical Physics Unit of *Universitat Rovira i Virgili* has participated in a project for the improvement of the automatic real-time environmental surveillance network of Catalonia (ES-E, Spain-East) (Casanovas et al., 2011). The main development of the project has been the implementation of gamma-ray scintillation spectrometry monitors with NaI(Tl) and $LaBr_3$(Ce) scintillation detectors all over the region and, specially, around the two nuclear power plants that operate in the area.

The monitors implemented in the Catalan network were developed for aerosol surveillance using a particulate filter (RARM-F) (Casanovas et al., 2014a) and for measuring directly to the environment using two shielded detectors (RARM-D2) (Casanovas et al., 2014b), with either NaI(Tl) or $LaBr_3$(Ce) detectors. Additionally, two water NaI(Tl) monitors (Casanovas et al., 2013) were developed for the surveillance of the water from Ebre river, which is used for cooling the two pressurised water reactors of one of the nuclear power plants.

Recently, a variety of direct monitors without shielding have been incorporated to the network, comprising different scintillation materials and crystals sizes: 1”×1” and 2”×2” $LaBr_3$(Ce) detectors and 2”×2” and 3”×3” NaI(Tl) detectors. At present, there are a total of 26 installed monitors in the network using scintillation gamma-ray spectrometry that are measuring in real-time, providing new spectra every 10 minutes. Thus, the total quantity of data to be analysed every day is very large.

Spectra registered in short integration times usually present high noise and low statistics due to environmental low dose rate measures, and hence, conventional peak analysis of gamma-ray spectra may not be accurate in providing real-time results. For this, other analysis methods that permit to establish early-warning alarms need to be developed to maximize the information extracted from these spectra, such as obtaining the ambient dose equivalent H*(10) from gamma-ray spectra (Casanovas et al., 2016) or using spectral windows analysis methods (IAEA - International Atomic Energy Agency, 1976)(Korbech and Nielsen, 1992)(IAEA - International Atomic Energy Agency, 1991)(Arnold et al., 2012)(Blum et al., 1997)(Cresswell et al., 2006).

In this study, a novel spectral windows method was developed to automatically monitor anthropogenic isotopes activity concentrations. The developed algorithm compensates the natural radioactivity oscillations, especially those associated with ^{222}Rn daughters (RD) that are related to meteorological variations (mainly rain and humidity variations). Besides, the algorithm not only considers the overlapping of the target anthropogenic isotopes peaks with the natural radiation ones but also accounts for the surplus of counts generated as a consequence of Compton dispersion arising from natural radiation that affects the entire spectrum.

The developed algorithm was optimized and tested for measuring ^{131}I and ^{137}Cs activity concentrations in real-time with a 2”×2” $LaBr_3$(Ce) detector measuring directly to the environment in different backgrounds.

2 Materials

2.1 Equipment and data acquisition

The detector used in this study was a 2”×2” $LaBr_3$(Ce) BrilLance^{TM}380 from Saint-Gobain Crystals® that was coupled to a digital multichannel analyser (Digibase from ORTEC®). Experimental data were obtained using radioactive sources: a point-like source of ^{137}Cs, a hermetically sealed source of ^{226}Ra in equilibrium with its gamma emitter daughters of ^{222}Rn (mainly ^{214}Pb and ^{214}Bi) and an encapsulated source of ^{131}I.

The detector and the radioactive sources were placed at 1.5 m above the ground, coupled to a stick, to guarantee an isotropic radiation field by avoiding its interference with the laboratory objects, walls and floor. All acquired spectra were collected during a 10 min integration time at different detector-source distances to simulate different airborne activity concentrations. The Gaussian peak analysis of spectra was performed using the commercial software ScintiVision^{TM} from ORTEC®, whereas the operations related with spectral windows were carried out by means of an internally developed software.

3 Methods

3.1 Spectra preparation before the analysis

Before the application of any analysis method, registered spectra need to be stabilised and calibrated in energy, resolution and efficiency.

3.1.1 Spectra stabilisation

Spectra stabilisation is required to correct the peak shift that is observed in spectra basically due to temperature variations. A self-developed software was used to apply a previously described

methodology that automatically searches for reference peaks and adjusts their position (Casanovas et al., 2012a).

3.1.2 Energy and resolution calibrations

Then, stabilised spectra were calibrated in energy and in resolution. The energy and resolution calibrations were performed using the radioactive sources listed in Section 2.1 and adjusting a 2nd degree polynomial, which was found to be an adequate function (Casanovas et al., 2012b).

3.1.3 Efficiency calibration

Finally, to obtain activity concentrations, an efficiency calibration was performed. Efficiency calibration was performed using Monte Carlo simulations with EGS5 code and assuming a homogeneous cylindrical source of equal radius and diameter of 500 m surrounding the $LaBr_3$(Ce) detector. More details about this calibration were given in a previous study (Casanovas et al., 2014b). It should be noted that the radioactive sources used in this study (see section 2.1) did not correspond to this geometry, but were considered as if.

3.2 Description of the method

3.2.1 ROI width determination

The width of the spectral windows or ROIs (Region of Interest) was determined by the width of the expected peaks of the isotopes of study, which is proportional to the Full Width at Half Maximum (FWHM) in function of the energy that is obtained in the resolution calibration:

$$n = n(E) = k \cdot FWHM(E) \quad (1)$$

where k is the proportionality constant to set the desired peak coverage and $FWHM(E)$ is a 2nd degree polynomial function of the energy (E). In this study, the widths of all the ROIs used where set at $k = 1.699$ for a 95.45% peak area coverage.

Given that the chosen width of the ROIs does not cover the entire Gaussian distribution arising from a gamma emission in a spectrum taken with scintillation detectors, the activity of the studied isotope in a ROI is calculated as:

$$A = \frac{cps}{\varepsilon \cdot p_\gamma \cdot G} \quad (2)$$

where cps is the number of counts per second in the given ROI, ε is the detector efficiency, p_γ is the emission probability of the gamma-ray and G is a term that corrects the proportion of Gaussian distribution that covers the width of the ROI, as it does not include the entire Gaussian distribution and hence, not all the cps originated from the gamma emission would be counted in the activity calculation.

3.2.2 Compton scattering and other contributions to spectra

When a gamma-ray spectrum is obtained with scintillation detectors, only a portion of the total cps is significant to calculate activity concentrations. These cps are those under the photo-peak

and above the baseline of the Gaussian distribution. The rest of cps of the spectrum is a result from different interactions between gamma-rays or beta particles and the detector materials, such as the Compton scattering.

In an environmental gamma-ray spectrum, the amount of cps arising from Compton scattering could be divided in two groups: the Compton contribution originated from gamma-ray emitting RD (mainly ^{214}Bi and ^{214}Pb) and the Compton contribution from all the other natural radionuclides such as ^{40}K and gamma-ray emitting isotopes from ^{232}Th decay chain (mainly ^{208}Tl, ^{228}Ac, ^{212}Pb or ^{212}Bi).

Moreover, other phenomena provide extra counts to gamma-ray spectra obtained with scintillation detectors. Among these are random summing, which is the continuum above the full energy-peaks, pair production (the annihilation peak at 511 keV) or Bremsstrahlung radiation that is registered in the low energy range of a spectrum and it is due to high-energy beta particles. In addition, in spectra obtained with lead shielded detectors peaks arising from characteristic X-rays or Compton backscattering in the region of 200-300 keV are also found (Gilmore, 2008).

In this regard, the developed methodology hypothesises that the amount of Compton scattering plus all the associated external counts from other interaction phenomena due to RD, in a certain window or ROI, is considered to be proportional to ^{214}Bi activity concentration (A_{Bi}), as the latter isotope is mainly in equilibrium with ^{214}Pb. Thus, the external contribution due to RD is:

$$RD\_cont_i = m_i \cdot A_{Bi} \tag{3}$$

where RD_cont_i is the external contribution from Compton scattering plus other interaction phenomena due to RD in ROI$_i$ (in cps), m_i is the fitting coefficient and A_{Bi} is ^{214}Bi activity concentration (Bq/m^3).

On the other hand, the amount of Compton scattering from the rest of natural radionuclides plus other possible types of contributions to a spectrum is considered to be constant. Thus, from Equation (3), the total extra cps contribution to a ROI can be written as:

$$cont_i = m_i \cdot A_{Bi} + c_i \tag{4}$$

where $cont_i$ is the total extra cps contribution in ROI$_i$ and c_i is the Compton scattering plus other interaction phenomena due to non-RD natural emissions. (The total extra contribution to a ROI is shown in black in Figure 1).

3.2.3 **Peak overlapping**

Peak overlapping occurs when some cps from two Gaussian distributions arising from different gamma emissions are found inside the same ROI. The components (in cps) of two adjacent ROIs centred in two gamma emissions of different isotopes that present peak overlapping can be identified as follows:

$$ROI_1 = cps_{11} + cps_{21} + cont_1 + Bkgd_1 \tag{5}$$

$$ROI_2 = cps_{22} + cps_{12} + cont_2 + Bkgd_2 \tag{6}$$

where ROI_1 are all the cps contained in the ROI centred around the gamma emission of isotope 1, cps_{11} are the cps of isotope 1 in ROI$_1$, cps_{21} are the cps of isotope 2 in ROI$_1$, $cont_1$ is the total extra

cps contribution in ROI_1 and $Bkgd_1$ are the cps of the intrinsic background in ROI_1. Analogously, ROI_2 are all the cps contained in the ROI centred around the gamma emission of isotope 2, cps_{22} are the cps of isotope 2 in ROI_2, cps_{12} are the cps of isotope 1 in ROI_2, $cont_2$ is the total extra cps contribution in ROI_2 and $Bkgd_2$ are the cps of the intrinsic background in ROI_2.

The term $Bkgd_i$ was included to take into account those detectors that have an intrinsic self-activity, such as $LaBr_3(Ce)$ or $LaCl_3(Ce)$ detectors (see Section 3.3). To apply the methodology at spectra obtained with detectors without self-activity, such as NaI(Tl), this term should not be considered.

Figure 1 shows the composition of two ROIs in cps, ROI_1 and ROI_2, corresponding to two close gamma emissions originated from $isotope_1$ and $isotope_2$ in a reproduction of a spectrum obtained with a $LaBr_3(Ce)$ detector. The Gaussian distributions of the emissions are drawn to identify the peak overlapping: the widths of ROI_1 and ROI_2 are smaller than the full energy peaks of the gamma emissions but contain cps of both isotopes.

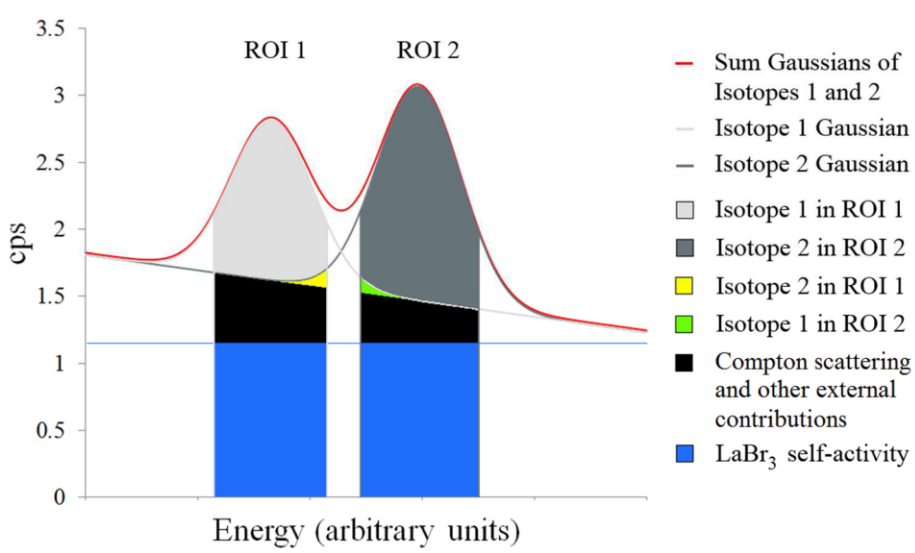

Figure 1. Composition of two ROIs in a partial reproduction of a $LaBr_3(Ce)$ spectrum with two overlapped energy peaks. (For interpretation of the references to colour in this figure legend, the reader is referred to the web version of this article.)

The cps originated from a gamma emission of an isotope *i* in a given ROI *j* can be written in terms of the isotope activity concentration using Equation (2):

$$cps_{ij} = A_i \cdot p_i \cdot \varepsilon_i \cdot G_{ij} \tag{7}$$

where cps_{ij} are the cps of isotope *i* in ROI *j*, A_i is the activity concentration of isotope *i*, p_i is the probability of the emission of isotope *i*, ε_i is the detector efficiency of the emission of isotope *i* and G_{ij} is the term that takes into account the proportion of the Gaussian distribution of isotope *i* inside ROI *j*.

Using Equations (4) and (7), Equations (5) and (6) can be written as:

$$ROI_1 = A_1 \cdot p_1 \cdot \varepsilon_1 \cdot G_{11} + A_2 \cdot p_2 \cdot \varepsilon_2 \cdot G_{21} + m_1 \cdot A_{Bi} + c_1 + Bkgd_1 \tag{8}$$

$$ROI_2 = A_2 \cdot p_2 \cdot \varepsilon_2 \cdot G_{22} + A_1 \cdot p_1 \cdot \varepsilon_1 \cdot G_{12} + m_2 \cdot A_{Bi} + c_2 + Bkgd_2 \tag{9}$$

Solving the equation system, the activities of the isotopes, A_1 and A_2, can be obtained:

$$A_1 = \frac{ROI_1 - Bkgd_1 - m_1 \cdot A_{Bi} - c_1 - \left(ROI_2 - Bkgd_2 - m_2 \cdot A_{Bi} - c_2\right)\left(\frac{G_{21}}{G_{22}}\right)}{p_1 \cdot \varepsilon_1 \left(G_{11} - \frac{G_{12} \cdot G_{21}}{G_{22}}\right)} \quad (10)$$

$$A_2 = \frac{ROI_2 - Bkgd_2 - m_2 \cdot A_{Bi} - c_2 - \left(ROI_1 - Bkgd_1 - m_1 \cdot A_{Bi} - c_1\right)\left(\frac{G_{12}}{G_{11}}\right)}{p_2 \cdot \varepsilon_2 \left(G_{22} - \frac{G_{21} \cdot G_{12}}{G_{11}}\right)} \quad (11)$$

3.2.4 **Determination of m_i and c_i**

As mentioned before in Equation (4), the total external contribution in a ROI was considered to be the Compton scattering contribution from RD, which is assumed to be m_i-proportional to A_{Bi}, plus the Compton scattering from the rest of natural emissions and other external contributions (c_i), which is assumed to be constant.

The determination of m_i and c_i was performed for the $LaBr_3$(Ce) detector using the radioactive sources listed in Section 2.1 to ensure that the algorithm is optimised for detecting small amounts of ^{137}Cs and ^{131}I over a natural background with changing radon and RD concentrations. The obtained spectra encompass different combinations of sources placed at different distances to simulate different activity concentrations of airborne isotopes. Determination of fitting coefficients was performed using a background spectrum, a ^{226}Ra spectrum, a ^{137}Cs spectrum and a ^{226}Ra with ^{131}I spectrum (it should be noted that the spectra used for the determination of the parameters are different from those used to test the methodology in Section 4).

The activity concentrations of different isotopes (^{214}Pb, ^{131}I, ^{208}Tl, ^{214}Bi and ^{137}Cs) were determined for each spectrum using ScintiVision™ software by fitting Gaussian peaks. The activity concentration of the chosen isotopes could be alternatively obtained applying Equations (10) and (11), considering that the ROIs of these isotopes partially overlap: ^{214}Pb (352 keV) overlaps with ^{131}I (365 keV), ^{208}Tl (583 keV) overlaps with ^{214}Bi (609 keV) and ^{137}Cs (662 keV) overlaps with ^{214}Bi (665 keV).

Therefore, the values of the obtained activities by Gaussian fitting for each spectrum were substituted in Equations (10) and (11), along with the other known parameters of the equations, such as the total value of the ROIs, the intrinsic background of the ROIs, the peak covertures G, the emission probabilities and the efficiencies. Thus, a set of equations that covered a variety of real radioactive sources contributions was obtained, where the only unknown parameters were m_i and c_i. Using a calculation programme, a least squares fit was applied to obtain the values of m_i and c_i that adjusted to all the equations at the same time.

3.2.5 **Peak overlapping with ^{214}Bi**

The method described to obtain the activities of overlapped peaks requires a previous assessment of ^{214}Bi activity concentration. The activity concentration of ^{214}Bi can be obtained from its most probable emission (609 keV) using Equation (10), as it partially overlaps with an emission from ^{208}Tl at 583 keV. Therefore, the term A_{Bi} in Equations (10) and (11) is calculated previously as:

$$A_{Bi} = \frac{ROI_{Bi} - Bkgd_{Bi} - c_{Bi} - \left(ROI_{Tl} - Bkgd_{Tl} - c_{Tl}\right)\left(\frac{G_{TlBi}}{G_{BiBi}}\right)}{p_{Bi}\cdot\varepsilon_{Bi}\left(G_{BiBi} - \frac{G_{BiTl}\cdot G_{TlBi}}{G_{TlTl}}\right) + m_{Bi} - m_{Tl}\frac{G_{TlBi}}{G_{TlTl}}} \tag{12}$$

where ROI_{Bi} is the ROI centred around the 609 keV peak of ^{214}Bi, $Bkgd_{Bi}$ is the $LaBr_3$(Ce) intrinsic background in ROI_{Bi}, c_{Bi} is the contribution from Compton scattering plus other interaction phenomena due to non-RD natural emissions to ROI_{Bi}, ROI_{Tl} is the ROI centred around the 583 keV peak of ^{208}Tl, $Bkgd_{Tl}$ is the intrinsic background in ROI_{Tl}, c_{Tl} is the contribution from Compton scattering plus other interaction phenomena due to non-RD natural emissions to ROI_{Tl}, G_{TlBi} is the amount of ^{208}Tl Gaussian distribution inside ROI_{Bi}, G_{BiBi} is the amount of ^{214}Bi Gaussian distribution inside ROI_{Bi}, p_{Bi} is the probability of the 609 keV emission from ^{214}Bi, ε_{Bi} is the detector efficiency at 609 keV, G_{BiTl} is the amount of ^{214}Bi Gaussian distribution inside ROI_{Tl}, G_{TlTl} is the amount of ^{208}Tl Gaussian distribution inside ROI_{Tl}, m_{Bi} is the fitting coefficient for the contribution from Compton scattering plus other interaction phenomena due to RD in ROI_{Bi} and m_{Tl} is the fitting coefficient for the contribution from Compton scattering plus other interaction phenomena due to RD in ROI_{Tl}.

Whenever a peak of an emission of interest is overlapped with an emission from ^{214}Bi, the calculation of the activity concentration of the isotope of interest can be easily determined without applying the method a second time, as the activity concentration of ^{214}Bi is already known. Thus, the cps corresponding to ^{214}Bi can be removed from the ROI of the isotope of interest simply using Equation (8) or (9).

For example, the 662 keV emission from ^{137}Cs overlaps with a low probability peak from ^{214}Bi at 665 keV that cannot be dismissed. Then, the activity concentration of ^{137}Cs, A_{Cs}, can be written as:

$$A_{Cs} = \frac{ROI_{Cs} - Bkgd_{Cs} - m_{Cs}\cdot A_{Bi} - c_{Cs} - A_{Bi}\cdot p_{Bi_{665}}\cdot\varepsilon_{Bi_{665}}\cdot G_{Bi_{665}Cs}}{p_{Cs}\cdot\varepsilon_{Cs}\cdot G_{CsCs}} \tag{13}$$

where ROI_{Cs} is the ROI centred around the 662 keV peak of ^{137}Cs, $Bkgd_{Cs}$ is the $LaBr_3$(Ce) intrinsic background in ROI_{Cs}, m_{Cs} is the fitting coefficient for the contribution from Compton scattering plus other interaction phenomena due to RD in ROI_{Cs}, A_{Bi} is the activity concentration of ^{214}Bi, c_{Cs} is the contribution from Compton scattering plus other interaction phenomena due to non-RD natural emissions to ROI_{Cs}, $p_{Bi_{665}}$ is the probability of the 665 keV emission from ^{214}Bi, $\varepsilon_{Bi_{665}}$ is the detector efficiency at 665 keV, $G_{Bi_{665}Cs}$ is the amount of the Gaussian distribution from ^{214}Bi peak at 665 keV inside ROI_{Cs}, p_{Cs} is the probability of the 662 keV emission from ^{137}Cs, ε_{Cs} is the detector efficiency at 662 keV, G_{CsCs} is the amount of ^{137}Cs Gaussian distribution inside ROI_{Cs}.

3.3 $LaBr_3$(Ce) intrinsic background determination

When the method is applied at spectra obtained with $LaBr_3$(Ce) detectors, it is necessary to obtain an intrinsic background spectrum to estimate the background of each ROI. $LaBr_3$(Ce) detectors self-activity, due to ^{138}La and ^{227}Ac in the detector crystal (Quarati et al., 2012), provide extra cps that must be subtracted. Therefore, the detector was placed inside a lead shielding for several hours. After the registration of the spectrum, the absence of any photopeak from natural origin was checked and an intrinsic background spectra was obtained.

3.4 Minimum Detectable Activity Concentration (MDAC)

The Minimum Detectable Activity Concentration corresponds to the activity measured from the detection limit, L_D. The detection limit is the minimum number of counts under a peak that one can be confident of detecting with a certain probability.

The MDAC can be determined as:

$$MDAC = \frac{L_D}{\varepsilon \cdot t \cdot p_\gamma} \tag{14}$$

where the detection limit L_D (with a 95% confidence limit) for a certain ROI is calculated using the expression for the standard deviation of the background (Currie, 1968):

$$L_D = 2.71 + 3.29\sigma_B \tag{15}$$

where σ_B is the standard deviation of the background (laboratory plus an intrinsic background in detectors such as $LaBr_3$(Ce)) measured in counts in the considered ROI. The width of the ROI is determined by Equation (1) with $k = 1.699$ for a 95.45% peak area coverage.

3.5 Spectra analysis discrimination criterion

A discrimination criterion to identify suspicious spectra was implemented in all the monitors of the surveillance network (Casanovas et al., 2011), which was adapted to the spectral windows analysis method. For that, the value of the activity concentration of the isotopes associated to each ROI of every registered spectrum is obtained (x_i) and the value is checked to be in the following interval:

$$\mu - \alpha\sigma_B \leq x_i \leq \mu + \alpha\sigma_B \tag{16}$$

where μ is the mean value of the activity concentration of the isotope registered in a long period corresponding to the monitor site background, σ_B the standard deviation and α a confidence factor.

In this study, the confidence factor α is set at 3. Since the background follows a Gaussian distribution, values above $\mu + 3\sigma_B$ would be only the 0.135% of the measurements. Therefore, when the activity concentration of an isotope, x_i, fails the established criterion above the interval, the suspicious spectrum is analysed in detail.

4 Results

4.1 Method application

Anthropogenic isotopes activity concentrations (Bq/m^3) are given for ^{131}I and ^{137}Cs, since these are typical isotopes that are susceptible of being released by a nuclear power plant in case of accident (Nuclear Energy Agency, 2002). ^{214}Bi and ^{214}Pb activity concentrations are presented as a representation of the contribution from RD.

To highlight the good performance of the proposed spectral windows analysis method, it is compared with simple spectral windows analysis, where the total cps of the analysed energy window are directly converted to Bq/m^3.

4.1.1 Simple spectral windows analysis method

Figure 2 shows the activity concentration of four spectral windows corresponding to ^{137}Cs, ^{131}I, ^{214}Bi and ^{214}Pb, obtained in a series of spectra registered with a $LaBr_3$(Ce) detector in the laboratory. The isotope activities were calculated using Equation (2), subtracting only the intrinsic background of the $LaBr_3$(Ce) detector and taking into account that the width of the ROIs included the 95.45% of the peak area.

Activity concentrations were calculated from spectra registered when the detector was exposed to different radioactive sources. The radioactive sources were changed every 50 spectra, resulting in a sequence of different source scenarios. It is worth mentioning that all the different radioactive sources scenarios registered include the laboratory background. Seven different scenarios are shown: no sources (laboratory background), ^{137}Cs, ^{137}Cs and ^{226}Ra (plus RD), ^{131}I, ^{131}I and ^{226}Ra (plus RD), ^{226}Ra (plus RD), and ^{226}Ra (plus RD) with very high activity. For illustrative purposes, the activity o concentration of the isotopes in the laboratory background was measured repeatedly along the sequence.

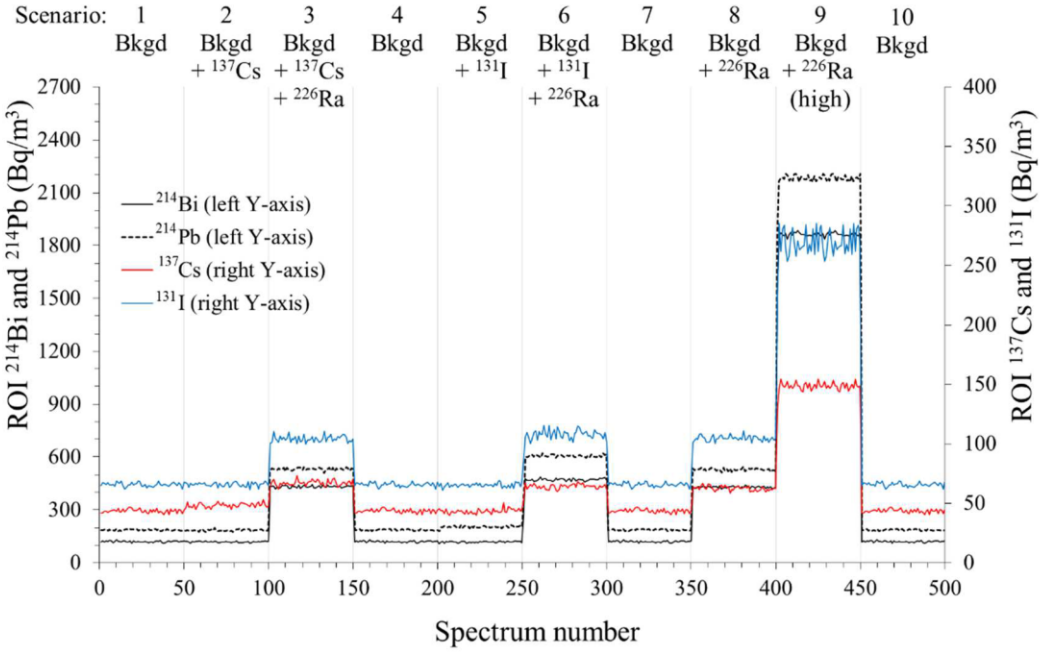

Figure 2. Activity concentrations of ^{214}Bi (black line, left Y-axis) and ^{214}Pb (dotted line, left Y-axis), ^{137}Cs (red line, right Y-axis) and ^{131}I (blue line, right Y-axis) using a simple windows

analysis method. (For interpretation of the references to colour in this figure legend, the reader is referred to the web version of this article.)

4.1.2 **Proposed spectral windows analysis method**

The activity concentrations obtained for the same isotopes when applying the proposed method can be observed in Figure 3. Detailed values of the activities (mean value and standard deviation) for both methods are presented in Table 1. Additionally, values of activity concentrations obtained with the commercial software ScintiVision™ are included for comparison purposes.

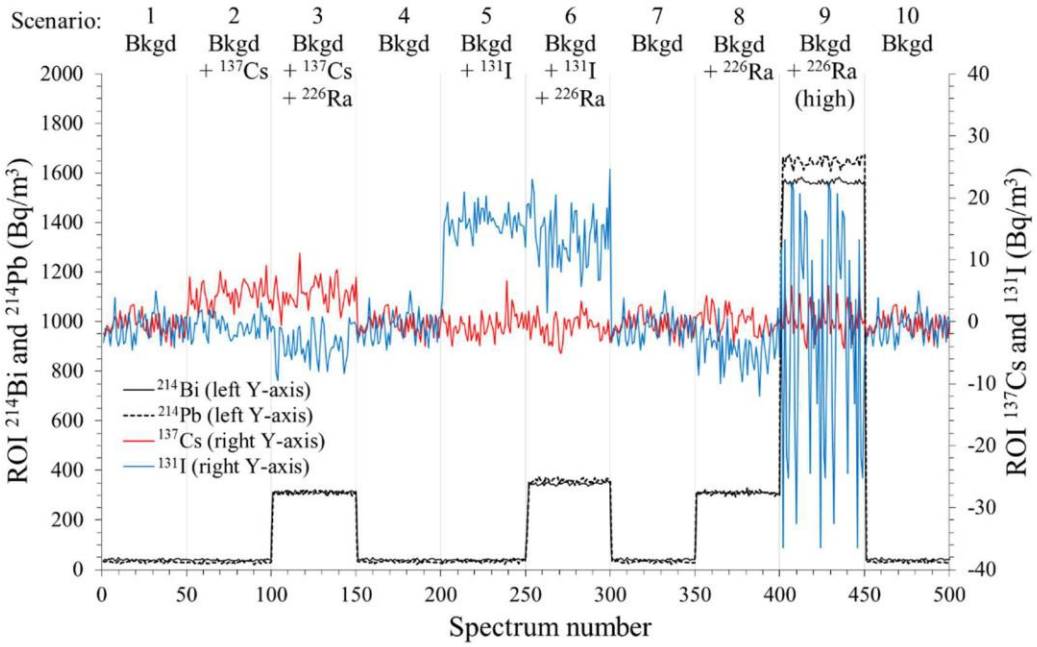

Figure 3. Activity concentrations of ^{214}Bi (black line, left Y-axis) and ^{214}Pb (dotted line, left Y-axis), ^{137}Cs (red line, right Y-axis) and ^{131}I (blue line, right Y-axis) calculated using equations of the proposed windows analysis method. (For interpretation of the references to colour in this figure legend, the reader is referred to the web version of this article.)

Scenario	External source[a]	Isotope	Activity concentration: Simple windows analysis[b] μ (Bq/m³)	Simple windows analysis[b] σ (Bq/m³)	Proposed windows analysis method μ (Bq/m³)	Proposed windows analysis method σ (Bq/m³)	Peaks Gaussian fit μ (Bq/m³)	Δ [c] (%)
1, 4, 7 and 10	--	^{137}Cs	43.6	1.6	-0.4	1.6	0.0	n.a.
		^{131}I	65.8	1.7	-0.9	2.2	0.0	n.a.
		^{214}Bi	120	3.9	40.0	3.4	42.8	-6.9
		^{214}Pb	186	3.7	31.4	3.9	33.1	-5.2
2	^{137}Cs	^{137}Cs	48.4	1.9	4.4	1.9	4.2	5.0
		^{131}I	65.8	1.7	-0.7	1.7	0.0	n.a.
		^{214}Bi	118	3.2	38.6	2.8	40.4	-4.7
		^{214}Pb	184	4.7	29.9	4.8	31.7	-6.2
3	^{137}Cs + ^{226}Ra	^{137}Cs	67.2	2.3	4.5	2.2	4.3	3.9
		^{131}I	104	2.7	-3.6	2.8	0.0	n.a.
		^{214}Bi	432	6.1	313	5.4	315	-0.7
		^{214}Pb	531	6.7	310	6.9	313	-0.9
5	^{131}I	^{137}Cs	43.4	2.0	-0.5	2.0	0.0	n.a.
		^{131}I	65.3	1.7	15.9	2.6	12.7	19.6
		^{214}Bi	118	3.7	38.5	3.2	38.8	-0.9
		^{214}Pb	204	6.2	33.7	5.2	34.7	-3.0
6	^{131}I + ^{226}Ra	^{137}Cs	64.0	2.6	-0.8	1.9	0.0	n.a.
		^{131}I	107	4.9	16.0	4.7	10.8	21.8
		^{214}Bi	468	30.1	344	26.3	348	-1.2
		^{214}Pb	601	33.1	356	27.7	361	-1.4
8	^{226}Ra	^{137}Cs	62.6	1.9	0.1	1.9	0.0	n.a.
		^{131}I	104	2.3	-4.4	3.0	0.0	n.a.
		^{214}Bi	430	4.9	310	4.4	312	-0.4
		^{214}Pb	529	6.7	310	7.2	306	1.1
9	^{226}Ra (high activity)	^{137}Cs	148	4.1	0.4	2.7	0.0	n.a.
		^{131}I	269	11.6	-2.9	18.2	0.0	n.a.
		^{214}Bi	1857	48.0	1558	42.0	1565	-0.4
		^{214}Pb	2176	53.4	1640	46.7	1652	-0.7

[a] Intrinsic background and laboratory natural background are always included

[b] Activity concentrations obtained using Equation (2) subtracting $LaBr_3(Ce)$ intrinsic background

[c] Relative percentage difference between the proposed windows analysis method and the peaks Gaussian fit results, calculated as $\Delta = 100\,(\mu_{Gaussian} - \mu_{proposed\_WM})/\mu_{Gaussian}$

Table 1. Comparison of the activity concentrations of ^{137}Cs, ^{131}I, ^{214}Bi and ^{214}Pb obtained with the simple and the proposed windows analysis method of the spectra registered with the different radioactive sources. Values of activity concentrations obtained with ScintiVision™ software are also presented.

Table 2 shows the MDAC and the discrimination criterion values of ^{137}Cs, ^{131}I, ^{214}Bi and ^{214}Pb obtained when applying the proposed windows analysis method at 10 min background spectra (scenarios 1, 4, 7 and 10). Additionally, MDAC and discrimination criterion values plus the mean background activity concentrations are presented for each isotope.

Isotope	MDAC (Bq/m^3)	μ + MDAC (Bq/m^3)	$\Delta 3\sigma_B$ (Bq/m^3)	$\mu + 3\sigma_B$ (Bq/m^3)
^{137}Cs	5.1	4.7	4.7	4.3
^{131}I	6.9	6.1	6.6	5.7
^{214}Bi	11.0	51.1	10.3	50.4
^{214}Pb	12.3	43.7	11.6	43.0

Table 2. MDAC and discrimination criterion values obtained for ^{137}Cs, ^{131}I, ^{214}Bi and ^{214}Pb, after the application of the method.

5 Discussion

5.1 RD activity concentrations

The activities obtained by the windows analysis method of the ROIs that correspond to RD (^{214}Bi and ^{214}Pb), in the different sources scenarios (Table 1), are in agreement with those obtained with ScintiVision™ software, giving a maximum absolute difference lower than 7% when computing the activity concentration of ^{214}Bi of the laboratory background. It is worth noting that the relative error increases with low activities due to the difficulty of fitting smaller peaks than fitting greater ones with the commercial software.

In the simple spectral windows analysis, the increase of the activity concentration of RD is overestimated in all configurations and it is remarkable when determining the activities of spectra registered in presence of the source of ^{226}Ra. For example, the activity concentration of ^{214}Bi in scenario 9 increases 1736 Bq/m^3 from the laboratory background, whereas, after calculating the activity concentration with the proposed method, the activity concentration increases 1518 Bq/m^3. This difference is mainly due to the correction of the Compton contribution of the RD source.

Scenarios 3, 6 and 8, registered with the source of ^{226}Ra, show activities that can be obtained occasionally in field monitors of the surveillance network but are not habitual, as these activities are very high. Thus, ^{214}Bi and ^{214}Pb activities shown in scenario 9, where the ^{226}Ra source was very close to the detector, are extremely high and are never found in field measurements. However, this scenario was included to test the goodness of the methodology.

5.2 ^{137}Cs activity concentrations

With simple windows analysis method, data show presence of ^{137}Cs in the laboratory background (43.6 Bq/m^3) whereas, after using the proposed windows method, ^{137}Cs activity concentration obtained is near 0 (see Table 1). In scenarios 2 and 3, the detector is exposed to a distant source of ^{137}Cs in order to register a small increase of the isotope activity. In Figure 2, before applying the method, the presence of ^{137}Cs is barely distinguishable from the background situation (scenarios 1 and 2) as the relative increase is low. After the application of the method, a small

increment is seen in scenarios 2 and 3 (Figure 3) and an activity concentration of 4.5 Bq/m^3 is obtained. This low activity concentration would trigger the analysis discrimination criterion for ^{137}Cs when using the proposed method, since activities over 4.3 Bq/m^3 would fulfil the criterion (see Table 2). The MDAC value obtained for ^{137}Cs for 10 min spectra is very similar to the discrimination criterion and to the 5 Bq/m^3 recommended for the minimum activity concentration of ^{137}Cs bound to aerosols detectable within 2 h in the Safety Standards of the German Nuclear Safety Standards Commission (Nuclear Safety Standards Commission (KTA), 2005).

A remarkable situation is shown in scenario 3 in Figure 3, where a source of ^{226}Ra is added to the ^{137}Cs source. In simple spectral windows analysis, the presence of natural radiation is computed as an increase of ^{137}Cs activity concentration (false-positive result). However, using the proposed method, the activity concentration of ^{137}Cs remains constant and equal to scenario 2 (only ^{137}Cs source). This effect is much more noticeable in scenario 9, where the high presence of RD increases in 104.7 Bq/m^3 the concentration of ^{137}Cs from the laboratory background. Therefore, the method proved to be an adequate system for establishing a ^{137}Cs early-warning alarm, as it is able to trigger the analysis criterion when low activity concentrations of ^{137}Cs are present but it does not generate false-positive results in situations with high presence of natural radiation from RD.

5.3 ^{131}I activity concentrations

Using simple spectral windows analysis method, the activities calculated show different situations resulting in misleading conclusions. On one hand, the activity concentration of ^{131}I computed without a ^{131}I source in spectra registered in the laboratory background or in presence of the ^{226}Ra source is not null, resulting in a false-positive presence of ^{131}I. On the other hand, the value of the activity concentration of ^{131}I when in presence of a ^{131}I source (65.3 Bq/m^3) is lower than the value obtained in the laboratory background spectra (65.8 Bq/m^3) causing a false-negative result (see Table 1).

Applying the proposed windows method, the mean value of ^{131}I activity concentration is near 0 in all registered scenarios without presence of the ^{131}I source. When the source of ^{226}Ra is present (see scenarios 3, 6 and 8 in Figure 3), the calculation of ^{131}I activity concentration increases the dispersion of the results, which is remarkably high when the activity concentration of ^{226}Ra is extremely great (scenario 9).

The proposed windows method overestimates ^{131}I activity concentrations compared to the Gaussian fit performed with ScintiVision™ in all scenarios (see Table 1). However, it should be mentioned that the Gaussian fit presented some complications since ^{131}I activity was very low and it overlapped with the ^{214}Pb emission at 352 keV of the laboratory background, which made it difficult to properly fit a double Gaussian.

The activity concentrations obtained for ^{131}I in presence of the source (scenarios 5 and 6) would trigger the analysis criterion, as these are larger than the 5.7 Bq/m^3 threshold (see Table 2). The MDAC obtained is of the same order as the threshold and lower than the minimum activity concentration of ^{131}I detectable within 2 h recommended by the German Nuclear Safety Standards Commission, which is set at 20 Bq/m^3 (Nuclear Safety Standards Commission (KTA), 2005). However, in view of the great dispersion of the obtained ^{131}I activity concentrations, these results should be interpreted with caution.

In scenario 6, where the detector is exposed to ^{131}I and ^{226}Ra sources, the method obtains a ^{131}I constant activity concentration, equal to that in the scenario without ^{226}Ra and only a ^{131}I source

(scenario 5). The values obtained by the Gaussian fitting software are lower than those obtained by the method (Table 1). As it has been mentioned before, the reason for this is probably due to the overlapping of ^{214}Pb and to the external cps contributions to ^{131}I ROI.

5.4 General considerations

The method described in this study was developed to be applied in spectra obtained by environmental real-time monitors using gamma-ray scintillation spectrometry with any kind of detector crystal. The results shown were particularised for a direct $LaBr_3$(Ce) monitor, however, the method can be adapted to any scintillation detector, shielding geometry or monitor type after determining the adequate parameters. For this reason, the method can be used for monitoring isotopes in monitors of spectrometry surveillance networks.

The method assumed that the Compton scattering contribution from natural isotopes that are not RD (e.g. ^{40}K and those from ^{232}Th decay chain, mainly ^{208}Tl, ^{228}Ac, ^{212}Bi, ^{212}Pb) plus all other types of external contributions to a spectrum was constant. In laboratory measurements, the activity concentrations from ^{40}K and ^{208}Tl were confirmed to be constant, but in field measurements the hypothesis may not still be valid, specially for ^{208}Tl. Thus, in case of finding variable external contributions to spectra when adjusting the c_i parameter for field monitors, a term $m_i' A_i$ could be added to take into account the fluctuations of non-RD isotopes.

In gamma-ray spectrometry monitors using NaI(Tl) detectors, the lower resolution of their crystal compared to $LaBr_3$(Ce) ones would contribute to a major peak overlapping. Even if the method is prepared to solve peak overlapping situations, better results are obtained for smaller overlapping of peaks inside a ROI. The overlapping could be minimised simply setting narrower ROI widths than the ones used in this study.

The analysis method presented in this paper is advantageous as it is computationally easy to implement. Moreover, the obtaining of the parameters used in the calculations can be fulfilled with a simple set of spectra measured with low dose rate radioactive sources. The possibility to fit the parameters to activity concentrations obtained with other analysis methods, for example by Gaussian fitting, guarantees that the obtained activity concentrations are in agreement with those obtained with a validated software, such as ScintiVision™.

6 Conclusions

The windows analysis method presented in this paper is a simple and useful tool for automatic monitoring of activity concentrations of natural and anthropogenic radionuclides in real-time environmental gamma-ray spectrometry with scintillation detectors. Although the results presented were obtained in laboratory conditions, the method can be adjusted to field monitors by calculating parameters related to the Compton scattering and to other external contributions arising from gamma-ray interactions with matter. Despite that the standard deviation of the obtained activity concentrations for ^{131}I was remarkable, the mean value was in agreement with the activity concentrations obtained with a commercial Gaussian fitting software. The method proved to be reliable when monitoring ^{137}Cs, since it did not generate false-positive neither false-negative results. Therefore, the proposed windows analysis method can be used for the

establishment of early-warning alarms in real-time environmental gamma-ray scintillation spectrometry.

References

Arnold, L.J., Duval, M., Falguères, C., Bahain, J.-J., Demuro, M., 2012. Portable gamma spectrometry with cerium-doped lanthanum bromide scintillators: Suitability assessments for luminescence and electron spin resonance dating applications. Radiat. Meas. 47, 6–18. doi:10.1016/j.radmeas.2011.09.001

Blum, P., Rabaute, A., Gaudon, P., Allan, J.F., 1997. Analysis of natural gamma-ray spectra obtained from sediment cores with the shipboard scintilation detector of the Ocean Drilling Program: Example from Leg 156. Proc. Ocean Drill. Program, Sci. Results 156.

Casanovas, R., Morant, J.J., López, M., Hernández-Girón, I., Batalla, E., Salvadó, M., 2011. Performance of data acceptance criteria over 50 months from an automatic real-time environmental radiation surveillance network. J. Environ. Radioact. 102, 742–748. doi:10.1016/j.jenvrad.2011.04.001

Casanovas, R., Morant, J.J., Salvado, M., 2014a. Development and calibration of a real-time airborne radioactivity monitor using gamma-ray spectrometry on a particulate filter. IEEE Trans. Nucl. Sci. 61, 727–731. doi:10.1109/TNS.2014.2299715

Casanovas, R., Morant, J.J., Salvadó, M., 2014b. Development and calibration of a real-time airborne radioactivity monitor using direct gamma-ray spectrometry with two scintillation detectors. Appl. Radiat. Isot. 89, 102–108. doi:10.1016/j.apradiso.2014.01.026

Casanovas, R., Morant, J.J., Salvadó, M., 2013. Implementation of gamma-ray spectrometry in two real-time water monitors using NaI(Tl) scintillation detectors. Appl. Radiat. Isot. 80, 49–55. doi:10.1016/j.apradiso.2013.06.003

Casanovas, R., Morant, J.J., Salvadó, M., 2012a. Temperature peak-shift correction methods for NaI(Tl) and LaBr3(Ce) gamma-ray spectrum stabilisation. Radiat. Meas. 47, 588–595. doi:10.1016/j.radmeas.2012.06.001

Casanovas, R., Morant, J.J., Salvadó, M., 2012b. Energy and resolution calibration of NaI(Tl) and LaBr 3(Ce) scintillators and validation of an EGS5 Monte Carlo user code for efficiency calculations. Nucl. Instruments Methods Phys. Res. Sect. A Accel. Spectrometers, Detect. Assoc. Equip. 675, 78–83. doi:10.1016/j.nima.2012.02.006

Casanovas, R., Prieto, E., Salvadó, M., 2016. Calculation of the ambient dose equivalent H*(10) from gamma-ray spectra obtained with scintillation detectors. Appl. Radiat. Isot. 118, 154–159. doi:10.1016/j.apradiso.2016.09.001

Cresswell, A.J., Sanderson, D.C.W., White, D.C., 2006. 137Cs measurement uncertainties and detection limits for airborne gamma spectrometry (AGS) data analysed using a spectral windows method. Appl. Radiat. Isot. 64, 247–253. doi:10.1016/j.apradiso.2005.07.013

Currie, L. a., 1968. Limits for qualitative detection and quantitative determination. Application to radiochemistry. Anal. Chem. 40, 586–593. doi:10.1021/ac60259a007

Gilmore, G.R., 2008. Practical gamma-ray spectrometry - 2nd edition, John Wiley {&} Sons, Ltd. doi:10.1016/S0584-8539(96)90113-0

IAEA - International Atomic Energy Agency, 1991. Airborne gamma ray spectrometer surveying, Technical Reports Series.

IAEA - International Atomic Energy Agency, 1976. Radiometric Reporting Methods and Calibration in Uranium Exploration, Technical Report Series No. 174.

Korbech, U., Nielsen, K.., 1992. A Simple Method for Early Detection of Fall-out. Radiat. Prot. Dosimetry 40, 103–109. doi:10.1093/oxfordjournals.rpd.a081197

Nuclear Energy Agency, 2002. Assessment of Radiological and Health Impacts 2002 Update of Chernobyl : Ten Years On. Chernobyl, Assess. Radiol. Heal. Impacts.

Nuclear Safety Standards Commission (KTA), 2005. Safety Standards KTA 1502 (2013-11) Monitoring Volumetric Activity of Radioactive Substances in the Inner Atmosphere of Nuclear Power Plants.

Quarati, F.G.A., Khodyuk, I. V., Van Eijk, C.W.E., Quarati, P., Dorenbos, P., 2012. Study of 138La radioactive decays using LaBr 3 scintillators. Nucl. Instruments Methods Phys. Res. Sect. A Accel. Spectrometers, Detect. Assoc. Equip. 683, 46–52. doi:10.1016/j.nima.2012.04.066

4. Discusión

Esta tesis ha contribuido a mejorar las principales tareas que la *Unitat de Física Mèdica* de la URV realiza en la Red de Espectrometría de la Generalitat de Catalunya. El trabajo desarrollado dentro del marco de la Red se ha estructurado en tres fases distintas. En primer lugar, se ha realizado investigación relacionada con el monitor de agua de río de la Red. Los estudios llevados a cabo han proporcionado información de interés respecto al comportamiento del monitor con dos tipos de cristal de centelleo distintos. En segundo lugar, se han aportado metodologías para el cálculo automático y en tiempo real del equivalente de dosis ambiental H*(10) a partir de medidas de espectrometría gamma. Por último, se ha desarrollado un método de análisis de datos espectrométrico aplicable a equipos de espectrometría gamma ambiental en tiempo real basado en las regiones espectrales. El método permite obtener de manera automática concentraciones de actividad de isótopos artificiales y naturales.

En este trabajo, se han adecuado los espectros obtenidos con un monitor de agua de espectrometría gamma con un detector de $LaBr_3$(Ce) (artículo **[I]**) para el análisis espectrométrico. Los espectros fueron estabilizados y el monitor de río fue calibrado en energía, resolución y eficiencia. La metodología usada para las calibraciones en energía y resolución fue detallada en un estudio previo donde los valores experimentales, espectros obtenidos mediante fuentes radiactivas de test, se ajustaron a polinomios de segundo orden [9]. Por otra parte, la eficiencia se obtuvo con métodos de Montecarlo con el código EGS5 validados para cálculos de eficiencia [9]. Teniendo en cuenta la mayor densidad y mayor rendimiento lumínico del cristal de $LaBr_3$(Ce) [10], los valores de eficiencia obtenidos resultaron mayores que aquéllos obtenidos por el monitor de agua de río con detector de NaI(Tl) [7].

Después de la calibración, el monitor de agua era capaz de obtener espectros gamma con información radiológica significativa. Para comprobar el funcionamiento de este monitor se estudió un período de medidas en el que se engloba un episodio de lluvia. Durante el estudio, el monitor de agua con el detector de $LaBr_3(Ce)$ que se calibró era aquél situado antes del paso del río Ebro por la central nuclear de Ascó (Río Norte), mientras que el monitor situado después del paso del río Ebro por la central (Río Sur) continuó funcionando con un detector de NaI(Tl). El citado episodio de lluvia se registró en ambos monitores y fue posible comparar los resultados obtenidos. Las medidas registradas durante el período seco presentaron muy baja tasa de dosis, mientras que, durante el episodio de lluvia, se determinaron concentraciones de actividad del isótopo ^{214}Bi con los dos tipos de monitores, obteniendo valores muy similares. Cabe destacar que la concentración de actividad del ^{214}Bi no tendría por qué ser exactamente la misma, ya que los monitores se ubican en sitios distintos aunque próximos entre sí.

Tanto el fondo obtenido en período seco como el aumento de cps registrado durante el episodio de lluvia fueron mayores para el monitor con detector de $LaBr_3(Ce)$ que con el detector de NaI(Tl). La explicación para este hecho recae en las mejores características técnicas del cristal de $LaBr_3(Ce)$ (principalmente eficiencia, rendimiento lumínico, densidad, resolución y linealidad) y a su fondo intrínseco creado por la contaminación interna de ^{138}La y ^{227}Ac [15]. Precisamente el fondo intrínseco, a pesar de las mejores características técnicas de los detectores de $LaBr_3(Ce)$ respecto a los detectores de NaI(Tl), conlleva un aumento de la dispersión de los valores medidos. Esta mayor dispersión implica que, aunque el monitor con detector de $LaBr_3(Ce)$ hubiera registrado incrementos de cps mayores, el aumento relativo respecto al fondo registrado fue mucho menor que el presentado por el monitor de NaI(Tl). Por otra parte, los espectros tomados por los monitores de la Red son sometidos a un criterio de discriminación establecido que se basa en calcular las cps totales de espectro y comprobar si superan 2 veces la desviación estándar del valor de cps de fondo ($\mu+2\sigma$). Por tanto, los espectros obtenidos con el monitor con detector de $LaBr_3(Ce)$ sobrepasaron dicho criterio en menor medida que los espectros registrados con NaI(Tl), aunque estos últimos presentaron menores incrementos absolutos.

Por todo lo expuesto, teniendo en cuenta la mejor resolución y eficiencia del detector de $LaBr_3(Ce)$, la implementación del citado detector en el monitor de agua de río sería una buena elección para analizar espectros gamma registrados en situaciones de alta tasa de

dosis, donde las cps del espectro gamma resultante fueran superiores a las del espectro de fondo. Por el contrario, el monitor de agua de río con un detector de NaI(Tl) sería un buen indicador de pequeños incrementos de tasa de dosis en situaciones de baja tasa de dosis.

Un valor de referencia importante por su implicación legal es el equivalente de dosis ambiental H*(10). En el artículo **[II]** se detalla la metodología para calcular el H*(10) a partir de espectros gamma. El cálculo de dicha dosis fue particularizado para un monitor con detector de $LaBr_3(Ce)$. Sin embargo, puede ser adaptado a otros tipos de monitores de espectrometría o a detectores de distinta forma y tamaño. Además, también se puede adecuar para otros rangos energéticos de rayos gamma.

En el desarrollo de la metodología se obtuvieron valores de conversión de fluencia a H*(10) que se corresponden con los facilitados por la publicación 74 de la ICRP [16]. No obstante, en aplicar el método a espectros gamma obtenidos por un monitor de espectrometría gamma con detector de $LaBr_3(Ce)$, los valores de H*(10) resultaron ser inferiores a los medidos por un contador GM calibrado. Se han analizado varios motivos que explican dicho resultado. La mayor respuesta a los rayos gamma del contador GM a partir de los 662 keV (energía de referencia correspondiente a la emisión gamma del ^{137}Cs) podría ser una causa para la obtención de valores más altos con dicho contador. Esta información fue proporcionada por el fabricante, aunque la mayor respuesta de los GM a energías mayores que 662 keV fue corroborada en una intercomparación con dosímetros TLD y cámaras de ionización [17]. Otro motivo podría ser la dificultad de medir por separado la radiación cósmica con un detector de $LaBr_3(Ce)$. La contribución de dicha radiación sería sustraída en el proceso de eliminación del fondo intrínseco, mientras que sí es detectada por el contador GM. Por este motivo, la contribución de la radiación cósmica debe ser determinada y añadida a la medida. Así, se consideró que, en la localización de los monitores de espectrometría utilizados en este estudio, la tasa de dosis de radiación cósmica era similar a 0,033 µSv/h, obtenida en Barcelona [18]. Además, la propia sustracción del fondo intrínseco se postuló como una posible fuente de incertidumbre que justificaría las discrepancias entre el H*(10) calculado y el determinado por el contador GM. De todos modos, cabe destacar que los incrementos registrados durante un episodio de lluvia por los dos tipos de detectores fueron de una magnitud similar.

Así, en vista de los resultados, se concluyó que era necesario desarrollar un estudio intercomparativo más extenso. Posteriormente a la publicación del artículo **[II]**, se llevó a

cabo un estudio de intercomparación para calibrar distintos tipos de detectores en H*(10), con valores obtenidos a partir de espectrometría gamma con detectores de $LaBr_3$(Ce) y NaI(Tl), un contador proporcional calibrado en H*(10), un contador GM y dosímetros TLD calibrados para medidas ambientales [19]. La media de H*(10) obtenida durante un mes por el contador proporcional obtuvo valores cercanos a los de los dosímetros TLD. Por este motivo, el resto de monitores se ajustó a las variaciones mostradas por el contador proporcional. Los resultados de dicho estudio determinaron que el cálculo de H*(10) a partir de espectrometría gamma aportaba una menor dispersión respecto al resto de monitores, además de la información isotópica que permite identificar los isótopos que provocan un aumento en el H*(10).

El valor del nivel de investigación (0,008 µSv/h) es un valor restrictivo del equivalente de dosis ambiental H*(10) a partir del cual los datos radiológicos son analizados en profundidad. El nivel de investigación es inferior a otros dos niveles que se relacionan con la legislación: el nivel de alerta establecido en 0,114 µSv/h [12] y el nivel de alarma (1 µSv/h) [20]. En el artículo **[II]**, se calcularon las concentraciones de actividad necesarias para sobrepasar la tasa de H*(10) establecida en el nivel de investigación que se obtendría a partir de espectros gamma obtenidos con un detector de $LaBr_3$(Ce). Las concentraciones mencionadas fueron determinadas para los isótopos ^{241}Am, ^{131}I, ^{137}Cs y ^{60}Co. A modo de ejemplo, la concentración de actividad de ^{137}Cs necesaria para alcanzar el nivel de investigación a partir de espectros gamma sería de 51,1 Bq/m^3. En un estudio previo, se calculó la concentración de actividad mínima detectable (MDAC) obtenida para espectros de 10 minutos registrados con un monitor de medida directa con detector de $LaBr_3$(Ce). La MDAC para el isótopo ^{137}Cs es de 5,3 Bq/m^3 [6] de manera que, concentraciones de actividad iguales o superiores a la MDAC serían detectables en un análisis espectrométrico. En consecuencia, un análisis espectrométrico convencional obtendría una mayor capacidad de detección que la determinación del H*(10), ya que, para obtener un incremento de H*(10) notable, son necesarias concentraciones de actividad de ^{137}Cs muy superiores al MDAC.

Aunque el cálculo del equivalente de dosis ambiental H*(10) es necesario para poder relacionar las medidas espectrométricas con los valores establecidos por la legislación, los resultados mencionados en el párrafo anterior demuestran que el análisis espectrométrico es más sensible. Por este motivo, se ha desarrollado una metodología de análisis para la

determinación de la concentración de actividad que se basa en la técnica de las regiones espectrales (artículo **[III]**).

El método de análisis por regiones espectrales fue desarrollado para realizar un análisis primario automático de los espectros registrados por los monitores de espectrometría gamma de centelleo de la Red de Espectrometría de Catalunya. El método propuesto obtiene concentraciones de actividad de manera automática de isótopos seleccionados, tanto isótopos naturales como isótopos artificiales, por ejemplo el ^{137}Cs y ^{131}I.

La necesidad de disponer de un método como el citado es consecuencia de dos motivos distintos. Por una parte, el volumen de datos para analizar ha ido creciendo debido al aumento de monitores de la Red. Éstos registran un espectro gamma cada 10 minutos para obtener datos en tiempo real. Por otra parte, los espectros gamma registrados en medidas ambientales se caracterizan por ser medidas de baja tasa de dosis que incluyen variaciones naturales de los emisores gamma descendientes del isótopo ^{222}Rn causadas por cambios meteorológicos (lluvia y humedad). Estos aspectos dificultan la determinación de la concentración de actividad de isótopos artificiales debido a la baja estadística, el solapamiento con emisiones naturales y la presencia de cuentas externas atribuidas a fenómenos de interacción entre fotones y materia, como la dispersión Compton.

Por todo ello, el método de análisis expuesto en el artículo **[III]** depura las regiones espectrales para obtener solamente las cps necesarias para determinar la concentración de actividad de ciertos isótopos. Así, el método elimina la contribución externa (dispersión Compton y otros efectos) y solventa el solapamiento de picos dentro de una región donde se encuentran cps provenientes de distintas emisiones. El método se ha particularizado para un monitor de medida directa con detector de $LaBr_3$(Ce) aunque es útil para cualquier otro tipo de monitor, configuración y detector de centelleo.

Las regiones espectrales determinadas por el ^{137}Cs y el ^{131}I incluyen cps de emisiones naturales cercanas, además de las cuentas externas. Dichas emisiones son la de 665 keV del ^{214}Bi en la región del ^{137}Cs y la de 352 keV del ^{214}Pb en la región del ^{131}I. Antes de la aplicación del método, las concentraciones de actividad tanto de ^{137}Cs como de ^{131}I resultaron positivas en espectros de fondo registrados en el laboratorio sin presencia de fuentes radiactivas externas (tan solo el fondo natural del laboratorio), dando un falso positivo. De la misma manera, también se registraron falsos positivos de ^{137}Cs y ^{131}I en

espectros registrados en presencia de la fuente emisora de descendientes del ^{222}Rn. Después de aplicar el método, los valores medios de concentración de actividad para dichos isótopos fueron nulos en ambos casos.

El método ha demostrado ser fiable para determinar la concentración de actividad del ^{137}Cs. Se registraron espectros con la fuente del citado isótopo de manera que el aumento de cps fuera casi imperceptible antes de la aplicación del método (ver Figura 2 del artículo **[III]**). Después de tomar 50 espectros se añadió una fuente que emitía descendientes del ^{222}Rn. Al aplicar el método, la concentración de actividad obtenida fue baja y constante en las dos situaciones y, además, en concordancia con los valores obtenidos por un programa comercial validado (ScintiVision™ de ORTEC®) de ajuste por Gaussianas. Además, se consiguió determinar un valor de concentración de actividad similar a la MDAC y al criterio de discriminación de análisis de espectros establecido.

Respecto a la concentración de actividad del ^{131}I, el valor medio obtenido fue correcto en todas las situaciones con distintas fuentes radiactivas presentadas. Sin embargo, se obtuvieron resultados ligeramente inferiores respecto al valor obtenido por el programa comercial. Se debería tener en cuenta que la actividad de la fuente de ^{131}I era baja y, además, la presencia de ^{214}Pb en el fondo del laboratorio dificultó el ajuste por Gaussianas con el programa. Es importante destacar que se han obtenido valores de dispersión notables en el caso de espectros registrados con la fuente emisora de descendientes del ^{222}Rn (ver Figura 3 del artículo **[III]**).

La hipótesis en la que se fundamenta el método (la contribución de la dispersión Compton de los isótopos no descendientes del ^{222}Rn más la contribución externa es constante) ha sido verificada en las medidas registradas en el laboratorio, obteniendo concentraciones de actividad constantes de ^{40}K, ^{208}Tl, ^{212}Bi y ^{212}Pb. Si la hipótesis no se cumple en aplicar el método a medidas de campo, se deberán adecuar los parámetros para tener en cuenta esta contribución variable.

Finalmente, cabe destacar que el método de análisis por regiones espectrales propuesto, aunque ha sido aplicado a un monitor con detector de $LaBr_3$(Ce) en el laboratorio, está dirigido a medidas registradas en campo con cualquier tipo de detector de centelleo.

5. Conclusiones

Los estudios presentados en el cuerpo central de esta tesis hacen referencia a distintas aportaciones que la *Unitat de Física Mèdica* de la URV ha realizado para la evaluación del significado radiológico de los datos adquiridos y en tareas de investigación en el marco del proyecto de la Red de Vigilancia Radiológica Ambiental de la Generalitat de Catalunya.

Las principales conclusiones alcanzadas en la realización de los diferentes estudios que ha abordado este trabajo son:

- Se han adecuado los espectros registrados por un monitor de agua de río con detector de $LaBr_3(Ce)$ para el análisis espectrométrico, aplicando metodologías para la estabilización de espectros y la calibración del equipo en energía, resolución y eficiencia.

- Se ha comparado su funcionamiento con otro monitor de agua de río con detector de NaI(Tl) durante un episodio de lluvia. La concentración de actividad calculada para el ^{214}Bi ha dado un resultado equiparable con ambos monitores.

- Debido a la gran dispersión de las medidas de fondo, aportada por el valor elevado del fondo intrínseco, el monitor de agua de río con detector de $LaBr_3(Ce)$ requiere un incremento de cps mucho mayor que el monitor de NaI(Tl) para superar el criterio de discriminación de análisis de espectros establecido en la Red.

- Se ha desarrollado una metodología para el cálculo del equivalente de dosis ambiental H*(10) en monitores de espectrometría gamma en tiempo real con detectores de centelleo que puede ser aplicada a todos los tipos de detectores de espectrometría, a distintas geometrías, materiales y rango de energías gamma.

- Se ha aplicado la metodología a un monitor con detector de $LaBr_3(Ce)$ y se han comparado los valores obtenidos de H*(10) con los proporcionados por un contador GM calibrado. Además, se han calculado las concentraciones de actividad necesarias para producir cierto incremento del equivalente de dosis ambiental H*(10).

- Se ha desarrollado un método de análisis por regiones espectrales para la monitorización de la concentración de actividad de isótopos artificiales en medidas ambientales de espectrometría gamma en tiempo real tomadas con detectores de centelleo.

- En cada región espectral, el método sustrae las contribuciones externas que sobreestiman la concentración de actividad de un cierto isótopo, como la dispersión Compton de la radiación natural o las cuentas provenientes de otras emisiones gamma cercanas.

- Se ha ajustado el método a un monitor de medida directa con detector de $LaBr_3(Ce)$, para evitar los falsos positivos de ^{137}Cs y ^{131}I en espectros de fondo y espectros con una notable presencia de descendientes del ^{222}Rn. En espectros registrados con fuentes de ^{137}Cs y ^{131}I, la metodología obtiene un valor de concentración de actividad equiparable con el obtenido por un programa comercial de ajuste de Gaussianas.

Referencias

[1] "2000/473/Euratom - Commission Recommendation of 8 June 2000," *Oficial Journal of the European Commission. no.191*. 2000.

[2] Council of the European Union, "Council Directive 96/29/Euratom," *Off. J. Eur. Union*, no. L, p. L159/1-159/114, 1996.

[3] Consejo de Seguridad Nuclear (CSN), "Informe sobre notificación de sucesos en centrales nucleares," 2008.

[4] R. Casanovas, J. J. Morant, M. López, I. Hernández-Girón, E. Batalla y M. Salvadó, "Performance of data acceptance criteria over 50 months from an automatic real-time environmental radiation surveillance network," *J. Environ. Radioact.*, vol. 102, no. 8, pp. 742–748, 2011.

[5] R. Casanovas, J. J. Morant, y M. Salvado, "Development and calibration of a real-time airborne radioactivity monitor using gamma-ray spectrometry on a particulate filter," *IEEE Trans. Nucl. Sci.*, vol. 61, no. 2, pp. 727–731, 2014.

[6] R. Casanovas, J. J. Morant, y M. Salvadó, "Development and calibration of a real-time airborne radioactivity monitor using direct gamma-ray spectrometry with two scintillation detectors," *Appl. Radiat. Isot.*, vol. 89, pp. 102–108, 2014.

[7] R. Casanovas, J. J. Morant, y M. Salvadó, "Implementation of gamma-ray spectrometry in two real-time water monitors using NaI(Tl) scintillation detectors," *Appl. Radiat. Isot.*, vol. 80, pp. 49–55, 2013.

[8] R. Casanovas, J. J. Morant, y M. Salvadó, "Temperature peak-shift correction methods for NaI(Tl) and LaBr3(Ce) gamma-ray spectrum stabilisation," *Radiat. Meas.*, vol. 47, no. 8, pp. 588–595, Aug. 2012.

[9] R. Casanovas, J. J. Morant, y M. Salvadó, "Energy and resolution calibration of NaI(Tl) and LaBr 3(Ce) scintillators and validation of an EGS5 Monte Carlo user code for efficiency calculations," *Nucl. Instruments Methods Phys. Res. Sect. A Accel. Spectrometers, Detect. Assoc. Equip.*, vol. 675, pp. 78–83, 2012.

[10] B. D. Milbrath, B. J. Choate, J. E. Fast, W. K. Hensley, R. T. Kouzes, y J. E. Schweppe, "Comparison of LaBr3: Ce and NaI (Tl) scintillators for radio-isotope identification devices," *Nucl. Instruments …*, no. PIET-43741-TM-488; PNNL-15831, p. 18, 2006.

[11] F. Quarati *et al.*, "X-ray and gamma-ray response of a 2'x2' $LaBr_3$:Ce scintillation detector," *Nucl. Instruments Methods Phys. Res. Sect. A Accel. Spectrometers, Detect. Assoc. Equip.*, vol. 574, no. 1, pp. 115–120, 2007.

[12] ICRP: ICRP Publication 103, "The 2007 Recommendations of the International Commission on Radiological Protection," *Ann. ICRP*, 2007.

[13] ICRU: ICRU Report 39, "Determination of Dose Equivalents Resulting from External Radiation Sources."

[14] Nuclear Energy Agency, "Assessment of Radiological and Health Impacts 2002 Update of Chernobyl : Ten Years On," *Chernobyl, Assess. Radiol. Heal. Impacts*, 2002.

[15] F. G. A. Quarati, I. V. Khodyuk, C. W. E. Van Eijk, P. Quarati, y P. Dorenbos, "Study of 138La radioactive decays using LaBr 3 scintillators," *Nucl. Instruments Methods Phys. Res. Sect. A Accel. Spectrometers, Detect. Assoc. Equip.*, vol. 683, pp. 46–52, 2012.

[16] ICRP, "ICRP Publication 74. Conversion Coefficients for use in Radiological Protection against External Radiation.," *Ann. ICRP*, 1996.

[17] J. C. Sáez-Vergara, a M. Romero, M. Vila Pena, R. Rodriguez, and J. L. Muñiz, "The use of passive environmental TLDs in the operation of the Spanish early warning network 'REVIRA'.," *Radiat. Prot. Dosimetry*, 2002.

[18] A. Camp y A. Vargas, "Ambient dose estimation H*(10) from $LaBr_3$(Ce) spectra.," *Radiat. Prot. Dosimetry*, 2014.

[19] E. Prieto, R. Casanovas, y M. Salvadó, "Estudio comparativo del equivalente de dosis ambiental H*(10) obtenido mediante diferentes tipos de detectores de radiación," in *IX Jornadas sobre el control de la radiactividad ambiental*, 2016.

[20] Consejo de Seguridad Nuclear (CSN), "Instrucción IS-10, revisión 1, de 30 de julio de 2014, del Consejo de Seguridad Nuclear, por la que se establecen los criterios de notificación de sucesos al Consejo por parte de las centrales nucleares. Disposición 9550 del BOE núm. 228 de 2014." 2014.

UNIVERSITAT ROVIRA I VIRGILI
ADECUACIÓN Y DESARROLLO DE MÉTODOS DE ANÁLISIS DE DATOS OBTENIDOS MEDIANTE ESPECTROMETRÍA GAMMA PARA LA MEDIDA DE LA RADIACTIVIDAD AMBIENTAL EN TIEMPO REAL
Elena Prieto Butillé

UNIVERSITAT ROVIRA I VIRGILI
ADECUACIÓN Y DESARROLLO DE MÉTODOS DE ANÁLISIS DE DATOS OBTENIDOS MEDIANTE ESPECTROMETRÍA GAMMA PARA LA MEDIDA DE LA RADIACTIVIDAD AMBIENTAL EN TIEMPO REAL
Elena Prieto Butillé

UNIVERSITAT
ROVIRA i VIRGILI